Conservative Numerical Schemes for Unsteady 1D Two Phase Flow (Esquemas Numéricos Conservativos para Flujo Bifásico 1D no Estacionario)

José Ramón García Cascales

A M^a Ángeles y Pepe

Agradecimientos

En primer lugar me gustaría agradecer a José Miguel Corberán y a Llanos Gascón su dedicación y ayuda durante todo el tiempo que ha llevado la realización de este trabajo.

Quisiera agradecer a José Gonzálvez la enorme ayuda prestada con Fortran, Latex y con mil cosas más, sin duda ha contribuido a que esto acabe mucho antes de lo previsto. Gracias a toda la gente del IMST que de una forma u otra siempre me ha ayudado y gracias a José Luis Muñoz-Cobo por su ayuda con las ecuaciones.

Me gustaría agradecer igualmente su apoyo y ayuda tanto en la consecución de esta tesis como a nivel docente a todos los compañeros del Departamento de Ingeniería Térmica y de Fluidos de la UPCT, a Francisco del Cerro y a Mariano Alarcón y al resto de amigos y compañeros de Cartagena, ya que sin ellos esto no habría llegado a su fin.

Agradecer también a la Universidad Politécnica de Cartagena, las ayudas económicas concedidas que me permitieron avanzar enormemente en el desarrollo de la tesis. Por supuesto hacer llegar mi agradecimiento a Randy Leveque y a Henri Paillere por su hospitalidad y ayuda durante el tiempo que pasé con ellos, así como a la gente del Departamento de Matemáticas Aplicada de Seattle y del SYSCO en Saclay por su amabilidad durante mis estancias allí.

Quisiera agradecer su apoyo durante todos estos años a mis familiares y amigos. Gracias a Clara y a Israel por ayudarme con el inglés y el valenciano respectivamente. Y bueno, un agradecimiento general a todos aquellos que no he citado y que de una forma u otra han contribuido al desarrollo de esta tesis.

Finalmente a Belén, que sin duda es la persona que más ha sufrido todo este proceso. Gracias por estar ahí.

Up the Irons!!

Resumen de la Tesis

Esta tesis está dedicada al modelado de mezclas bifásicas no estacionarias de líquido y vapor. Está motivada por la gran cantidad de aplicaciones industriales en las que podemos encontrar estos fenómenos. Los transitorios en flujo bifásico son un aspecto muy importante en diferentes aplicaciones químicas, nucleares e industriales. En el caso de la industria nuclear, el estudio de transitorios en flujo bifásico es fundamental, debido a la importancia que tiene prevenir accidentes con pérdida de refrigerante (LOCA), así como garantizar un buen funcionamiento del circuito del refrigerante. Mediante la introducción de algunos de los códigos más importantes desarrollados en las dos últimas décadas, así como las técnicas de mallado que utilizan justificamos el presente desarrollo que se ha centrado en la extensión de algunos esquemas explícitos conservativos para obtener soluciones aproximadas del sistema de ecuaciones en flujo bifásico unidimensional. Éstos han sido esquemas centrados y "upwind" para resolver problemas con flujo multifásico, muchos de ellos basados en la solución exacta o aproximada de problemas de Riemann usando métodos tipo Godunov tales como "Approximate Riemann Solvers" o métodos "Flux Vector Splitting". Fundamentalmente hemos estudiado los esquemas TVD, TVD Adaptados y la familia de esquemas AUSM.

En primer lugar introducimos el sistema de ecuaciones de flujo bifásico con el que trabajaremos a lo largo de esta tesis. Para ello vamos desde las ecuaciones instantáneas al sistema de ecuaciones doblemente promediadas en tiempo y área. Posteriormente estudiamos los distintos regímenes de flujo bifásio y algunas de las relaciones de cierre más importantes que nos permitirán cerrar el sistema de ecuaciones. A diferencia de lo que ocurre en el caso de flujo monofásico, la existencia de tales regímenes impide conocer la verdadera posición de los fluidos cada instante. También describimos brevemente algunos de estos fenómenos tales como transmisión de calor o fricción a través de las paredes y de la interfase haciendo algunas consideraciones sobre las ecuaciones de estado.

En el capítulo 3 consideramos los sistemas de ecuaciones más utilizados dependiendo del modelo que consideremos. Así introducimos el modelo homogéneo, el modelo isoentrópico y el modelo separado son tratados con un poco de detalle. Otros modelos son considerados de forma resumida. Nos centramos en los sistemas de ecuaciones que consideran una sola presión, así como el problema que implica la existencia de valores propios complejos, lo cual conduce a soluciones no físicas del sistema. Avanzamos que este problema lo evitamos mediante el uso de términos de corrección de presión, aunque términos como la masa virtual u otros de regularización pueden ser considerados.

El capítulo 4 analiza la evaluación de los valores y vectores propios de flujo bifásico homogéneo y separado. Además se analizan algunos de los modelos más utilizados

para determinar los valores propios. Un método general para determinar de forma analítica los vectores propios es también estudiado. En la segunda parte del capítulo nos concentramos en revisar los esquemas desarrollados y aplicados más recientemente a flujo bifásico.

En el capítulo 5 extendemos a flujo bifásico diferentes esquemas conservativos cuyo buen comportamiento en flujo monofásico ha sido sobradamente probado. Ellos son básicamente los esquemas de Lax-Wendroff, esquemas TVD, los Lax-Wendroff y TVD Adaptados desarrollados por Gascón y Corberán y la familia de esquemas AUSM primeramente introducida por Steffen y Liou y después desarrollada y mejorada por Liou entre otros. El primer grupo, los esquemas TVD, corresponden a los esquemas del tipo "Flux Difference Splitting" (FDS) y los segundos a la categoría "Flux Vector Splitting" (FVS). La mayoría de las extensiones desarrolladas en esta tesis se basan en incluir los términos no conservativos de la ecuación de momento y energía en el término fuente. Siguiendo el esquema de desarrollo anterior, en primer lugar, demostramos la pobre resolución de los esquemas centrados bajo algunos de los test propuestos. Hemos presentado los esquemas TVD y una versión extendida de los mismos, estudiando tanto las versiones de primer como de segundo orden. Este último conseguido mediante la utilización de la estrategia MUSCL-Hancock y con limitadores de pendientes para limitar oscilaciones. El esquema ATVD es el siguiente esquema introducido, es construído con la idea de la inclusión del término fuente en el vector de flujo. Se ha hecho una inclusión parcial, únicamente los términos con derivadas espaciales. Finalmente hemos desarrollado una segunda versión del esquema ATVD, que hemos llamado ATVD2, en la que hemos desacoplado las fases. En un primer paso cada sistema de ecuaciones es analizado separadamente cuando resolvemos el problema de Riemann en la interfase. En una segunda etapa componemos ambos flujos con el fin de determinar las variables que caracterizan los puntos en estudio. En cierta forma esta es la misma idea que aplicaremos en el desarrollo de los esquemas AUSM.

Con respecto a los esquemas AUSM, hemos estudiado dos esquemas, el AUSM+ y el AUSMDV. Están basados en la descomposición del vector de flujos en una parte convectiva y otra de presión. Su implementación de primer y segundo orden son también tratadas. Para conseguir segundo orden hemos probado diferentes opciones usando la estrategia MUSCL junto con limitadores de pendientes para quitar el caracter oscilatorio del segundo orden, diferentes limitadores han sido probados. El comportamiento de cada desarrollo ha sido analizado mediante los siguientes test tipo:

- Grifo de agua (Water faucet).
- Tubo de choque (Shock tube).
- Sedimentación (Sedimentation).
- Manometro oscilatorio (Oscillating manometer).
- Tubo de ebullición (Boiling tube, only for the homogeneous model).

Toda la programación ha sido realizada en Fortran.

Este trabajo nos ha permitido concluir que ambos esquemas, TVD y AUSM son capaces de modelar problemas de flujo bifásico en los que las fases son compresibles. Demostrar además que son capaces de competir con otros de los recientes métodos numéricos aplicados a flujo bifásico. En particular los esquemas AUSM han demostrado algunas ventajas tales como:

- Ser computacionalmente más eficientes debido al hecho de que no es necesario realizar diagonalización alguna en cada interfase lo cual los hace muy atractivos incluso cuando cambiamos de sistema de ecuaciones o de modelo para los fluidos.
- Tener buena representación de las discontinuidades. A lo largo de los distintos test estudiados mostramos su buen nivel de exactitud en la representación de choques y de discontinuidades de contacto.

Summary of the Thesis

The thesis is devoted to the modelization of non steady two phase mixtures of liquid and vapour. It has been motivated by the great amount of industrial applications in which we find these phenomena. Transient two phase flow is a very important issue in nuclear, chemical and industrial applications. In the case of the nuclear industry due to the importance of preventing loss of coolant accidents (LOCA) and guarranteing a good perfomance of the coolant system in power plants. By means of the introduction of the most important codes developed during the last two decades and their associated mesh techniques we justify the present development which is centred on the extension of some conservative and explicit schemes to obtain approximate solutions of the system of equations in one dimensional one pressure two phase flow. They have been Centred and Upwind Schemes to solve multiphase flow problems, most of them based on the exact or approximate solution of Riemann problems using Godunov's like methods such as Approximate Riemann Solvers or Flux Splitting methods. We have studied mainly TVD schemes, Adapted TVD schemes (ATVD) and the AUSM family of schemes.

Firstly we introduce the 1D two phase flow system of equations with which we will work. Thus, we go from the instantaneous equations to the double area and time averaged system of equations. Afterward we study different two phase flow regimes and some important closure relationships which will allow us to close the system of equations. Unlike what happens with single fluid flow, the existance of such regimes do not permit to know the true position of the fluids at each instant. We also describe briefly some phenomena such as heat transfer and friction through the wall of the conduct and the interfaces and make some consideration about the equations of state.

We consider in chapter 3 the systems of equations more used depending on the model. Thus we introduce the homogeneous model, the isentropic model and the separated model will be treated in some detail. Others are summarized briefly. After this, we comment how the 1D one pressure model system of equations is ill-posed in the sense that the Jacobian matrix of the flux vector has complex eigenvalues that make the system produces non physical solutions. We advance that we will avoid this problem by using a pressure correction terms, although virtual mass terms and other regularizing terms could be used as well.

Chapter 4 analyses the evaluation of the eigenstructure of the homogeneous and the separated two phase flow. Different methods to determine the eigenvalues are presented. A general method to determine the eigenvectors is studied as well. In the second part of the chapter we focus on a review of the most recent schemes developed to solve two phase flow problems.

In chapter 5 we extend to two phase flow different conservative schemes whose good behaviour in single phase has been well proved. They are basically TVD schemes, the Adapted TVD schemes developed by Gascón and Corberán and the AUSM family of schemes, firstly introduced by Steffen and Liou and after developed among others. The first one corresponds to the Flux Difference Splitting (FDS) category and the second one belongs to the Flux Vector Splitting (FVS) category.

Most of the extensions developed in this thesis are based on including the non conservative terms of the equations of momentum and energy in the source term.

To demonstrate the bad behaviour of centred schemes we have tested the Lax and Wendroff and the Adapted Lax and Wendroff schemes. The last one also introduced by Gascón and Corberán. We show their poor resolution under some of the proposed tests. Afterward, we present TVD schemes and it is extended version. The Adapted TVD is the following scheme introduced, it is constructed with the idea of the inclusion of the source term in the flux vector. We have done a partial inclusion, only the terms with spatial derivatives. Finally we have developed a second version of Adapted TVD scheme (ATVD2) in which we have decoupled the phases, analising each system of equations separately when we solve the Riemann problem at the interface and in a second step we have composed both fluxes in order to get the variables that characterize each point in study. In certain form, this is the same idea we will apply in the application of AUSM schemes to two phase flow.

With respect to the AUSM schemes, we have studied two schemes, namely, AUSM+ and AUSMDV. Their first and second order implementations have been treated as well. They are based on a splitting of the flux vector in a convetive part and in a pressure part. The behaviour of each development has been analysed by means of the following benchmarks:

- Faucet test.
- Shock tube.
- Sedimentation.
- Oscilating manometer.
- Boiling tube (only for the homogeneous model).

We remark that some of them have not been able to solve all the problems with success.

This work has led us to conclude that both type of schemes, TVD and AUSM are able to model two phase problems in which phases are compressible and can compite with other recent models applied to two phase flow. In particular the AUSM type of schemes has demonstrated that presents some advantages regarding to

- Computation time, AUSM schemes have demostrated to be very low time consuming schemes due to we do not need evaluate the eigenstructure of the system at each intercell which makes them much more attractive.

- Good representation of discontinuities, we have shown the very good level of accuracy in the representation of shocks and contact discontinuities in the results herein.

Resum de la tesi

Esta tesi està dedicada al modelat de mescles bifàsic no estacionàries de líquid i vapor. Està motivada per la gran quantitat d'aplicacions industrials en les que podem trobar aquestos successos. Com el seu títol avança, alguns dels esquemes conservatius, recentment aplicats a problemes monofàsics han sigut estesos a fluix bifàsics. Amb este motiu, la tesi ha estat estructurada en cinc capítols com a comentem d'ací en davant.

En primer lloc comencem destacant l'importància del fluix bifàsic en l'indústria. Els transitoris en fluix bifàsic són un aspecte molt important en diferents aplicacions químiques, nuclears e industrials.

En el cas de l'indústria nuclear, l'estudi de transitoris en fluix bifàsic es fonamental, degut a l'importància que té previndre accidents amb perdua de refrigerant (LOCA), així com garantir un correcte funcionament del circuit de refrigerant.

D'esta forma introduïm alguns dels més importants codis desenvolupats en les dos ultimes dècades, entre d'ells, els clàssics, TRAC, RELAP i CATHARE o més recentment FLICA o TRIO-U en el camp nuclear o d'altres com OLGA, PLAC O TACITE en l'indústria del petroli. Molts d'ells han sigut desenvolupats per resoldre algunes de les dificultats que apareixen al tractar problemes involucrats amb fluix bifàsic.

Per a justificar els nostres desenvolupaments assenyalem que els primers codis utilitzen técniques de mallat "staggered" associades amb el principi de "donor cell", el qual produïx solucions estables en els casos en què proporcionem prou difusió. Allò ocorre quan considerem mallats grossers, ja que són molt difusius i afegixen suficient difusivitat numèrica per a suprimir possibles oscil·lacions. Este estat de l'art es completa esmentant els últims avanços en l'aplicació de diferents esquemes centrats i "upwind" per a resoldre problemes amb fluix multifàsic, molts d'ells basats en la solució exacta o més propera dels problemes de Riemann utilitzant mètodes "Flux Vector Splitting". No ens oblidem d'esmentar treballs pioners con els de Ramson i Toro, abans de tindre en compte les contribucions més rellevants en este camp, entre les que destaquem les "Aproximate Riemann Solvers" de Toumi, els esquemes de Fluix de Ghidaglia, els esquemes "Flux Vector Splitting" de Sung-Jae Lee, els treballs de Masella, Sainssaulien i Berger. I per descomptat els esquemes no conservatius de Tiselj i Petelin.

La nostra contribució està dirigida en l'extensió d'alguns esquemes explícits conservatius per obtindre solucions properes del sistema d'equacions en fluix bifàsic unidimensional. Aquestos són els esquemes TVD, TVD Adaptats i la família d'esquemes AUSM.

La finalitat del capítol 1 és introduir el sistema d'equacions de fluix bifàsic amb el que treballarem al llarg d'esta tesi. D'esta forma anirem des de les equacions instantànies al sistemes d'equacions doble mitjana en temps i àrea.

En el capítol 2 estudiem els diferents règims de fluix bifàsic i alguns de les relacions de tancament més importants que ens permetran tancar el sistema d'equacions. A diferència de què succeïx en l'exemple de fluix monofàsic, l'existència d'aquestos règims no permet conéixer la vertadera posició dels fluids cada instant. També descrivim breument alguns d'aquestos fenòmens com el de la transmissió de calor o fricció mitjançant les parets i de la interfase fent algunes de les consideracions sobre les equacions d'estat.

Sota diferents hipòtesis podem trobar diversos sistemes d'equacions els quals són descrits en el capítol 3. El model homogeni, el model isoentròpic i el model separat són tractats amb més detall. Uns altres models són considerats de forma més resumida. Després d'allò, comentem els sistemes d'equacions que consideren una sola presió, així com el problema que implica l'existència de valors propis complexos després de la diagonalització de la matriu jacobiana del sistema, el qual conduïx cap a solucions no físiques de sistema. Avancem que este problema l'evitem mitjançant l'ús de formes de correcció de presió, encara que termes com la massa virtual i altres de regularització poden ser considerats.

El capítol 4 analitza l'avaluació dels valores i vectors propis del fluix bifàsic homogeni i separat. A més a més s'analitzen alguns dels models més utilitzats per a determinar els valors propis. Un mètode general per a determinar de forma analítica els vectors propis es també estudiat. En la segona part del capítol ens centrem a revisar els esquemes desenvolupats i aplicats més recentment a fluix bifàsic.

En el capítol 5 estenem a fluix bifàsic diferents esquemes conservatius en els quals el seu comportament en fluix monofàsic ha sigut sense cap dubte provat. Aquestos són bàsicment els esquemes TVD, els ATVD desenvolupats per Gascón i Corberán i la família d'esquemes AUSM primerament introduïda per Steffen i Liou i després desenvolupada i millorada per Liou entre d'altres. El primer grup, els esquemes TVD, corresponen als esquemes del tipus "Flux Difference Splitting" (FDS) i els segons a la categoria "Flux Vector Splitting" (FVS). La majoria de les extensions desenvolupades en esta tesi es basen en incloure els termes no conservatius de l'equació de moment i energia en el terme font.

Per a demostrar el mal comportament dels esquemes centrats hem analitzat l'aplicació dels esquemes de Lax-Wendroff i Lax- Wendroff Adaptat, este últim introduït per Gascón i Corberán. Hem demostrat pobre resolució sota alguns dels tests proposats. Després presentem els esquemes TVD i una versió estesa dels mateixos, estudiant tant les versions de primer com de segon ordre. Al segon ordre de precisió s'arriba mitjançant l'utilització de l'estratègia MUSCL-Hancock i amb limitadors de pendents per limitar oscil·lacions. L'esquema ATVD es el següent esquema introduït i construït amb l'idea d'incloure el terme font en el vector de fluix. S'ha fet una inclusió parcial, només els termes amb derivades espacials. Finalment hem desenvolupat una segona versió de l'esquema ATVD, que hem esmentat ATVD2, en la que hem desacoblat les fases. En un primer moment cada sistema d'equacions s'analitza separadament quan resolem el

problema de Riemann en la interfase. En la segona etapa componem els dos fluixes amb la finalitat de determinar les variables que caracteritzen els punts en estudi. Així doncs es la mateixa idea que aplicarem en el desenvolupament dels esquemes AUSM.

En relació als esquemes AUSM, hem estudiat els dos esquemes, el AUSM+ i el AUSMDV. Estan basats en la descomposició del vector de fluixes en una part convectiva i una altra de presió. La seua implementació de primer i segon ordre són també tractades. Per aconseguir segon ordre hem provat diferents opcions utilitzant l'estratègia MUSCL seguit de limitadors de pendent per a restar el caràcter oscil·latori el segon ordre, diferents limitadors han sigut provats. Després de cada un dels desenvolupaments hem analitzat el seu comportament mitjançant els següent test tipus:

- Aixeta d'aigua (Water faucet).
- Tub de xoc (Shock tube).
- Sedimentació (Sedimentation).
- Manòmetre oscil·latori (Oscillating manometer).
- Tub d'ebullició (Boiling tube, only for the homogeneous model).

Tota la programació ha sigut realitzada en Fortran.

Este treball ens ha permés concloure que els dos esquemes, TVD i AUSM són capaços de modelar problemes de fluix bifàsic en els que les fases són compreses i que a més a més són capaços de competir en altres dels recents mètodes numèrics aplicats a fluix bifàsic.

En particular els esquemes AUSM han demostrat alguns avantatges com:

- Són computacionalment més eficients degut al fet que no es necessari realitzar diagonalització alguna en cadascuna interfase allò els fà molt atractius fins i tot quan canviem de sistema d'equacions o models per als fluids.
- Bona representació de discontinuïtats. Al llarg dels diferents tests estudiats mostrem el seu bon nivell d'exactitud en la representació de xocs i discontinuïtats de contacte. Este capítol es completa amb d'altres conclusions dels resultats numèrics obtinguts i futurs direccions a seguir.

Nomenclature

Subscripts:
ρ : derivative of a variable respect to the density.
c : related to the mass equation.
e : derivative of a variable respect to the internal energy.
e : related to the energy equation.
f : saturation state for the liquid.
g : saturation state for the vapour.
h : derivative of a variable respect to the enthalpy.
i : component i of a vector.
i : interface variable.
I : interface.
ij : component ij of a matrix.
$k = v, l$, v for the vapour phase and l for the liquid phase.
m : related to the momentum equation.
t : time derivative.
w : wall.
x : spatial derivative in x direction.
z : projection of a vector over the z axis.
z : spatial derivative in the z direction.

Variables and other parameters:
α : void fraction.
Γ : mass transfer through the interface.
ε : void fraction.
δ_{ij} : Kroeneker's delta.
θ : angle between a conduct and the horizontal plane.
λ : eigenvalue.
ν : eigenvalue.
π : 3.1416...
ψ : general variable to be balanced.
ϕ : volume source.
ϕ : source term.
φ : dissipative term.
ρ : density.
τ : shear tensor.
∂ : partial derivative.

A : cross section.
b : volume forces (frequently gravity).
c : speed of sound.

d : total derivative.
dt : differential of time.
dA : differential of surface.
dS : differential of surface.
dV : differential of volume.
e : internal energy.
e_i : unitary vector in the direction of axis i.
E : total energy ($e + \frac{u^2}{2}$).
F : flux vector.
g : gravity.
h : enthalpy.
h_i : interfacial heat transfer coefficients.
h_w : wall heat transfer coefficients.
H : total enthalpy ($h + \frac{u^2}{2}$).
J: general outward flux.
J : jacobian matrix.
$\dot{m}_k$: mass transfer from phase k to the other phase.
$\hat{n}_k$: outwards normal vector to the surface of phase k.
n : normal vector to a surface.
p : pressure.
q'' : surface heat flux.
q''' :volume heat source.
q_i : interfacial heat transfer.
S : source term vector.
$\vec{r}$: position vector.
s : entropy.
S_c : surface of the control volume.
S_I : surface of the interface.
t : time.
$\vec{t}$: stress in a determined direction.
$\bar{T}$: stress tensor.
$\vec{u}$: velocity of a point.
$\vec{u}_c$: velocity of the surface of the control volume S_c.
$\vec{U}$: velocity of a particle.
V : vector of primitive variables.
V_c : control volume.
W : vector of conserved variables.
z : axis coordinate.

Introduction

This work is devoted to the modelling of non steady two phase mixtures of liquid and vapour or gas. The great amount of industrial applications in which we find these phenomena has motivated the present thesis. Transient two phase flow is a very important issue in nuclear applications, heat exchangers industry, oil industry and other chemical and industrial applications. The interest has been greater in the nuclear industry due to the importance of preventing loss of coolant accidents (LOCA) and guaranteeing a good performance of the coolant system in power plants. Many codes have been developed during the last two decades, some of them are TRAC [**8**], RELAP [**60**] and CATHARE [**6**]. In the last decade, new codes have been or are being developed such as FLICA or TRIO-U for nuclear analysis and others like OLGA, PLAC or TACITE for the oil industry. Lots of them have been developed in order to overcome some of the difficulties that appear in dealing with two phase flow problems, mainly those due to the characterization of the geometry of the two phase mixture and the ill-posed system of equations that appears in these sort of problems. The first two phase flow codes utilized the ICE method, a staggered mesh technique associated with the donor cell principle. These codes produce stable solutions in cases where enough numerical damping is provided to the system. Their main problem is the introduction of too much diffusion in some problems, appearing oscillations with a large number of cells. As commented by Toumi in [**81**], this may be due to either the ill-posed character of the model or to the numerical scheme we are using.

Different Centred and Upwind Schemes are being utilized and applied to solve a great variety of multiphase flow problems, they are based on the exact or approximate solution of Riemann problems using Godunov's like methods such as Approximate Riemann Solvers or Flux Splitting methods. Pioneer works are [**56**] by Ramson and Hicks or [**75**] by Toro, for instance. Ramson applied a Lax and Wendroff two step scheme to the two fluids considering one and two pressure models, on the other hand Toro treated the equations of two phase reactive flow (gas and solid) in a very original form which identifies two hyperbolic homogeneous systems of equations and solves them in a decoupled way. More recently, other successful approaches have been made, it has been as much in the conservative field as in the non conservative. Among the most relevant contributions we can cite the VFFC (Volumes Finis à Flux Caractéristiques) scheme [**27**], Toumi's Approximate Riemann Solver [**77**], Städtke's Flux Vector Splitting Scheme [**64**], Masella's Godunov Method [**47**], Sainsaulieu's Models for two phase flow formed by liquid or solids and gas [**57**], the application of Godunov type schemes by Berger and Colombeau in [**7**], the non conservative models of Tiselj and Petelin in [**71**] or the one by Hwang [**37**] for example, the Sung-Jae Lee's Flux Vector Splitting scheme [**40**], etc.

Our contribution is centred in the extension of some conservative and explicit schemes to obtain approximate solutions of the system of equations in one dimensional, one pressure two phase flow, namely TVD schemes, Adapted TVD schemes (ATVD) and the AUSM family of schemes. In the following we summarize this work. In the first chapter the system of equations that governs two phase flow is introduced, we go from the instantaneous equations to the double area and time averaged system of equations, we will be concerned with 1D two phase flow.

In chapter 2 we study different two phase flow regimes and some important closure relationships which will allow us to close the system of equations. They include phenomena such as heat transfer and friction through the wall of the conduct and the interfaces, some consideration about the equations of state are also included. Unlike what happens with single fluid flow, the existence of such regimes do not permit to know the true position of the fluids at each instant. This is the main reason that obeys to average the system of equations.

Under distinct hypotheses we can find various systems of equations which will be studied in chapter 3. The homogeneous model, the isentropic model and the separated model will be treated in some detail. Others will be described briefly. As it is well known the system of equations is ill-posed in the sense that the jacobian matrix of the flux vector has complex eigenvalues that make the system produces non physical solutions. To avoid this behaviour we will use pressure correction terms, although virtual mass term and other regularizing terms could be used as well.

We have structured chapter 4 in two parts, firstly we analyse the evaluation of the eigenstructure of the homogeneous and the separated two phase flow. Different methods to determine the eigenvalues are presented, among them perturbation, Taylor series expansion and analytical methods. A general method to determine the eigenvectors is studied as well. In the second part of the chapter we focus on a review of the most recent schemes developed to solve two phase flow problems.

In chapter 5 we extend to our system different conservative schemes whose good behaviour in single phase has been well proved. They are basically the ATVD schemes developed by Gascón and Corberán in [**15**], [**24**] or [**25**] and the AUSM family of schemes, firstly introduced by Steffen and Liou in [**45**] and after developed in [**43**], [**49**] or [**44**]. The first one corresponds to the Flux Difference Splitting (FDS) category of schemes and the second one belongs to the Flux Vector Splitting (FVS) category. The description and extension of the AUSM schemes to two phase flow, namely, AUSM+ and AUSMDV and their first and second order implementations are also treated in this chapter. After some numerical results we close this work with some conclusions and future directions. In the final appendices we include a description of some interesting Mathematical tools and the numerical benchmark we have used to validate the schemes presented and extended to two phase flow.

Contents

List of Figures

Chapter 1

System of Equations in Two Phase Flow

1.1. Introduction

In single phase flow the behaviour of the fluid is characterized by a system of equations written in partial derivatives when the point in study does not belong to a surface of discontinuity. Unlike single phase, in the study of two phase flow some surfaces of discontinuity appear, they are called interfaces and separate the phases. Thus we have

- Conservation equations for each phase (p.d.e.).
- Interfacial equations or jump conditions.

Let us consider the control volume of figure 1.1, which is comprised of two phases, one liquid (l) and the other gas or vapour (g or v), then we have for each phase the following volumes

$$V_{cv}(t) = \sum_i V_{cv}^{(i)}(t); \qquad V_{cl}(t) = \sum_i V_{cl}^{(i)}(t)$$

where

$$V_c(t) = V_{cv}(t) + V_{cl}(t)$$

and

$$S_I(t) = \sum_i S_I^{(i)}(t).$$

If S_I is the interface surface and $S_{ck}(t)$ is the common surface between the surface of phase k and the boundary of the control volume, the portion of surface of the control

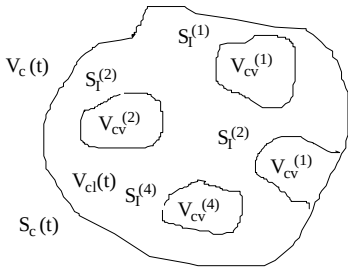

FIGURE 1.1. Control volume.

volume that is common to them will be given by

$$S_{ck}(t) - S_I(t),$$

and the boundary of the control volume

$$S_c(t) = \sum_{k=v,l} S_{ck}(t) - S_I(t).$$

1.2. Integral Form of the Conservation Equations

1.2.1. Equation for Mass Conservation

The equation for mass conservation for a control volume that has a velocity of $\overrightarrow{u}_c(t)$, different from the velocity of each fluid, is

$$\frac{d}{dt}\int_{V_c(t)} \rho_k dV = -\int_{S_c(t)} \rho_k(\vec{u} - \vec{u}_c)\cdot d\vec{S}. \tag{1.2.1}$$

As the control volume is moving with a different velocity then the mass flow rate through the control surface is done with $\vec{u} - \vec{u}_c$.

Applying equation 1.2.1 to each phase we have

$$\frac{d}{dt}\int_{V_{ck}(t)} \rho_k dV = -\int_{S_{ck}(t)} \rho_k(\vec{u}_k - \vec{u}_{ck})\cdot d\vec{S}_k. \tag{1.2.2}$$

If we decompose the surface of phase k in two, the common surface to the control surface and the common surface that corresponds to the interface we have

$$S_{ck}(t) = (S_{ck} - S_I) + S_I.$$

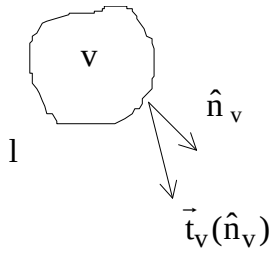

FIGURE 1.2. Surface stress.

If $\vec{u}_I$ is the velocity of the interface the mass equation for the phase k is

$$\frac{d}{dt}\int_{V_{ck}(t)} \rho_k dV = -\int_{S_{ck}-S_I} \rho_k(\vec{u}_k - \vec{u}_{ck})\cdot\hat{n}_k dS_k - \int_{S_I} \rho_k(\vec{u}_k - \vec{u}_I)\cdot\hat{n}_k dS_k. \tag{1.2.3}$$

By adding the mass equations for each phase, we recover equation 1.2.1.

$$\frac{d}{dt}\int_{V_{cl}(t)} \rho_l dV + \frac{d}{dt}\int_{Vcv(t)} \rho_v dV = -\int_{S_{cl}-S_I} \rho_l(\vec{u}_l - \vec{u}_{cl})\cdot\hat{n}_l dS_l$$
$$-\int_{S_{cv}-S_I} \rho_v(\vec{u}_v - \vec{u}_{cv})\hat{n}_v dS_v - \sum_{k=v,l}\int_{S_I} \rho_k(\vec{u}_k - \vec{u}_I)\cdot\hat{n}_k dS_k.$$

As $V_c = V_{cl}\cup V_{cv}$, $\rho(\vec{r},t) = \begin{cases} \rho_l \ if \ \vec{r}\in V_{cl} \\ \rho_v \ if \ \vec{r}\in V_{cv} \end{cases}$ and equation 1.2.1 is satisfied by the control volume we have the following jump condition for the mass equation

$$\sum_{k=g,l}\int_{S_I} \rho_k(\vec{u}_k - \vec{u}_I)\cdot\hat{n}_k dS_k = 0. \tag{1.2.4}$$

1.2.2. Equation for Momentum Conservation

The momentum equation applied to the control volume of figure 1.1 is

$$\frac{d}{dt}\int_{V_c(t)} \rho\vec{u} dV = \int_{V_c(t)} \rho\vec{g} dV + \int_{S_c(t)} \vec{t}(\hat{n}) dS - \int_{S_c(t)} \rho\vec{u}(\vec{u} - \vec{u}_c)\cdot d\vec{S} \tag{1.2.5}$$

where the stress in each direction is given by

$$\vec{t}(\hat{n}) = \hat{n}\cdot\bar{T}$$

with $\overline{T}$ the stress tensor.

If we apply equation 1.2.5 to each phase

$$\frac{d}{dt}\int_{V_{ck}(t)}\rho_k\vec{u}_k dV = \int_{V_{ck}(t)}\rho_k\vec{g}dV + \int_{S_{ck}(t)}\hat{n}_k\bar{T}_k dS - \int_{S_{ck}(t)}\rho_k\vec{u}_k(\vec{u}_k-\vec{u}_{c_k})\cdot d\vec{S}_k.$$

Taking into account that $S_{ck}(t) = (S_{ck} - S_I) + S_I$ we can write

$$\frac{d}{dt}\int_{V_{ck}(t)}\rho_k\vec{u}_k dV = \int_{V_{ck}(t)}\rho_k\vec{g}dV + \int_{S_{ck}(t)}\hat{n}_k\cdot\bar{T}_k dS -$$

$$\int_{S_{ck}(t)-S_I(t)}\rho_k\vec{u}_k\cdot(\vec{u}_k-\vec{u}_{ck})\cdot\hat{n}_k dS_k - \int_{S_I(t)}\rho_k\vec{u}_k\cdot(\vec{u}_k-\vec{u}_I)\cdot\hat{n}_k dS_k. \tag{1.2.6}$$

Summing the momentum equations for both phases we recover 1.2.5

$$\frac{d}{dt}\int_{V_{cl}(t)}\rho_l\vec{u}_l dV + \frac{d}{dt}\int_{V_{cv}(t)}\rho_v\vec{u}_v dV = \int_{V_{cl}(t)}\rho_l\vec{g}dV + \int_{V_{cv}(t)}\rho_v\vec{g}dV$$
$$+\int_{S_{cl}(t)-S_I(t)}\hat{n}_l\cdot\bar{T}_l dS_l + \int_{S_{cv}(t)-S_I(t)}\hat{n}_v\cdot\bar{T}_v dS_v - \sum_{k=v,l}\int_{S_{ck}(t)-S_I(t)}\rho_k\vec{u}_k\cdot(\vec{u}_k-\vec{u}_{ck})\cdot\hat{n}_k dS_k$$
$$+\int_{S_I(t)}\hat{n}_l\cdot\bar{T}_l dS_l + \int_{S_I(t)}\hat{n}_v\cdot\bar{T}_v dS_v - \sum_{k=v,l}\int_{S_I(t)}\rho_k\vec{u}_k\cdot(\vec{u}_k-\vec{u}_I)\cdot\hat{n}_k dS_k.$$

This leads us to the following jump conditions for the momentum equation

$$\int_{S_I(t)}\hat{n}_l\cdot\bar{T}_l dS_l + \int_{S_I(t)}\hat{n}_v\cdot\bar{T}_v dS_v - \sum_{k=v,l}\int_{S_I(t)}\rho_k\vec{u}_k\cdot(\vec{u}_k-\vec{u}_I)\cdot\hat{n}_k dS_k = 0. \tag{1.2.7}$$

1.2.3. Equation for Total Energy Conservation

If the specific total energy is defined by $E = e + \frac{u^2}{2}$ the total energy equation is given by

$$\frac{d}{dt}\int_{V_c(t)}\rho E dV = \int_{V_c(t)}\rho q''' dV - \int_{S_c(t)}\vec{q}''\cdot d\vec{S}$$
$$+\int_{V_c(t)}\rho\vec{g}\cdot\vec{u}dV + \int_{S_c(t)}\vec{t}(\hat{n})\cdot\vec{u}dS - \int_{S_c(t)}\rho E(\vec{u}-\vec{u}_c)\cdot d\vec{S}. \tag{1.2.8}$$

For each phase we have

$$\frac{d}{dt}\int_{V_{ck}(t)}\rho_k E_k dV = \int_{V_{ck}(t)}\rho_k q_k''' dV - \int_{S_{ck}(t)}\vec{q}_k''\cdot d\vec{S}_k + \int_{V_{ck}(t)}\rho_k\vec{g}\cdot\vec{u}_k dV$$
$$+\int_{S_{ck}(t)}\vec{t}_k(\hat{n}_k)\cdot\vec{u}_k dS_k - \int_{S_{ck}(t)}\rho_k E_k(\vec{u}_k-\vec{u}_{ck})\cdot d\vec{S}_k. \tag{1.2.9}$$

Summing both conservation laws, we have

$$\frac{d}{dt}\int_{V_{cv}(t)}\rho_v E_v dV+\frac{d}{dt}\int_{V_{cl}(t)}\rho_l E_l dV=\sum_{k=v,l}[\int_{V_{ck}(t)}\rho_k q_k'''dV+\int_{V_{ck}(t)}\rho_k\vec{g}\cdot\vec{u}_k dV]+$$

$$\sum_{k=v,l}[-\int_{S_{ck}(t)-S_I(t)}\vec{q}_k''\cdot d\vec{S}_k+\int_{S_{ck}(t)-S_I(t)}\vec{t}_k(\hat{n}_k)\cdot\vec{u}_k dS_k-\int_{S_{ck}(t)-S_I(t)}\rho_k E_k(\vec{u}_k-\vec{u}_{ck})\cdot d\vec{S}_k]$$

$$+\sum_{k=v,l}[-\int_{S_I(t)}\vec{q}_k''\cdot d\vec{S}_k+\int_{S_I(t)}\vec{t}_k(\hat{n}_k)\cdot\vec{u}_k dS_k-\int_{S_I(t)}\rho_k E_k(\vec{u}_k-\vec{u}_I)\cdot d\vec{S}_k]$$

and as we have done for the other two conservation equations, the energy equation for the mixture (eq. 1.2.8), gives us the following jump condition

$$\sum_{k=v,l}[-\int_{S_I}\vec{q}_k''\cdot\hat{n}dS_k+\int_{S_I}\hat{n}\cdot\overline{T}\cdot\vec{u}_k dS_k-\int_{S_I}\rho_k E_k\dot{m}_k dS_k]=0 \tag{1.2.10}$$

where $\dot{m}_k=\rho_k(\vec{u}_k-\vec{u}_I)\cdot\hat{n}_k$ for $k=v,l$, it is the mass transfer from one phase to another through the interface by unit of surface.

1.3. Differential Form for Conservation Equations

1.3.1. Equation for Mass Conservation

Applying the Leibniz theorem in 1.2.3 we have

$$\int_{V_{ck}(t)}\frac{\partial\rho_k}{\partial t}dV+\int_{S_{ck}}\rho_k\vec{u}_{ck}\cdot\hat{n}_k dS_k=-\int_{S_{ck}}\rho_k(\vec{u}_k-\vec{u}_{ck})\cdot\hat{n}_k dS_k.$$

Using the Gauss theorem

$$\int_{V_{ck}(t)}(\frac{\partial\rho_k}{\partial t}+\vec{\nabla}\cdot(\rho_k\vec{u}_k))dV=0\quad\text{for }\vec{r}\in\text{ phase }k.$$

Owing to the arbitrary character of $V_{ck}(t)$ the differential form of the mass equation is

$$\frac{\partial\rho_k}{\partial t}+\vec{\nabla}(\rho_k\vec{u}_k)=0\quad\text{for }\vec{r}\in\text{ interface }S_I$$

and the jump condition is

$$\rho_l(\vec{u}_l-\vec{u}_I)\hat{n}_l+\rho_v(\vec{u}_v-\vec{u}_I)\hat{n}_v=0$$

or using the notation defined above

$$\dot{m}_l+\dot{m}_v=0.$$

1.3.2. Equation for Momentum Conservation

Applying the Leibniz and the Gauss theorems in equation 1.2.6 we have for each phase

$$\int_{V_{ck}(t)} \frac{\partial \rho_k \vec{u}}{\partial t}_k dV + \int_{S_{ck}(t)} \rho_k \vec{u}_k \vec{u}_{ck} d\vec{S}_k = \int_{V_{ck}(t)} \rho_k \vec{g} dV + \int_{V_{ck}(t)} \vec{\nabla} \cdot \bar{T}_k dV - \int_{S_{ck}(t)} \rho_k \vec{u}_k \vec{u}_k d\vec{S}_k + \int_{S_{ck}(t)} \rho_k \vec{u}_k \vec{u}_{ck} d\vec{S}_k.$$

Due to the arbitrary character of $V_{ck}(t)$ the differential form of the momentum equation is

$$\frac{\partial \rho_k \vec{u}_k}{\partial t} + \vec{\nabla} \cdot (\rho_k \vec{u}_k \vec{u}_k) = \rho_k \vec{g} + \vec{\nabla} \cdot \bar{T}_k \tag{1.3.1}$$

where $\vec{u}_k \vec{u}_k = \vec{u}_k \otimes \vec{u}_k$ (diadic product).

The jump condition in this case is

$$\hat{n}_l \cdot \bar{T}_l + \hat{n}_v \cdot \bar{T}_v - \sum_{k=v,l} \rho_k \vec{u}_k (\vec{u}_k - \vec{u}_{_I}) \cdot \vec{n}_k = 0.$$

By using the definition of $\dot{m}_k$, the jump condition is:

$$\hat{n}_l \cdot \bar{T}_l + \hat{n}_v \cdot \bar{T}_v - \sum_{k=v,l} \dot{m}_k \vec{u}_k = 0.$$

1.3.3. Equation for Total Energy Conservation

Applying the Leibniz theorem to equations. 1.2.9 we have for each phase

$$\int_{V_{ck}(t)} \frac{\partial}{\partial t}(\rho_k E_k) dV + \int_{S_{ck}(t)} \rho_k E_k \vec{u}_{ck} \cdot d\vec{S}_k = \int_{V_{ck}(t)} \rho_k q_k''' dV - \int_{S_{ck}(t)} \vec{q}_k'' \cdot d\vec{S}_k + \int_{V_{ck}(t)} \rho_k \vec{g} \cdot \vec{u}_k dV + \int_{S_{ck}(t)} \vec{t}_k(\hat{n}_k) \cdot \vec{u}_k dS_k - \int_{S_{ck}(t)} \rho_k E_k (\vec{u}_k - \vec{u}_{ck}) \cdot d\vec{S}_k.$$

Simplifying and applying Gauss theorem we have

$$\frac{\partial}{\partial t}(\rho_k E_k) + \vec{\nabla} \cdot (\rho_k E_k \vec{u}_{ck}) = \rho_k q_k''' - \vec{\nabla} \cdot \vec{q}_k'' + \rho_k \vec{g} \cdot \vec{u}_k dV + \vec{\nabla} \cdot \overline{T} \cdot \vec{u}_k$$

or grouping

$$\frac{\partial}{\partial t}(\rho_k E_k) + \vec{\nabla} \cdot (\rho_k E_k \vec{u}_{ck} + \vec{q}_k'' - \overline{T} \cdot \vec{u}_k) = \rho_k q_k''' + \rho_k \vec{g} \cdot \vec{u}_k.$$

This equation can be expressed as a function of the total enthalpy defined as

$$H_k = E_k + \frac{p}{\rho_k} = h_k + \frac{u_k^2}{2}$$

and the term that involves the stress tensor

$$\vec{\nabla}\overline{T}_k \cdot \vec{u}_k = -\vec{\nabla} \cdot (p\vec{u}_k) + \vec{\nabla} \cdot \overline{\tau}_k \cdot \vec{u}_k$$

we have

$$\frac{\partial}{\partial t}(\rho_k E_k) + \vec{\nabla} \cdot (\rho_k H_k \vec{u}_k + \vec{q}_k^{''} - \overline{\tau} \cdot \vec{u}_k) = \rho_k q_k^{'''} + \rho_k \vec{g} \cdot \vec{u}_k,$$

and therefore the jump condition for the energy equation is

$$\sum_{k=v,l} [-\vec{q}_k^{''} \cdot \vec{n}_k + \hat{n}_k \cdot \overline{\tau}_k \cdot \vec{u}_k - \rho_k E_k \dot{m}_k] = 0$$

with $\overline{\tau}_k$ the viscosity shear stress tensor of phase k.

1.4. General Form of the Conservation Equations

We can write the integral conservation equations of the mixture in general form as

$$\frac{d}{dt}\int_{V_c(t)} \rho\psi dV = \int_{V_c(t)} \phi dV - \int_{S_c(t)} \vec{J} \cdot \hat{n} dS - \int_{S_c(t)} \rho\psi(\vec{u} - \vec{u}_c) \cdot \hat{n} dS.$$

For the phase k

$$\frac{d}{dt}\int_{V_{ck}(t)} \rho_k\psi_k dV = \int_{V_{ck}(t)} \phi_k dV - \int_{S_{ck}(t)} \vec{J}_k \cdot \hat{n} dS_k - \int_{S_{ck}(t)} \rho_k\psi_k(\vec{u}_k - \vec{u}_{ck}) \cdot \hat{n} dS_k.$$

With the jump condition

$$\sum_{k=v,l} [\int_{S_I} \vec{J}_k \cdot \hat{n}_k dS_k + \int_{S_I} \rho_k\psi_k(\vec{u}_k - \vec{u}_I) \cdot \hat{n}_k dS_k] = 0.$$

In these equations the variables ψ_k, $\vec{J}_k$ and ϕ_k depend on the conservation equation considered and represent

- ψ_k : Magnitude to be balanced.
- $\vec{J}$: Non convective flux term, it is defined such that $\vec{J} \cdot \vec{n} dS$ is the rate of a magnitud that flows through a surface element dS of the control surface $S_c(t)$ in the direction of $\vec{n}$.
- ϕ : Volume sources of the considered property.

Thus, the general conservation equations in differential form for the phase k are

$$\frac{\partial}{\partial t}\rho_k\psi_k + \vec{\nabla} \cdot (\rho_k\psi_k\vec{u}_k + \vec{J}_k) = \phi_k \qquad k = l, v \tag{1.4.1}$$

Conservation Equation	ψ_k	$\vec{J}_k$	ϕ_k
Mass	1	0	0
Momentum	$\vec{u}_k$	$-\overline{T}_k$	$\vec{g}$
Energy	E_k	$-\overline{T}\cdot\vec{u}_k+\vec{q}_k^{\,\prime\prime}$	$\vec{g}\cdot\vec{u}_k+\frac{q_k^{\prime\prime\prime}}{\rho_k}$

TABLE 1. Values of ψ_k, J_k and ϕ_k.

with the jump conditions given by

$$\sum_{k=v,l}\left[\vec{J}_k\cdot\vec{n}_k+\rho_k\psi_k(\vec{u}_k-\vec{u}_I)\cdot\vec{n}_k\right]=0 \qquad \forall\vec{r}\in S_I. \tag{1.4.2}$$

This set of conservation laws are locals and instantaneous. They cannot be applied directly as they cannot be integrated, this is due to the fact that we cannot know the form of the interface every instant. To solve this problem, the thermohydraulic models used to characterize two phase flows by means of averaged equations. We can make different averaging procedures:

- Space average
  - Instantaneous Area Averaged Equations,
  - Instantaneous Volume Averaged Equations
- Local time average and Double time average
- Space/Time and Time/Space average and
- Statistical Average

A detailed description of the averaging operators can be found in [**20**]. In the following we are going to describe briefly the space/time (equivalently time/averaged) equations. Their interest resides in that almost all the practical two phase flow problems are dealt with using these equations. Other good descriptions of derivation of the equations can be found in [**32**] or [**38**].

1.5. Instantaneous Area-Averaged Equations

We are going to average the instantaneous equations over the cross section of a duct with impermeable walls and variable cross section, for this purpose, let us consider the cross section of figure 1.3 and let us integrate over the area $A_k(z,t)$ which is limited by the boundaries $C(z,t)$ with the other phase and $C_k(z,t)$ with the pipe wall, so

$$\int_{A_k(z,t)}\frac{\partial}{\partial t}A_k\rho_k\psi_k dA+\int_{A_k(z,t)}\vec{\nabla}\cdot(\rho_k\psi_k\vec{U}_k)dA+\int_{A_k(z,t)}\vec{\nabla}\cdot\vec{J}_k dA-\int_{A_k(z,t)}\rho_k\phi_k dA=0.$$

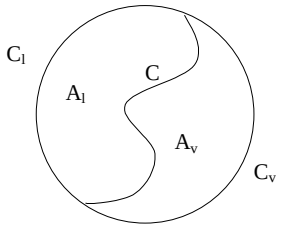

FIGURE 1.3. Cross section of a duct.

Applying the limiting forms of the Leibniz and the Gauss theorems (see [**20**] for details) we have

$$\frac{\partial}{\partial t}A_k < \rho_k\psi_k >_2 + \frac{\partial}{\partial z}(A_k < \hat{n}_z \cdot (\rho_k\psi_k\vec{U}_k) >_2) + \frac{\partial}{\partial z}A_k < \hat{n}_z \cdot \vec{J}_k >_2 - A_k < \rho_k\phi_k >_2$$
$$= -\int_{C(z,t)} (\dot{m}_k\dot{\psi}_k + \hat{n}_k \cdot \vec{J}_k)\frac{dC}{\hat{n}_k \cdot \hat{n}_{kC}} - \int_{C_k(z,t)} \hat{n}_k \cdot \vec{J}_k \frac{dC}{\hat{n}_k \cdot \hat{n}_{kC}}$$

where

$$< f_k >_2 = \frac{1}{A_k}\int_{A_k(z,t)} f_k(x,y,z,t)dA$$
$$\dot{m}_k = \rho_k(\vec{U}_k - \vec{U}_I) \cdot \hat{n}_k.$$

Considering the expressions of ψ_k, J_k and ϕ_k collected in table 1 we have the following conservation equations for each phase.

Mass equation

$$\frac{\partial}{\partial t}A_k < \rho_k >_2 + \frac{\partial}{\partial z}A_k < \rho_k U_{kz} >_2 = -\int_{C(z,t)} \dot{m}_k \frac{dC}{\hat{n}_k \cdot \hat{n}_{kC}}.$$

Momentum equation

The momentum equation after projecting along the conduct axis is:

$$\frac{\partial}{\partial t}A_k < \rho_k U_k >_2 + \frac{\partial}{\partial z}A_k < \rho_k U_{kz}^2 > - A_k < \rho_k b_{kz} >_2 + \frac{\partial}{\partial z}A_k < p_k >_2$$
$$- \frac{\partial}{\partial z}A_k < (\hat{n}_z \cdot \bar{\tau}_k) \cdot \hat{n}_z >_2 = - \int_{C(z,t)} \hat{n}_z \cdot (\dot{m} U_k - \hat{n}_k \cdot \bar{\tau}_k) \frac{dC}{\hat{n}_k \cdot \hat{n}_{kC}} +$$
$$\int_{C_k(z,t)} \hat{n}_z \cdot (\hat{n}_k \cdot \bar{\tau}_k) \frac{dC}{\bar{n}_k \cdot \bar{n}_{kC}}.$$

Energy equation

$$\frac{\partial}{\partial t} < \rho_k (\frac{1}{2}\vec{U}_k^2 + e_k) >_2 + \frac{\partial}{\partial z}A_k < \rho_k (\frac{1}{2}U_k^2 + h_k) U_k >_2 - A_k < \rho_k \vec{b}_k \cdot \vec{U}_k >_2 -$$
$$\frac{\partial}{\partial z}A_k (\bar{\tau} \cdot \vec{U}_k) \cdot \hat{n}_k + \frac{\partial}{\partial z}A_k < \vec{q}_k \cdot \hat{n}_k >_2 =$$
$$- \int_{C(z,t)} [\dot{m}_k (\frac{1}{2}U_k^2 + u_k) - (\bar{T} \cdot \vec{U}_k) \cdot \hat{n}_k + \vec{q}_k] \frac{dC}{\hat{n}_k \cdot \hat{n}_{kC}} + \int_{C_k(z,t)} \vec{q}_k \cdot \hat{n}_k \frac{dC}{\hat{n}_k \cdot \hat{n}_{kC}}.$$

where $\vec{q}_k$ is the heat through the surface of phase k. We remark that in the previous equation volume sources of heat have not been considered.

1.6. Double Area-Time Averaged Equations

Once we have determined the instantaneous area averaged equations, we have to time-average them to get the double averaged system (space and time) which will be used in our modelling process. After such a process we arrive to the following general form of the conservation laws

$$\frac{\partial}{\partial t}\overline{A_k < \rho_k \psi_k >_2} + \frac{\partial}{\partial z}\overline{A_k < \hat{n}_z \cdot (\rho_k \psi_k \vec{U}_k) >_2} + \frac{\partial}{\partial z}\overline{A_k < \hat{n}_z \cdot \vec{J}_k >_2}$$

(1.6.1)

$$-\overline{A_k < \rho_k \psi_k >_2} = -\overline{\int_{C(z,t)} (\dot{m}_k \psi_k + \hat{n}_k \cdot \vec{J}_k) \frac{dC}{\hat{n}_k \cdot \hat{n}_{kC}}} - \overline{\int_{C_k(z,t)} \hat{n} \cdot \vec{J}_k \frac{dC}{\hat{n}_k \cdot \hat{n}_{kC}}}.$$

By using the definitions fo ψ_k, J_k and ϕ_k of table 1 we can obtain a more practical set of equations. It will be written in terms of dependent variables such as α_k (with $\alpha_l + \alpha_v = 1$), ρ_k, p_k, $\vec{u}_k$ and h_k (sometimes is prefered e_k). Using the notation of [**32**] we have the following one dimensional conservation equations.

Mass equation

$$\frac{\partial}{\partial t}(A\alpha_k\rho_k) + \frac{\partial}{\partial z}(A\alpha_k\rho_k u_k) = (A\Gamma)_{kI}$$

where

$$(A\Gamma)_{kI} = \lim_{\Delta z\to 0}[-\frac{1}{\Delta z}\overline{\int_{A_I}\rho_k(\vec{U}_k - \vec{U}_I)\cdot\hat{n}_k dA}].$$

For the balance of mass, the jump condition results

$$\sum_k (A\Gamma)_{kI} = 0.$$

Momentum equation

$$\frac{\partial}{\partial t}(A\alpha_k\rho_k u_k) + \frac{\partial}{\partial z}(A\alpha_k\rho_k u_k^2) + \frac{\partial}{\partial z}(A\alpha_k p_k) - \frac{\partial}{\partial z}(A\alpha_k\tau_k\cdot\hat{n}_z)\hat{n}_z = A\alpha_k\rho_k\vec{b}\cdot\hat{n}_z$$
$$+A(FF)_{kI} + A(FP)_{kI} + A(FF)_{kW} + A(FP)_{kW} + A(\Gamma U)_{kI}.$$

where
$A(\Gamma U)_{kI} = \lim_{\Delta z\to 0}(-\frac{1}{\Delta z}\int_{A_I}\rho_k(\vec{U}_k - \vec{U}_I)\cdot\hat{n}_k\vec{U}_k dA)\cdot\hat{n}_z$,
$A(FP)_{kI} = \lim_{\Delta z\to 0}(-\frac{1}{\Delta z}\int_{A_I} p_k\hat{n}_k dA)\cdot\hat{n}_z$,
$A(FP)_{kW} = \lim_{\Delta z\to 0}(-\frac{1}{\Delta z}\int_{A_I} p_k\hat{n}_k dA)\cdot\hat{n}_z$.

For the momentum equation the jump conditions are

$$\sum_k [A(FF)_{kI} + A(FP)_{kI} + A(\Gamma U)_{kI}] - A(I\sigma)_I = 0$$

with
$A(I\sigma)_I = \lim_{\Delta z\to 0}(\frac{1}{\Delta z}\overline{\int_{A_I}[\vec{\nabla}_s\sigma - \sigma(\vec{\nabla}_s\cdot\hat{n}_v)\hat{n}_v]dA})$.

Energy equation

After using the Leibniz and Gauss theorems we have that the energy equation is

$$\frac{\partial}{\partial t}(A\alpha_k\rho_k(h_k + \frac{1}{2}u_k^2)) + \frac{\partial}{\partial z}(A\alpha_k\rho_k u_k(h_k + \frac{1}{2}u_k^2 - \frac{\partial}{\partial t}(A\alpha_k p_k) -$$
$$\frac{\partial}{\partial z}(A\alpha_k(\bar{\tau}_k\cdot\hat{n}_z)\cdot\vec{U}_k) + \frac{\partial}{\partial z}(A\alpha_k\vec{q}_k\cdot\hat{n}_z) = A\alpha_k\rho_k(\vec{U}_k\cdot\vec{b})\cdot\hat{n}_z + A(\Gamma H)_{kI} +$$
$$A(\Gamma C)_{kI} + A(EF)_{kI} + A(EP)_{kI} + A(EQ)_{kI}$$
$$+A(EF)_{kW} + A(EP)_{kW} + A(EQ)_{kW}$$

where

$A(\Gamma H)_{kI} = \lim_{\Delta z \to 0} \left[-\frac{1}{\Delta z} \int_{A_I} (\rho_k (\vec{U}_k - \vec{U}_I) \cdot \hat{n}_k) h_k dA \right]$,
$A(\Gamma C)_{kI} = \lim_{\Delta z \to 0} \left[-\frac{1}{\Delta z} \int_{A_I} \frac{1}{2} (\rho_k (\vec{U}_k - \vec{U}_I) \cdot \hat{n}_k) \vec{U}_k^2 dA \right]$
and the pressure terms
$A(EP)_{kI} + A(EP)_{kW} = \lim_{\Delta z \to 0} \left[-\frac{1}{\Delta z} \int_{A_I} p_k \vec{U}_I \cdot \hat{n}_k dA \right]$
$+ \lim_{\Delta z \to 0} \left[-\frac{1}{\Delta z} \int_{A_W} p_k \vec{U}_I \cdot \hat{n}_k dA \right]$.
We remark that $A(EP)_{kW} = 0$ if we consider $U_W = 0$, which is usual.
The other terms are friction and heat transfer terms.

We conclude with the jump condition for the energy equation

$$\sum_k [A(\Gamma H)_{kI} + A(\Gamma C)_{kI} + A(EF)_{kI} + A(EP)_{kI} + A(EQ)_{kI}] - A(E\sigma)_I = 0$$

with $A(E\sigma)_I = \lim_{\Delta z \to 0} \left[\frac{1}{\Delta z} \overline{\int_{A_I} \vec{\nabla}_s \cdot (\sigma \vec{U}^t) dA} \right]$.

1.7. System of Equations used by the TRAC-BF1/MOD1 Code

This is a code for analysing thermal-hydraulic transients in boiling water reactors, it allows to study one and three dimensional two phase flow by solving the set of equations describing the behaviour of the fluids, the flow of energy in the fuel and the structural reactor core. The three dimensional conservation equations for a two-fluid mixture which is flowing in a duct of constant cross section are the following

Equations for mass conservation

Vapour phase

$$\frac{\partial (\alpha \rho_v)}{\partial t} + \vec{\nabla} \cdot (\alpha \rho_v \vec{u}_v) = \Gamma.$$

Liquid phase

$$\frac{\partial ((1-\alpha) \rho_l)}{\partial t} + \vec{\nabla} \cdot [(1-\alpha) \rho_l \vec{u}_l] = -\Gamma.$$

Mixture

$$\frac{\partial ((1-\alpha) \rho_l + \alpha \rho_v)}{\partial t} + \vec{\nabla} \cdot [(1-\alpha) \rho_l \vec{u}_l + \alpha \rho_v \vec{u}_v] = 0.$$

Equations for momentum conservation

Vapour phase

$$\frac{\partial \vec{u}_v}{\partial t} + \vec{u}_v \cdot \vec{\nabla}\vec{u}_v + k_{vm}\frac{\rho_c}{\alpha\rho_v}\frac{\partial}{\partial t}(\vec{u}_l - \vec{u}_v) =$$
$$-\frac{1}{\rho_v}\vec{\nabla}p - \frac{C_i}{\alpha\rho_v}(\vec{u}_v - \vec{u}_l)\,|\vec{u}_v - \vec{u}_l| - \frac{C_{wv}}{\alpha\rho_v}\vec{u}_v\,|\vec{u}_v| +$$
$$\vec{g} - k_{vm}\frac{\rho_c}{\alpha\rho_v}\vec{u}_D\vec{\nabla}(\vec{u}_v - \vec{u}_l) + \frac{\vec{\nabla}p_s}{\alpha\rho_v}.$$

Liquid phase

$$\frac{\partial \vec{u}_l}{\partial t} + \vec{u}_l \cdot \vec{\nabla}\vec{u}_l + k_{vm}\frac{\rho_c}{(1-\alpha)\rho_l}\frac{\partial}{\partial t}(\vec{u}_l - \vec{u}_v) =$$
$$-\frac{1}{\rho_l}\vec{\nabla}p + \frac{C_i}{(1-\alpha)\rho_l}(\vec{u}_v - \vec{u}_l)\,|\vec{u}_v - \vec{u}_l| - \frac{C_{wl}}{(1-\alpha)\rho_l}\vec{u}_l\,|\vec{u}_l| +$$
$$\vec{g} - k_{vm}\frac{\rho_c}{(1-\alpha)\rho_l}\vec{u}_D\vec{\nabla}(\vec{u}_l - \vec{u}_v) + \frac{\vec{\nabla}p_s}{(1-\alpha)\rho_l}.$$

Equations for internal energy conservation

Vapour phase

$$\frac{\partial(\alpha\rho_v e_v)}{\partial t} + \vec{\nabla}\cdot(\alpha\rho_v e_v \vec{u}_v) =$$
$$-p\frac{\partial\alpha}{\partial t} - p\vec{\nabla}\cdot(\alpha\vec{u}_v) + q_{wv} + q_{dv} + q_{iv} + \Gamma h'_v.$$

Liquid phase

$$\frac{\partial[(1-\alpha)\rho_l e_l]}{\partial t} + \vec{\nabla}\cdot[(1-\alpha)\rho_l e_l \vec{u}_l] =$$
$$-p\frac{\partial(1-\alpha)}{\partial t} - p\vec{\nabla}\cdot[(1-\alpha)\vec{u}_l] + q_{wl} + q_{dl} + q_{il} - \Gamma h'_l.$$

Mixture

$$\frac{\partial[(1-\alpha)\rho_l e_l + \alpha\rho_v e_v]}{\partial t} + \vec{\nabla}\cdot[(1-\alpha)\rho_l e_l\vec{u}_l + \alpha\rho_v e_v\vec{u}_v] =$$
$$-p\vec{\nabla}\cdot[(1-\alpha)\vec{u}_l + \alpha\vec{u}_v] + q_{wl} + q_{wv} + q_{dl} + q_{dv}.$$

Where

C_i : interfacial drag coefficient.

C_{wl} : wall drag coefficient.

k_{vm} : virtual mass coefficient. Although the addition of the magnitude of this variable does not affect the solution very much it is included in order to add dumping to the solution procedure.

ρ_c : density of continuous phase.

The product of these variables is given by

$$k_{vm}\rho_c = \begin{cases} 0.5\alpha \left(\frac{1+2\alpha}{1-\alpha}\right) \rho_l & 0 < \alpha < \alpha_{tr} \\ 0.5(1-\alpha) \left(\frac{3-2\alpha}{\alpha}\right) \rho_v + (\rho_l^{vm} - \rho_v^{vm}) \left(\frac{1-\alpha}{1-\alpha_t r}\right)^3 & 1 > \alpha > \alpha_{tr} \end{cases}$$

where ρ_l^{vm} and ρ_v^{vm} are function of α_{tr}, the transition void fraction from bubbly/churn to annular flow.

$\vec{u}_D$: velocity of dispersed phase.

$\vec{\nabla} p_s$: pressure force per unit volume due to void gradient between adjacent cells in horizontal direction. It takes into account the force resulting from the difference in the hydrostatic heads in adjacent computational cells.

q_{dl} and q_{dv} : volumetric sources of heat.

Mass equations are written in fully conservative form to permit the conservation of mass. A partially conservative form of the energy equations make numerical solution simpler than it would be if the fully conservative form were used. The same occurs with the momentum equations although it is necessary a fully conservative form when we have sharp changes of the void fraction. TRAC-BF1/MOD1 uses a staggered-mesh scheme in which the velocities are defined at the mesh-cell surfaces as opposed to the volume properties which are defined at the mesh-cell center. Additional information on the numerical models and correlations used in TRAC can be found in [**8**].

1.8. System of Equations used by the RELAP Code

The RELAP code is a tool for estimating transient simulations of light water reactor coolant systems with large and small break loss of coolant accidents and other operational transients. The space-time balance equations used by RELAP are mass, momentum and energy for vapour and liquid, it only allows the study of one dimensional problems.

Equation for mass conservation

Vapour phase

$$\frac{\partial}{\partial t}(\alpha\rho_v) + \frac{1}{A}\frac{\partial}{\partial z}(\alpha A \rho_v u_v) = \Gamma_v.$$

Liquid phase

$$\frac{\partial}{\partial t}((1-\alpha)\rho_l) + \frac{1}{A}\frac{\partial}{\partial z}((1-\alpha)A\rho_l u_l) = -\Gamma_v.$$

Equation for momentum conservation

Vapour phase

$$\alpha\rho_v\frac{\partial}{\partial t}u_v + \frac{1}{2}\alpha\rho_v\frac{\partial}{\partial z}u_v^2 = -\alpha\frac{\partial}{\partial z}p + \alpha\rho_v g\cos\theta - \frac{1}{2}\alpha\rho_v\frac{f_{vw}}{D}u_v\left|u_v\right|$$
$$+\Gamma_v(u_{vi}-u_v) - \frac{C_D}{8}\rho_c a_{vl}\left|u_r\right|u_r - C_{vm}\alpha(1-\alpha)\rho_m\frac{\partial}{\partial t}u_r.$$

Liquid phase

$$(1-\alpha)\rho_l\frac{\partial}{\partial t}u_l + \frac{1}{2}(1-\alpha)\rho_l\frac{\partial}{\partial z}u_l^2 = -(1-\alpha)\frac{\partial}{\partial z}p + (1-\alpha)\rho_l g\cos\theta$$
$$-\frac{1}{2}(1-\alpha)\rho_l\frac{f_{lw}}{D}u_l\left|u_l\right| - \Gamma_v(u_{li}-u_l) + \frac{C_D}{8}\rho_c a_{vf}\left|u_r\right|u_r + C_{vm}\alpha(1-\alpha)\rho_m\frac{\partial}{\partial t}u_r.$$

Equations for energy conservation

Vapour phase

$$\frac{\partial}{\partial t}(\alpha\rho_v e_v) + \frac{1}{A}\frac{\partial}{\partial z}(\alpha A\rho_v e_v u_v) =$$
$$-p\frac{\partial\alpha}{\partial t} - \frac{p}{A}\frac{\partial}{\partial z}(\alpha A u_v) + q_{wv} + q_{iv} + \Gamma h_v' + \frac{1}{2}\alpha\rho_v\frac{f_{vw}}{D}u_v^2\left|u_v\right|.$$

Liquid phase

$$\frac{\partial}{\partial t}((1-\alpha)\rho_l e_l) + \frac{1}{A}\frac{\partial}{\partial z}((1-\alpha)\rho_l e_l u_l] =$$
$$-p\frac{\partial(1-\alpha)}{\partial t} - \frac{p}{A}\frac{\partial}{\partial z}((1-\alpha)u_l] + q_{wl} + q_{il} - \Gamma h_l' + \frac{1}{2}(1-\alpha)\rho_l\frac{f_{lw}}{D}u_l^2\left|u_l\right|.$$

Where
a_{vl} : interface surface area.
C_D : coefficients of interface friction.
C_{vm} : virtual mass coefficient.
f_{kw} : wall drag coefficient of phase k.
ρ_m : density of mixture.
u_r : relative velocity $(u_v - u_l)$.

The physical models, the numerical methods it uses and the modelling process are documented in the RELAP manuals, see [**60**] for a review of the numerical techniques.

1.9. System of Equations used by the CATHARE Code

CATHARE is another code designed for safety research and development studies in nuclear industry. Despite the previous codes, it has been developed for the simulation of pressure water reactors loss of coolant accidents. Here we have included the one dimensional system of equations the code solves.

Equation for mass conservation

Vapour phase

$$A\frac{\partial}{\partial t}(\alpha\rho_v) + \frac{\partial}{\partial z}(\alpha A\rho_v u_v) = A\Gamma.$$

Liquid phase

$$A\frac{\partial}{\partial t}((1-\alpha)\rho_l) + \frac{\partial}{\partial z}((1-\alpha)A\rho_l u_l) = -A\Gamma.$$

Equation for momentum conservation

Vapour phase

$$A\alpha\rho_v\frac{\partial}{\partial t}u_v + A\alpha\rho_v u_v\frac{\partial}{\partial z}u_v = -A\alpha\frac{\partial}{\partial z}p - Ap_i\frac{\partial\alpha}{\partial z} + \alpha\rho_v g_z - M_A$$
$$-A\tau_i - \chi_f\tau_{pv} + A\Gamma(u_i - u_v) + \frac{R(1-\alpha)}{4}p_i\frac{\partial A}{\partial z}.$$

Liquid phase

$$A(1-\alpha)\rho_l\frac{\partial}{\partial t}u_l + A(1-\alpha)\rho_l u_l\frac{\partial}{\partial z}u_l = -A(1-\alpha)\frac{\partial}{\partial z}p + Ap_i\frac{\partial\alpha}{\partial z} + (1-\alpha)\rho_l g_z + M_A$$
$$+A\tau_i - \chi_f\tau_{pl} + A\Gamma(u_i - u_l) + \frac{R\alpha}{4}p_i\frac{\partial A}{\partial z}.$$

Equation for energy conservation

Vapour phase

$$A\frac{\partial}{\partial t}(\alpha\rho_v(h_v + \frac{u_v^2}{2})) + \frac{\partial}{\partial z}(\alpha A\rho_v(h_v + \frac{u_v^2}{2})u_v) - A\alpha\frac{\partial p}{\partial t} =$$
$$-\chi_h q_{wv} + Aq_{iv} + A\Gamma(h_v + \frac{u_v^2}{2}) + A\alpha\rho_v u_v g_z.$$

Liquid phase

$$A\frac{\partial}{\partial t}((1-\alpha)\rho_l(h_l + \frac{u_l^2}{2})) + \frac{\partial}{\partial z}((1-\alpha)A\rho_l(h_l + \frac{u_l^2}{2})u_l) - A(1-\alpha)\frac{\partial p}{\partial t} =$$
$$-\chi_h q_{wl} + Aq_{il} - A\Gamma(h_l + \frac{u_l^2}{2}) + A(1-\alpha)\rho_l u_l g_z.$$

Where
χ_f : friction perimeter.
χ_h : heating perimeter.
R : rate of stratification.
g_z : axial projection of gravity contribution ($g \cos\theta$).
M_A : added mass term.

An assessment of the CATHARE code can be found in [**6**]. A description of the different terms and the necessary closure laws appearing in the previous set of equations can be found in [**17**] as well.

Chapter 2

Closure Relationships

2.1. Introduction

In this chapter we will study some helpful equations called closure laws that play an important role for the solution of the system of equations in two phase flow problems. They appear due to the information lost in the averaging procedure and are empirical correlations that allow to recover it. These relationships have to agree with the Physics of the processes they model, characterizing phenomena such as

- Interfacial heat transfer (q_{ig} and q_{il}),
- Wall heat transfer (q_{wg} and q_{wl}),
- Interfacial friction, defined by mean of interfacial drag coefficients (C_i),
- Mass transfer through the interface, usually denoted by (Γ),
- Wall friction, by mean of the shear stress coefficients (C_{wg} and C_{wl}).
- Virtual mass terms, $k_{vm}\rho_c$ or gravity terms as $\overrightarrow{\nabla} p_s$ that involve additional terms that will be added in the momentum and energy equations and
- Thermodynamics properties by means of more or less complicated equations of state.

The calculation in most of them needs to know the regime developed by the fluids, in codes like TRAC it is taken into account by means of a parameter called transition void fraction, that accounts for the use of one correlation or another. In the following sections we summarize the most common regimes that appear in two phase flow and we will make some comments about the closure equations associated to them.

2.2. Two Phase Flow Regimes

One of the major difficulties in two phase flow is the characterization of the geometry of the flow, it is not known a priori but it is a part of the solution. In single phase we know the geometry of the fluid in a tube of fluid and we can determine the velocity profile, the shear stress distribution, the pressure drops and so on.

In two phase flow, these calculations will depend on the distribution of the phases in the conduct. This leads us to consider different flow patterns that will depend on the inclination of the conduct, its geometry, the pressure, the velocities of the phases, the properties of the fluids, etc.

The main flow patterns we can find in co-current two phase flow depend on whether we have vertical or horizontal flow. They are briefly commented in this section.

Flow patterns in vertical co-current flows

- Bubble flow, gas is dispersed as discrete bubbles in a more or less continuous liquid.
- Slug flow, when quality increases, bubbles coalesce and form larger bubbles.
- Churn flow, when velocity of phase is increased, the slugs break down into unstable regime.
- Annular flow, the liquid flow is on the wall as a film, the vapour phase is a continuous phase in the centre of the tube.
- Wispy annular flow, when the velocity of the liquid phase increases some amount of liquid is in the gas core.

In figure 2.1 we can see a representation of these patterns.

Flow patterns in horizontal co-current flows

The main difference with the vertical patterns is that in horizontal flow, gravity tends to stratify the fluids. Hence we have the following patterns:

- Bubble flow, bubbles are dispersed in the continuous liquid.
- Stratified flow, the phases are separated with liquid at the bottom of the conduct and vapour on the top. We can find two kinds of stratified flow, depending on the velocity of the gas phase, they are stratified smooth and stratified wavy flows.
- Annular flow, the liquid fluid is on the wall and the gas is in the centre, this is kept with higher velocities of the gas.
- Plug flow, is an intermittent flow that occurs at low flow rates and moderate liquid rate. We have some plug of liquid separated by zones of large gas bubbles.
- Slug flow, it appears when velocity is increased in plug flow.

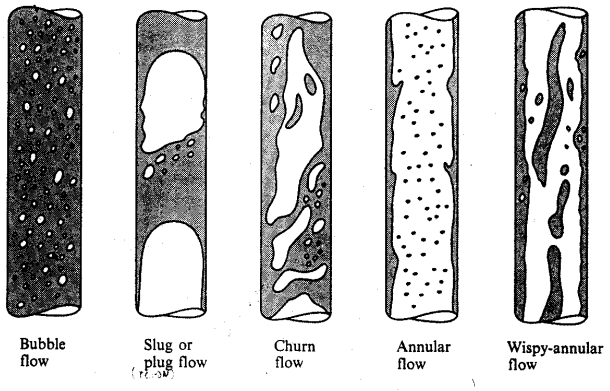

FIGURE 2.1. Flow patterns in vertical flow

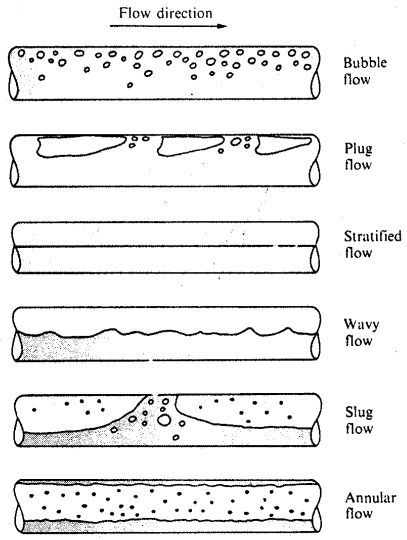

FIGURE 2.2. Flow patterns in horizontal flow

In figure 2.2, we have a representation of these patterns.

Annular flow (pure, wispy and with some bubbles in the liquid film) is the typical regime in condensers, evaporators, boilers and even in BWR.

There are also maps that allow to know the pattern we have. They are two-dimensional graphs that separate the space into areas which depend on the pattern, the regime mostly depends on the value of some ratios or variables (densities, velocities and viscosities of the phases). Examples of them are the Baker map and its modification by Scott for horizontal flow, the Hewitt and Roberts map for vertical upflow and the Taitel and Dukler for flow pattern determination in horizontal flows in a tube. A more complete description of them can be found in the two phase flow literature (see [**11**], [**33**] and [**53**]).

2.3. Closure Relationships for Heat Transfer Terms

There are different heat transfer phenomena that can be found in two phase flow problems, in the next section we will pay attention to interfacial heat transfer and wall heat transfer.

2.3.1. Interfacial Heat Transfer

The mass transfer flow rate, Γ through the interface is determined taking into account the jump condition for the energy equation, so we have for TRAC and RELAP codes

$$\Gamma = \Gamma_{wall} - \frac{q_{ig} + q_{il}}{(h_v - h_l)_i}$$

where

Γ_{wall} : heat flux between wall and interface

$q_{ig} = h_{ig} A_i \frac{T_{sv} - T_g}{vol}$ and $q_{il} = h_{il} A_i \frac{T_{sv} - T_l}{vol}$ with

h_{il} and h_{ig} : heat transfer coefficients between the interface and the phase k, there are correlations to determine them depending on the regime we have.

vol: the considered volume.

h_v and h_l are the enthalpies of vapour and liquid respectively, evaluated at the interface conditions.

In the same manner for CATHARE we have that

$$\Gamma = -\frac{q_{ig} + q_{il} - \frac{\chi_h}{A} q_{wi}}{h_v - h_l}.$$

For the calculation of the heat transfer coefficients, h_{ig} and h_{il}, there are a lot of correlations that depend on the regime we consider (annular, wispy, bubbly, stratified, etc.). A complete description of those relationships can be found in the Codes' manuals such as [**8**] or [**60**]. A good compilation of them can be found in [**33**] as well.

2.3.2. Wall Heat Transfer

The terms related to heat transfer through the wall are

$$q_{wl} = h_{wl} A_w \frac{T_w - T_l}{vol} \quad \text{and} \quad q_{wg} = h_{wg} A_w \frac{T_w - T_g}{vol}$$

with

A_w : wall surface.

h_{wl} and h_{wg} : heat transfer coefficients between the wall and the phase k. There are also expressions to determine them, they vary depending on the regime we have and the code we use.

For a better understanding of the heat transfer process, let us consider the boiling curve of figure 2.3 which shows the mechanisms of boiling. We can distinguish some heat transfer processes

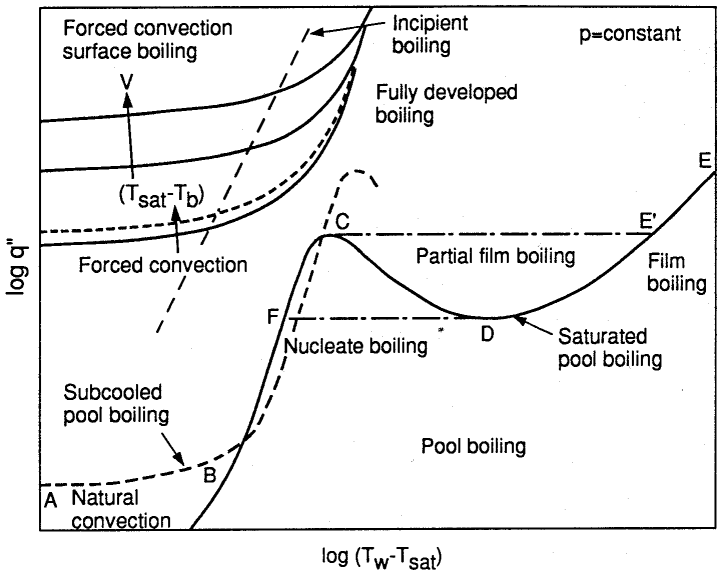

FIGURE 2.3. Boiling curve

- Natural or force convection in liquid phase.
- Nucleate boiling where vapour are formed, mainly at the wall surface.
- Convective boiling, in which the heat is conducted through a film of liquid to the vapour with no bubble formation.

- Transition boiling, under low heat flux an intense evaporation happens that prevents a good contact between the liquid and the wall, there are parts of the surface under nucleate boiling and parts in film boiling.
- Film boiling, radiation from the walls to the two phase mixture gain importance and heat transfer increases considerably.
- Convection in superheated vapour phase.

The form of the boiling curve depends on the geometry of the conduct, the mass flow rate and the properties of the fluid.

Heat transfer from the fluid to the wall (fluid cooling) implies some of the following processes:

- Natural or forced convection in the liquid phase.
- Condensation of the vapour of the two phase mixture.
- Natural or forced convection in the vapour phase.

2.4. Closure Relationships for Friction Terms

In this section we will study the terms related to interfacial and wall friction, they appear in the momentum and energy equations

2.4.1. Interfacial Friction

The interfacial friction terms are characterized by the interfacial drag force, they derive from the study of momentum equation in steady state. These forces are expressed in terms of the difference of densities and the void fraction, using TRAC notation we have

$$F_{\mathrm{lg}} = \overline{C}_i \frac{\left|\overline{V}_{gj}\right| \overline{V}_{gj}}{< 1-\alpha >^2} + \Delta\rho g < \alpha(1-\alpha) >$$

in which $\overline{C}_i$ includes $\frac{1}{\eta^2}$ that is the factor that relate drift and relative velocities, $\overline{V}_{gj}$ and $\overline{V}_r$ respectively. In the TRAC code $\overline{C}_i$ is defined as

$$\overline{C}_i = \frac{1}{2} C_D \left(\frac{3}{2}\frac{1}{d_i}\right) \rho_c \frac{1}{\eta^2}$$

where $\frac{3}{2}\frac{1}{d_i}$ is the friction area per unit volume and ρ_c is the density of the continious phase.

The form of the relation is

$$F_{\mathrm{lg}} = \overline{C}\left[\overline{V}_r\right]^N = \overline{C}\left|C_1\overline{V}_g - C_0\overline{V}_l\right|\left(C_1\overline{V}_g - C_0\overline{V}_l\right).$$

The exponent varies between 2 and 4, due to the effect of the regime upon the interfacial area. This effect has to do with the variable $\overline{C}_i$.

On the other hand the coefficient, $C_1 = \frac{1-\alpha C_0}{1-\alpha}$takes into account radiative heat transfer phenomenon.

2.4.2. Wall Friction

In the momentum equations, the general form of the friction coefficients with the wall for each phase is

$$C_{wl} = \frac{\left.\frac{\partial p}{\partial z}\right|_w}{\rho_l (V_l)^2}, \qquad C_{wg} = \frac{\left.\frac{\partial p}{\partial z}\right|_w}{\rho_g (V_g)^2}$$

where $\left.\frac{\partial p}{\partial z}\right|_w$ is the static pressure drop due to wall friction. These terms are obtained by considering two and single phase correlations. Their calculation is based on the so-called multipliers.

It is convenient to relate the pressure drop in a channel or conduct to the single phase (liquid or vapour) pressure drop. For this purpose it is necessary the introduction of multipliers ϕ_g and ϕ_l

$$\phi_g^2 = \frac{\left(-\frac{\partial p}{\partial z}\right)_w}{\left(-\frac{\partial p}{\partial z}\right)_{wg}}, \qquad \phi_l^2 = \frac{\left(-\frac{\partial p}{\partial z}\right)_w}{\left(-\frac{\partial p}{\partial z}\right)_{wl}}, \qquad \phi_{lo}^2 = \frac{\left(-\frac{\partial p}{\partial z}\right)_w}{\left(-\frac{\partial p}{\partial z}\right)_{wlo}},$$

where $\left(-\frac{\partial p}{\partial z}\right)_{wk}$ is the vapour or liquid only pressure drop flowing with a mass flow rate of W_k, depending on $k = g$ or l respectively. With the subscript lo a mass flow rate of $W_v + W_l$ is supposed. In the literature can be found different correlations to determine these multipliers, see [**11**] or [**53**] for instance.

2.5. Equations of State

2.5.1. General Equations of State

In the solution of the system of equations in two phase flow, different equations of state can be used to close the problem, some differences have been found in the variables that researchers consider as independent, codes such as CATHARE, FLICA

y TRIO4 consider the equations of the densities choosing as independent variables pressure and enthalpy,

$$\rho_k = \rho_k(p, h_k),$$

so the speeds of sound of the phases are written as functions of the derivatives of density respect to these variables, $\left.\frac{\partial \rho_k}{\partial p}\right|_{h=cte}$ and $\left.\frac{\partial \rho_k}{\partial h_k}\right|_{p=cte}$

$$c_k^2 = \frac{1}{\left.\frac{\partial \rho_k}{\partial p}\right|_{h_k=cte} + \frac{1}{\rho_k}\left.\frac{\partial \rho_k}{\partial h_k}\right|_{p=cte}}.$$

RELAP prefers considering both densities but using as independent variables pressure and internal energy

$$\rho_k = \rho_k(p, e_k),$$

in this case the speeds of sound will be functions of $\left.\frac{\partial \rho_k}{\partial p}\right|_{e_k=cte}$ y $\left.\frac{\partial \rho_k}{\partial e_k}\right|_{p=cte}$

$$c_k^2 = \frac{p}{\rho_k^2}\left.\frac{\partial p}{\partial e}\right|_{\rho_k=cte} + \left.\frac{\partial p}{\partial \rho}\right|_{e_k=cte}.$$

For the calculation of these derivatives we have two options:

- Using tabulated expressions of the derivatives which is the common procedure followed by the codes mentioned above.
- Determining them numerically, this way produces an additional difficulty when we go from the single phase region to the two phase one and vice versa as we find a discontinuity in the derivatives at the saturation lines.

In our case, we have analysed some possibilities, among them:

- Utilizing the NIST/ASME's routines (see [**31**]) that provide relationships for $\left.\frac{\partial \rho_k}{\partial p}\right|_{T=cte}$ and $\left.\frac{\partial \rho_k}{\partial T_k}\right|_{p=cte}$. So we have yielded the following expressions helpful only in the single phase regions

$$\left.\frac{\partial \rho_k}{\partial p}\right|_{h=cte} = \left.\frac{\partial \rho_k}{\partial p}\right|_{T=cte} - \frac{1}{c_{pk}}\left.\frac{\partial \rho_k}{\partial T_k}\right|_{p=cte}\left(v + Tv^2\left.\frac{\partial \rho_k}{\partial T_k}\right|_{p=cte}\right)$$

$$\left.\frac{\partial \rho_k}{\partial h_k}\right|_{p=cte} = \frac{1}{c_{pk}}\left.\frac{\partial \rho_k}{\partial T_k}\right|_{p=cte}$$

$$c_k^2 = \frac{1}{\left.\frac{\partial \rho_k}{\partial p}\right|_{T=cte} - Tv^2\left.\frac{\partial \rho_k}{\partial T_k}\right|_{p=cte}}.$$

- Numerical calculation of the derivatives by means of the NIST/ASME routines for calculation of the state properties of steam and water.

A program has been developed to observe the discontinuity of such derivatives, for that we have considered points (ρ, h) along the isobaric line of 0.1 MPa. Using the NIST/ASME Steam Database program the point of saturated liquid is characterized by a value of enthalpy $h_f = 417.5$ kJ/kg and a value of the speed of sound of $c_f = 1544$ m/s. The point of saturated vapour is given by an enthalpy $h_v = 2675$ kJ/kg and a speed of sound $c_g = 472$ m/s. In the following we are going to analyse the variation of the derivatives of density and speeds of sound of the phases.

Subcooled liquid: $\left.\frac{\partial \rho_l}{\partial p}\right|_{h_l=cte}$, $\left.\frac{\partial \rho_l}{\partial h_l}\right|_{p=cte}$ and c_l. In figure 2.4, we show how the speed of sound of the liquid goes to the value of 1544 m/s. The derivatives approximate to some finite values when we go to the saturation line from the left.

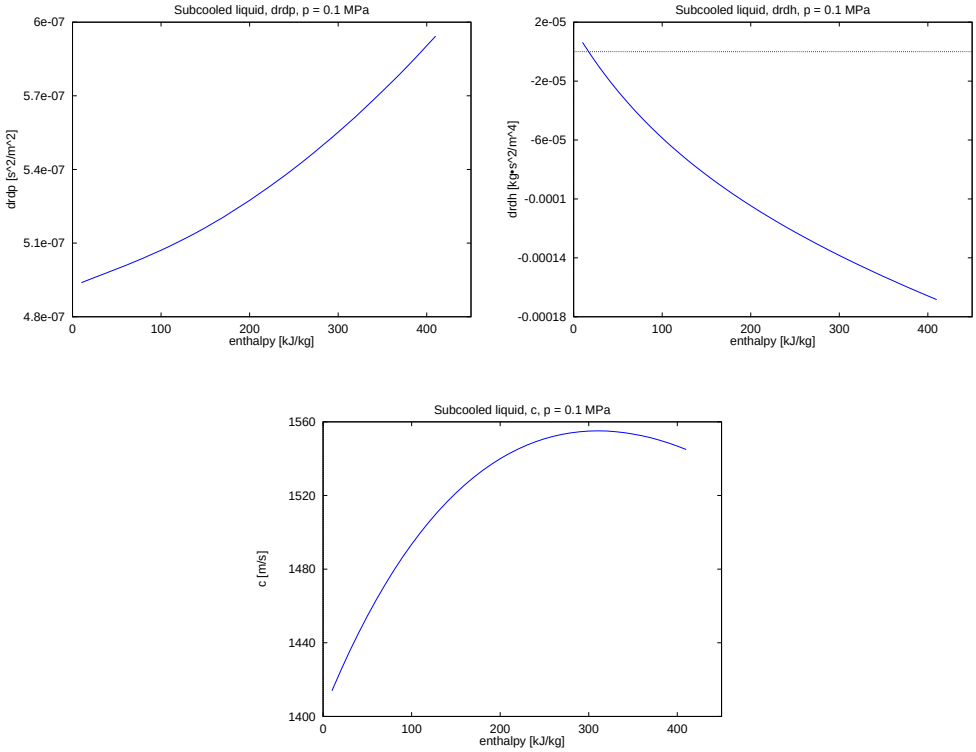

FIGURE 2.4. Derivatives of liquid density respect to pressure at constant enthalpy and respect to enthalpy at constant pressure, at the bottom speed of sound of the liquid phase

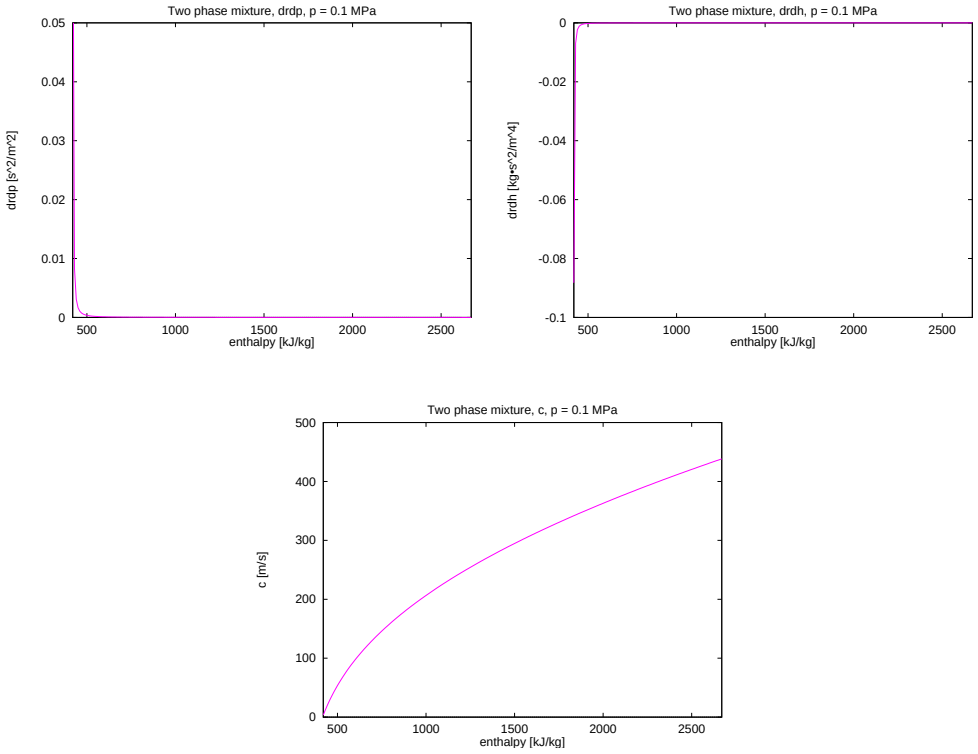

FIGURE 2.5. Derivatives of two phase density with respect to pressure at constant enthalpy and respect to enthalpy at constant pressure, at the bottom pseudo speed of sound of the mixture

Two phases: $\left.\frac{\partial \rho}{\partial p}\right|_{h=cte}$, $\left.\frac{\partial \rho}{\partial h}\right|_{p=cte}$ and c, in figure 2.5 we can watch the asymptotic behaviour of the derivatives of density, so that

$$\left.\frac{\partial \rho}{\partial p}\right|_{h=cte} \rightarrow \quad +\infty$$
$$\left.\frac{\partial \rho}{\partial h}\right|_{p=cte} \rightarrow \quad -\infty.$$

When we approach to the liquid saturation line from the right. Instead, as was commented previously, c goes to a value near to 0 when we are near the liquid saturation line from the left On the other hand, when we approximate to the vapour saturation line from the right, this derivatives go to a finite value lower that 450 m/s, different from the speed of sound of saturated vapour, 472 m/s, which proves the existence of another discontinuity through this line as well.

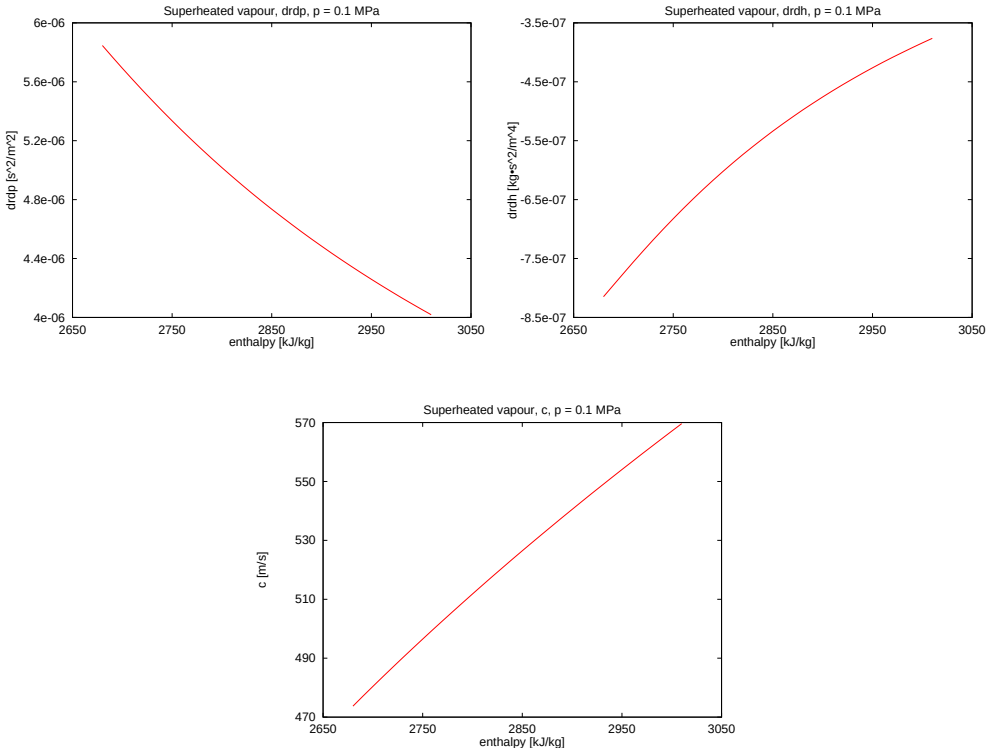

FIGURE 2.6. Derivatives of vapour density respect to pressure at constant enthalpy and respect to enthalpy at constant pressure, at the bottom speed of sound of the vapour

Superheated vapour: $\left.\frac{\partial \rho_v}{\partial p}\right|_{h_v=cte}$, $\left.\frac{\partial \rho_v}{\partial h_v}\right|_{p=cte}$ and c_v. In figure 2.6 we can observe the opposite behaviours of the derivatives of density as enthalpy increases with constant pressure of $p = 0.1$ Pa, and how the speed of sound of vapour also increases with the enthalpy.

2.5.2. Final Remark on the Speed of Sound of the Mixture

In the study of the homogeneous two phase flow we will use a pseudo-speed of sound of the mixture, defined by

$$c = \left(\left.\frac{\partial \rho}{\partial p}\right|_h + \frac{1}{\rho} \left.\frac{\partial \rho}{\partial h}\right|_p \right)^{-\frac{1}{2}}$$

it is the acoustic speed of sound which does not match with the speed of sound of the mixture that is given by

$$c_{mixture} = \left(\frac{\alpha\rho}{\rho_v} a_v^{-2} + \frac{(1-\alpha)\rho}{\rho_l} a_l^{-2} \right)^{-\frac{1}{2}}.$$

In figure 2.7, we show a comparison between these two speeds of sound.

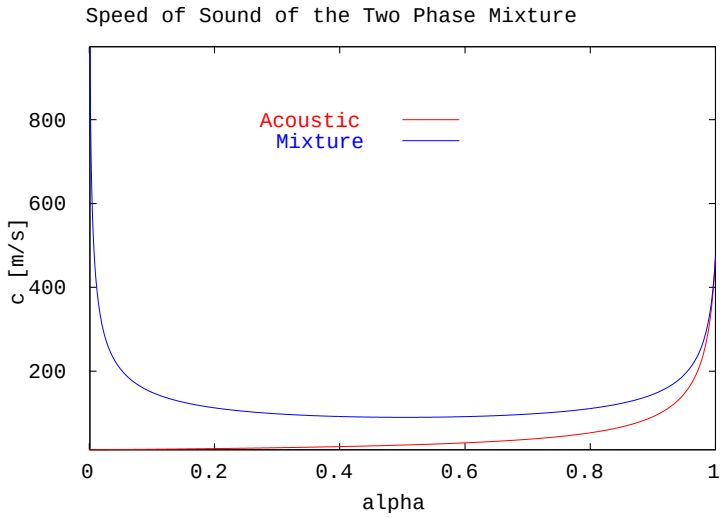

FIGURE 2.7. Acoustic speed of sound vs mixture speed of sound

In the case we study separated two phase flow we should not have any problem, because we will have are the derivatives of the densities of each phase respect to pressure and enthalpy. Problems will appear when we want to study the change of phase process using the homogeneous model as we will have to go through a discontinuity when we go from the liquid or the vapour to the two phase mixture or vice versa. Perhaps the solution would be to make some kind of average between the values of the derivatives at each side of the saturation line.

2.5.3. Simplified Equations of State for Water and Air

Sometimes the regions of interest can be modelled with simple equations of state that permit to simplify considerably the problems. In this section we will talk about them as in some of the tests studied along this work we will go to simpler equations of state, in particular the stiffened gas and the perfect gas equations of state. Examples

of this can be found in the literature, we can cite [**19**] or [**52**] for example, where for the homogeneous model studied below the authors have utilized tabulated equations respectively or the Taitl equation. We want to stand out the second case where liquid phase is considered as a barotropic substance (pressure only depends on density) by means of

$$p(\rho) = A\left[\left(\frac{\rho}{\rho_0}\right)^{\gamma} - 1\right]$$

where $A = 3001$ atm and $\gamma = 7.15$ for water. ρ is the liquid density and $\rho_0 = 1000$ kg/m^3. Perfect gas equation of state was used for the vapour phase.

For the six equation model, and in tests with air and water, a more general version of this equation has been used for both phases, it is the *stiffened equation*. Different versions can be found in the literature, Saurel in [**58**], states that nearly all equations of state can be written under the Mie-Gruneisen form, this is

$$p = (\gamma(\rho) - 1)\rho e - \gamma(\rho)\pi(\rho) \tag{2.5.1}$$

and in the cases of ideal gas or stiffened equations of state γ and π are constants. Berger in [**7**], Saurel in [**58**] and Shyue in [**61**] are examples of the application of the stiffened gas equation of state to two phase flow, in the case of Shyue he uses a hybrid equation by considering van der Waals's equation as well and applying it to homogeneous two phase flow. Therefore, and for the sake of simplicity in the benchmark developed for mixtures of air and water we are going to use the following equations of state:

Liquid phase (stiffened gas)

$$p_l(\rho_l, e_l) = (\gamma_l - 1)\rho_l e_l - p_\infty \gamma_l$$

or as a function of density and temperature

$$p_l(\rho_l, e_l) = \frac{\gamma_l - 1}{\gamma_l}\rho_l c_{pl} T_l - p_\infty,$$

$$e_l(T, \rho) = \frac{c_{pl} T_l}{\gamma_l} + \frac{p_\infty}{\rho_l} \tag{2.5.2}$$

so we can obtain a relationship for the density

$$\rho_l = \gamma_l \frac{p + p_\infty}{(\gamma_l - 1)c_{pl} T_l} \tag{2.5.3}$$

and the speed of sound is

$$c_l^2 = \frac{\gamma_l (p + p_\infty)}{\rho_l} = c_{pl}(\gamma_l - 1)T_l.$$

For water we have
$\gamma_l = 1.8$,
$p_{\infty l} = 6 \times 10^8$Pa.

That corresponds to the values of $\kappa = 0.505$, $\chi = 440 \times 10^3$ and $(\kappa + 1)p_0 = 7900 \times 10^5$.

Vapour phase (perfect gas)

$$p = (\gamma_v - 1)\rho_v e_v - p_\infty \gamma_v$$

and

$$c_v^2 = \frac{\gamma_v p}{\rho_v} = c_{pv}(\gamma_v - 1)T_v$$

as $p_\infty = 0$ and $\gamma_v = 1.4$.

Additionally we have taken into account that

$$R_{air} = 288.2 \text{ J/(kg·K)}, \qquad R_{H_2O} = 461.8 \text{ J/(kg·K)}.$$

In figure 2.8 we show a comparison between the data obtained with the NIST routines and the one obtained using the stiffened gas equation of state, only densities and internal energies have been compared, the first for a constant temperature of $T = 323$ K and the second for constant pressure of $p = 0.1$ MPa, we can conclude that the results obtained are coherent enough for the ranges and the cases we are going to deal with.

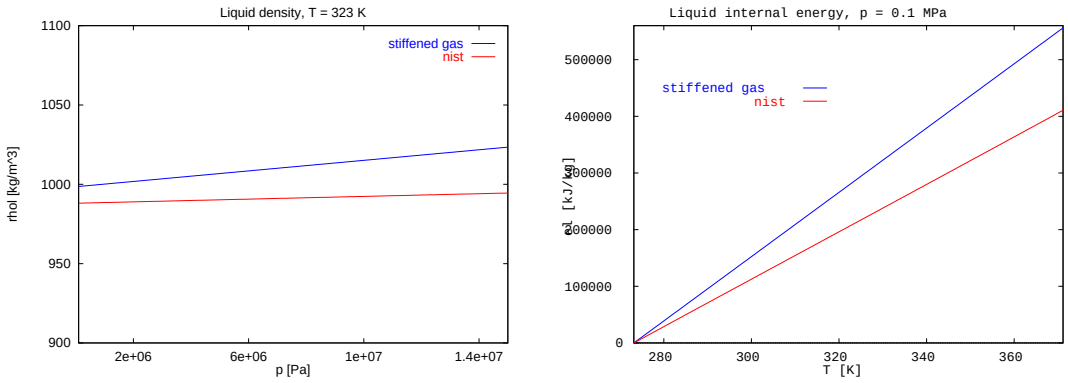

FIGURE 2.8. Density of liquid as a function of enthalpy at constant temperature and internal energy of liquid as a function of enthalpy at constant pressure

Chapter 3

Different Models in 1D Two Phase Flow

3.1. Introduction

So far we have introduced the double area-time averaged one dimensional system of equations and the closure laws we need to close the system in order to model our two phase flow problems properly. In this chapter we are going to make some considerations about the number of equations and some of the commonest simplifications that researchers used to do in order to arrive to a well posed initial value problem in the Hadamard sense. The search of such models is motivated by the necessity of finding and developing improved two fluids models for transient two phase flow. Some influent factors will be the regimes in study, the mathematical character of the equations and other considerations we describe below. In the following sections we present the six equations model, the four equations (isentropic model), the homogeneous and other models that are briefly summarized (the drift model for example). A very good review of the one dimensional models can be found in [**5**] for instance.

3.2. Six Equations Models

The most general 1D model is the two pressure one in which each phase has different pressures, this implies to consider an additional equation to close the system, the void fraction propagation equation is often used. An important contribution on the advantages of using two pressures models can be found in [**1**] and [**4**] for example.

In this work we will be concerned with the six equations model, our study will begin by considering some common approximations, these approaches are based on the way the interfacial pressure terms are integrated, such a topic was an important cause of controversy in the 70's, see [**59**] for example. We are going to describe briefly some of the most important approximations, and how to overcome the problems they involve. These mainly reside in the complex characteristics introduced by the model which are avoided by the inclusion of some damping terms that will affect to the the mathematical character of the system of equations (hyperbolic, parabolic or elliptic). For that purpose, let us recall the 1D system of six equations, which can be written, after the averaging procedure as:

Mass equation

$$A\frac{\partial}{\partial t}(\alpha_k\rho_k) + \frac{\partial}{\partial z}(\alpha_k A\rho_k u_k) = \phi'_{ck}.$$

Momentum equation

$$A\frac{\partial}{\partial t}(\alpha_k\rho_k u_k) + \frac{\partial}{\partial z}(\alpha_k A\rho_k u_k^2) + \int_{A_i}\vec{n}_z\cdot\vec{n}_k\cdot p_k dS + \int_{A_k}\vec{n}_k\cdot\vec{n}_z p_k dS = \phi'_{mk}.$$

Energy equation

$$A\frac{\partial}{\partial t}(\alpha_k\rho_k E_k) + \frac{\partial}{\partial z}(\alpha_k A\rho_k E_k u_k) + \int_{A_i}\vec{n}_z\cdot\vec{n}_k\cdot p_k\cdot u_i\cdot dS + \int_{A_k}\vec{n}_k\cdot\vec{n}_z p_k\cdot u_k\cdot dS = \phi'_{ek}$$

where source terms have been grouped in those ϕ' terms.

We can derive by parts, including all the derivatives of the cross section, A in the source terms and after dividing by A, we have a more common system:

Mass equation

$$\frac{\partial}{\partial t}(\alpha_k\rho_k) + \frac{\partial}{\partial z}(\alpha_k\rho_k u_k) = \phi''_{ck}.$$

Momentum equation

$$\frac{\partial}{\partial t}(\alpha_k\rho_k u_k) + \frac{\partial}{\partial z}(\alpha_k\rho_k u_k^2) + \int_{A_i}\vec{n}_z\cdot\vec{n}_k\cdot p_k dS + \int_{A_{wk}}\vec{n}_k\cdot\vec{n}_z p_k dS = \phi''_{mk}.$$

Energy equation

$$\frac{\partial}{\partial t}(\alpha_k\rho_k E_k) + \frac{\partial}{\partial z}(\alpha_k\rho_k E_k u_k) + \int_{A_i}\vec{n}_z\cdot\vec{n}_k\cdot p_k\cdot u_i\cdot dS + \int_{A_{wk}}\vec{n}_k\cdot\vec{n}_z p_k\cdot u_k\cdot dS = \phi''_{ek}.$$

The integral $\int_{A_{wk}} \vec{n}_k \cdot \vec{n}_z p_k dS$ in the momentum equation is usually neglected or is zero when we have constant cross section.

The integral $\int_{A_{wk}} \vec{n}_k \cdot \vec{n}_z p_k \cdot u_k \cdot dS$ is zero because the velocity of the particles beside the wall is zero.

With respect to the pressure terms, we can find different approaches in the literature. In this section, we are going to consider some of them. We will study the pressure terms of the momentum equations, similar developments can be done for the energy equations.

- Case 1. p_k is constant, it is the pressure of the phase k, this is what Boure does in [**10**] in order to derive a two pressure model.

$$\int_{A_i} \vec{n}_z \cdot \vec{n}_k \cdot p_k dS = -p_k \frac{\partial \alpha_k A}{\partial z}.$$

- Case 2. Near the interface $p_k = p_i =$ constant

  Yadigaroglu et al. in [**84**] derive the one dimensional two phase flow system

  taking into account that

$$\int_{A_i} \vec{n}_z \cdot \vec{n}_k \cdot p_k dS = -p_i \frac{\partial \alpha_k A}{\partial z}.$$

  Banerjee in [**33**] also arrives at the same result by introducing an average pressure $< p_k >$ in phase k, he considers that the pressure difference between a point of phase k and another near the interface is $\Delta p_{ki} = p_{ki} - < p_k >$, so

$$\int_{A_i} \vec{n}_z \cdot \vec{n}_k \cdot p_k dS = \int_{A_i} \vec{n}_z \cdot \vec{n}_k \cdot (< p_k > + \Delta p_{ki}) dS = -(< p_k > + \Delta p_{ki}) \frac{\partial \alpha_k A}{\partial z}.$$

  It reduces the model to the one pressure model by considering only that $\Delta p_{ki} = p - p_i = 0$

- Case 3. A virtual mass term is considered. If we consider that pressure varies from point to point at the interface and we express the integral of the pressure terms as

$$\int_{A_i} \vec{n}_z \cdot \vec{n}_k \cdot p_k dS = -(< p_k > + \Delta p_{ki}) \frac{\partial \alpha_k A}{\partial z} + \int_{A_i} \vec{n}_z \cdot \vec{n}_k \cdot \Delta p'_{ki} dS.$$

  The term $\int_{A_i} \vec{n}_z \cdot \vec{n}_k \cdot \Delta p'_{ki} dS = F_{VM} = C_{vm} \rho_l a_{vm}$ is called virtual mass, the parameter C_{vm} is a function of α and a_{vm} is a function of the velocity derivatives.

Depending on the researcher, and in order to guarantee hyperbolicity, either a virtual mass term or a pressure difference term are taken into account. Examples of them are Nguyen in [**50**] who tries to improve [**5**], [**3**] and [**10**] by considering

$$p_k - p_i = L_{\alpha k}[\frac{\partial \alpha_k}{\partial t} + w_k \frac{\partial \alpha_k}{\partial z}],$$

for the resolution of the system he needed a seventh equation, it was the void propagation equation as has been used by others before. In this sense Lee et al. [**41**] write the pressure difference as

$$p_k - p_i = L_k[1 \pm \frac{R_k}{2}\frac{\partial a_i}{\partial z}],$$

giving expressions for L_k which depend on the two phase flow regime. With respect to the interfacial area, a_i, in [**40**], one can find different expressions, which lead to consider a seventh partial differential equation, the propagation of the interfacial area.

Others, in the analysis of two phase flow in pipelines have developed models more or less simplified by introducing hydrostatical considerations, an example of this is Taitel in [**68**] who studies stratified flux in circular cross section pipes. De Henau in [**18**], considered an average pressure

$$p = (1-\alpha)p_f + \alpha p_g$$

and wrote p for stratified flux by considering only the hydrostatical pressure. This has been used successfully by Masella in [**48**] to model the behaviour of two phase flows formed by oil and gas in conducts, he calls these terms "suppression terms".

We will centre our study in the one pressure model, getting hyperbolicity by means of a pressure correction of type *(Case 2)*. The more important approximations used for these terms are enumerated in the following

- Toumi et al. in [**78**] and [**80**] use the following expression, with an arbitrary δ that guarantees hyperbolicity,

$$p - p_i = \alpha\rho_l\delta(u_v - u_l)^2. \tag{3.2.1}$$

  It is based on a formulation by Hancox.
- Lahey introduced in [**39**] a correction for bubbly flows for the liquid phase given by

$$p - p_l^i = C_p(\alpha)\rho_l(u_v - u_l)^2. \tag{3.2.2}$$

- CATHARE expression, used also in [**26**] following the ideas of Bestion [**17**]

$$(p - p^i) = \sigma\frac{\alpha(1-\alpha)\rho_v\rho_l}{\alpha\rho_l + (1-\alpha)\rho_v}(u_v - u_l)^2. \tag{3.2.3}$$

3.3. Four Equations Model

When the flow is considered isentropic for each phase the six equations model is reduced to a set of four equations where the balances of energy disappear. In this case we have

Mass equations

$$\frac{\partial}{\partial t}(\alpha\rho_v) + \frac{\partial}{\partial x}(\alpha\rho_v u_v) = \phi_{cv},$$
$$\frac{\partial}{\partial t}((1-\alpha)\rho_l) + \frac{\partial}{\partial x}((1-\alpha)\rho_l u_l) = \phi_{cl}.$$

Momentum equations

$$\frac{\partial}{\partial t}(\alpha\rho_v u_v) + \frac{\partial}{\partial x}(\alpha\rho_v u_v^2) + \alpha\frac{\partial p}{\partial x} = \phi_{mv},$$
$$\frac{\partial}{\partial t}((1-\alpha)\rho_l u_l) + \frac{\partial}{\partial x}((1-\alpha)\rho_l u_l^2) + (1-\alpha)\frac{\partial p}{\partial x} = \phi_{ml}.$$

In the analysis of the mathematical character of the system by its eigenstructure, the consideration of the speeds of sound of each phase will be very helpful, in this case it is given by

$$c_k = \left(\left.\frac{\partial\rho_k}{\partial p}\right|_{s_k}\right)^{-\frac{1}{2}}.$$

3.4. The Homogeneous Model

It is one of the most simplified models used to analyse transient two phase flow. It is characterized by

$$u_g = u_f = u$$

or equivalently by means of the slip ratio

$$S = \frac{u_g}{u_f} = 1.$$

Its validity is limited to low unsteady flows, as speed of vapour used to be much higher than the speed of the liquid. In steady state its validity depends very much on the components of the pressure gradients. Although for the acceleration pressure gradient results are not very good, it gives reasonable predictions for the gravitational and frictional gradients, the homogeneous void fraction is a good estimate for $\frac{\rho_l}{\rho_v} < 10$

or if $G > 2000$ kg/m^{2}s, see [**53**] for example, for steam-water mixtures this condition is reached when $p > 120$ bar.

The system of equations that represents the fluid behaviour flowing in a pipe and considering constant cross section is

Mass equation

$$\frac{\partial}{\partial t}[\rho] + \frac{\partial}{\partial z}[\rho u] = 0. \tag{3.4.1}$$

Momentum equation

$$\frac{\partial}{\partial t}[\rho u] + \frac{\partial}{\partial z}[\rho u^2 + p] + \left(\frac{\partial p}{\partial z}\right)_F + \rho g \sin\theta = 0. \tag{3.4.2}$$

Energy equation

$$\frac{\partial}{\partial t}[\rho E] + \frac{\partial}{\partial z}[\rho H u] + \rho u g \sin\theta + \frac{q''_w}{A} = 0. \tag{3.4.3}$$

where $E = e + \frac{u^2}{2}$ and $H = e + \frac{u^2}{2} + \frac{p}{\rho}$.

Depending on whether we consider the phases in thermal equilibrium or not we will have the Homogeneous Equilibrium Model (HEM) or a more general homogeneous model sometimes called the "slip model".

3.5. Other Important Models

An important model is the drift flux model, it was introduced in [**85**]. It is useful for modelling steady or quasi steady two phase flow and provides good results in bubbly and churn flow regimes although it is a bit artificial in separated two phase flow as is pointed out in [**33**]. It is based on the definition of the so-called drift velocities. If the cross sectional volumetric fluxes are

$$j_k = \alpha_k u_k$$

and the velocity of the volumetric flux averaged over the cross section is

$$J = j_v + j_l$$

so the local drift velocities are defined as

$$\begin{aligned} u_{vj} &= u_v - J \\ u_{lj} &= u_l - J. \end{aligned}$$

The resultant system of equations is function of the drift velocities defined above.

Finally we introduce the case in which the system is formed by the three conservation laws of the mixture. Thus, we have the following set of equations:

Mass equation

$$A\frac{\partial}{\partial t}[\rho] + \frac{\partial}{\partial z}[\dot{m}A] = 0.$$

Momentum equation

$$\frac{\partial}{\partial t}[\dot{m}] + \frac{1}{A}\frac{\partial}{\partial z}A[\alpha\rho_v u_v^2 + (1-\alpha)\rho_l u_l^2] = -\frac{\partial p}{\partial z} - \left(\frac{\partial p}{\partial z}\right)_F + \rho g \sin\theta.$$

Energy equation

$$\frac{\partial}{\partial t}[\alpha\rho_v E_v + (1-\alpha)\rho_l E_l] + \frac{\partial}{\partial z}[\alpha\rho_v H_v u_v + (1-\alpha)\rho_l H_l u_l] = \rho u g \sin\theta + \frac{q''_w}{A}.$$

The interest of such an approximation is its simplicity, however we have to add some relationships that help us to determine all the unknowns of the problem, for example we need equations that relate void fraction and slip ratio to mass flow rate, pressure, enthalpy, etc.

Taken from [**33**], we have summarized in table 1 most of the two fluid models we can find.

Constraints	n ^{o}of equations	Clouser laws supplied externally	Free variables	
1 none	2 phase mass	$\Gamma_{l,g}$	p, α	p
	2phase momentum	$\tau_{wl}, \tau_{wv}, \tau_i$	u_l, u_v	$\dot{m}, x, \alpha$
	2 phase energy	$q_{wl}, q_{wv}, q_{il}, q_{iv}$	h_l, h_v	h_l, h_v
2, relation between	2 phase mass	$\Gamma_{l,g}$	p, α	p
phase velocities or	1 mixture momentum	τ_w	u_l, u_v	$\dot{m}, x$
for α	2 phase energy	$q_{wl}, q_{wv}, q_{il}, q_{iv}$	h_l, h_v	h_l, h_v
3, on energy	2 phase mass	$\Gamma_{l,g}$ from energy j.c.	p, α	p
of one phase,	2 phase momentum	$\tau_{wl}, \tau_{wv}, \tau_i$	u_l, u_v	$\dot{m}, x, \alpha$
h_{sat},e.g.	1 mixture energy	q_w, q_{wl}, q_{wv}	h_l, h_v	
4, on mass exhange	1 mixture mass		p, α	p
between phases	2 phase momentum	$\tau_{wl}, \tau_{wv}, \tau_i$	u_l, u_v	$\dot{m}, x, \alpha$
	2 phase energy	$q_{wl}, q_{wv}, q_{il}, q_{iv}$	h_l, h_v	h_l, h_v
5, relation between	1 mixture mass		p, α	p
phase velocities	1 mixture momentum	τ_w	u_l, u_v	$\dot{m}, x$
or for α	2 phase energy	$q_{wl}, q_{wv}, q_{il}, q_{iv}$	h_l, h_v	h_l, h_v
6, on energy	2 phase mass	$\Gamma_{l,g}$	p	p
of phases	1 mixture momentum	τ_w	u_l, u_v	$\dot{m}, x$
	1 mixture energy	q_w	h_l, h_v	h_l, h_v
7, two constraints	1 mixture mass		p, α	p
on energy of phases	2 phase momentum	$\tau_{wl}, \tau_{wv}, \tau_i$	u_l, u_v	p, α
	1 mixture energy	q_w		$\dot{m}, x$
8 two on energy	1 mixture mass		p	p
and one for α	1 mixture momentum	τ_w	u_l, u_v	$\dot{m}, x$
	1 mixture energy	q_w		

TABLE 1. Summary of different two phase models

Chapter 4

Numerical Methods Applied to the Solution of Two Phase Flow Problems

4.1. Introduction

We usually model two phase flow by means of a system of equations, that in general, is based on the equations for the conservation of mass, momentum and energy or entropy for both components. During the last years many models have been developed, their features have been always conditioned by the field of application interested in its development, nuclear engineering, oil or chemical industry, etc. The codes developed to analyse two phase flow (RELAP and TRAC among them) traditionally have utilized semi implicit or implicit numerical methods, using staggered mesh techniques with the donor cell principle to solve the two phase system of equations. These methods produce stable solutions in cases where enough numerical damping is provided to the system. This occurs when coarse meshes are used as they are very diffusive and the numerical diffusion acts to suppress any spurious oscillation. Problems appear when fine meshes are utilized, in this case the schemes do not provide enough numerical damping to suppress oscillations. The application of the method of characteristics and other explicit and implicit methods have contributed enormously to the advance in the solution of two phase problems.

From the numerical point of view it would be desirable to work with conservative and explicit schemes but the non conservative character of the momentum and energy

equations is a problem which makes the utilization of explicit schemes a complicated issue, mainly due to two problems already mentioned:

- Hyperbolicity and
- Conservation.

When we try to write the one pressure two phase system of equations in conservative form, we find that is not possible due to the pressure terms in the momentum and energy equations. This has been the reason that has motivated a great amount of researchers to write the system in non conservative form. Even doing this we find that the system is not hyperbolic because it has complex characteristics.

Many researchers have studied the hyperbolicity of the system of equations. Among them, we will refer to some of the most important contributions. In [**29**], Gidaspow et al. exposed and discussed the problem of the ill-posed initial value problem that appears when the one dimensional system of equations is considered, in particular the isentropic case (four equations model). They stated that the solution is to consider additional terms by means of a two pressure model or a mass force (virtual mass). In this sense Ramshaw et al. considered in [**55**] a two pressure model and studied the isothermal case. The general paper by Lyczkowski et al., [**46**] analyses the one pressure model with and without an acceleration term with derivatives of the velocities, like the above mentioned virtual mass.

Banerjee et al. analyse in [**5**] the hyperbolicity of different models of the system of equations, they study the one pressure model with different velocities and temperatures, the homogeneous model and the two pressure model.

Stewart shows in [**66**] that the problem of complex characteristics can be avoided by considering a semi-implicit method to solve the system of equations, he studied the one pressure isothermal two phase model. Other interesting papers appeared with regard to this problem, Ransom et al. in [**56**], considered a two-pressure model and the pressure difference between phase and interface. In their review article [**67**], Stewart and Wendroff talked about these aspects and some others. Holm et al., in [**36**], dealt with the problem as well but in terms of a Hamiltonian formulation.

Lately, many of these aspects have been gathered in some papers like [**78**] and [**80**] by Toumi, [**70**] by Tiselj et al. or [**37**] by Hwang.

The consequence of having complex characteristics is that the initial value problem does not depend continuously on the initial values and therefore it is ill-posed. In order to obtain stable results the introduction of numerical dumping terms is necessary. Many of the cited researchers solve the problem with the presence of non viscous terms that make the model well posed, as commented before they are virtual mass or pressure terms. Sometimes they have generated different analyses of the equations,

some examples are Ghidaglia et al. in the VFFC schemes [**27**] or more general development by Städtke in [**64**], the first one introduces a pressure correction term and the second the virtual mass. Tiselj in his non conservative version utilizes a variation of the conventional virtual mass terms of RELAP (see [**72**] for example), similarly we can find other non conservative applications such as the one by Hwang in [**37**]. A bit different can be the formulation developed by Toumi [**78**] that even considers a mixture equation, combined with perfect gas equations of state and incompressibility of the liquid to derive his model.

In the first part of this chapter we are going to focus on analysing the hyperbolicity of the homogeneous model and the six equations one pressure separated model. The first one is an extreme case, the system is hyperbolic and the application of traditional upwind schemes can be more or less an easy issue. Despite its apparent simplicity the problem results very complex due to other appearing handicaps such as the discontinuities of the derivatives at the saturation lines. For both models we will study their eigenstructures, in the case of the six equation model we will study the conservative and the non conservative versions. On the other hand and in order to complete our developments we will describe some of the most successful numerical schemes applied to these two phase flow models.

4.2. Mathematical Analysis of the Homogeneous Two-Phase Flow System

Traditionally, the system of equations in homogeneous two phase flow (eqs. 3.4.1, 3.4.2 and 3.4.3) has been solved by considering its non conservative form. The application of conservative schemes is more recent, we stand out [**19**], [**52**] or [**77**] among others. In this section, we will study the eigenstructure of the conservative and non conservative versions of this system of equations.

Conservative Case

We can write the conservative version of the system of equations in vector form as

$$W_t + F(W)_z + S(W) = 0 \tag{4.2.1}$$

where the vector of conserved variables is

$$W = \begin{bmatrix} \rho \\ \rho u \\ \rho E \end{bmatrix} = \begin{bmatrix} \omega_1 \\ \omega_2 \\ \omega_3 \end{bmatrix}$$

the flux vector

$$F(W) = \begin{bmatrix} \rho u \\ \rho u^2 + p \\ \rho H u \end{bmatrix} = \begin{bmatrix} \omega_2 \\ \frac{\omega_2^2}{\omega_1} + p \\ \omega_3 \frac{\omega_2}{\omega_1} + p \frac{\omega_2}{\omega_1} \end{bmatrix}$$

only pressure cannot be explicitly expressed as a function of the conserved variables w_i, but as an implicit relationship stated by

$$p = p(\rho, e) \tag{4.2.2}$$

this expression for the pressure can be fitted by polynomials in the range of study.

The source term is

$$S(W) = \begin{bmatrix} 0 \\ \left(\frac{\partial p}{\partial z}\right)_F + \rho g \sin\theta \\ \rho u g \sin\theta + \frac{q''_w}{A} \end{bmatrix}.$$

The jacobian matrix is then given by

$$J(W) = \frac{\partial F(W)}{\partial W} = \begin{bmatrix} 0 & 1 & 0 \\ -u^2 + \frac{\partial p}{\partial w_1} & 2u + \frac{\partial p}{\partial w_2} & \frac{\partial p}{\partial w_3} \\ -(e + \frac{u^2}{2})u + \frac{\partial p}{\partial w_1} u - p\frac{u}{\rho} & e + \frac{u^2}{2} + \frac{\partial p}{\partial w_2} u + \frac{p}{\rho} & u + \frac{\partial p}{\partial w_3} u \end{bmatrix} \tag{4.2.3}$$

taking into account eq. 4.2.2

$$\begin{aligned} \frac{\partial p}{\partial w_1} &= \frac{\partial p}{\partial \rho}\frac{\partial \rho}{\partial w_1} + \frac{\partial p}{\partial e}\frac{\partial e}{\partial w_1} \\ \frac{\partial p}{\partial w_2} &= \frac{\partial p}{\partial \rho}\frac{\partial \rho}{\partial w_2} + \frac{\partial p}{\partial e}\frac{\partial e}{\partial w_2} \\ \frac{\partial p}{\partial w_3} &= \frac{\partial p}{\partial \rho}\frac{\partial \rho}{\partial w_3} + \frac{\partial p}{\partial e}\frac{\partial e}{\partial w_3} \end{aligned} \tag{4.2.4}$$

and since

$$\begin{aligned} \rho &= w_1 \\ u &= \frac{w_2}{w_1} \\ e &= \frac{w_3}{w_1} - \frac{w_2^2}{2w_1^2} \end{aligned}$$

we can stand for the derivatives (eqs. 4.2.4) as functions of the primitive variables

$$\begin{aligned}\frac{\partial p}{\partial w_1} &= \frac{\partial p}{\partial \rho} - \frac{1}{\rho}\left(e - \frac{u^2}{2}\right)\frac{\partial p}{\partial e} \\ \frac{\partial p}{\partial w_2} &= -\frac{u}{\rho}\frac{\partial p}{\partial e} \\ \frac{\partial p}{\partial w_3} &= \frac{1}{\rho}\frac{\partial p}{\partial e}\end{aligned}$$

and write the jacobian matrix

$$J(W) = \begin{bmatrix} 0 & 1 & 0 \\ -u^2 + p_\rho - \frac{1}{\rho}\left(e - \frac{u^2}{2}\right)p_e & 2u - \frac{u}{\rho}p_e & \frac{1}{\rho}p_e \\ -(e + \frac{u^2}{2})u + p_\rho u - p\frac{u}{\rho} - \frac{u}{\rho}\left(e - \frac{u^2}{2}\right)p_e & e + \frac{u^2}{2} - \frac{u^2}{\rho}p_e + \frac{p}{\rho} & u + \frac{u}{\rho}p_e \end{bmatrix}$$

where $p_\rho(\rho, e) = \left.\frac{\partial p}{\partial \rho}\right|_{e=const.}$ and $p_e(\rho, e) = \left.\frac{\partial p}{\partial e}\right|_{\rho=const.}$. These partial derivatives, which are needed to find numerical solutions of the system 4.2.1, can be found analytically or numerically at every calculation point (ρ, e) from equation 4.2.2. In the case of using simplified equations of state we can evaluate them, but when we consider real two phase mixtures, these derivatives cannot be evaluated explicitly so that we can consider two options:

- A map of the different values of them can be built for each pair of values of ρ and e.
- Evaluating the unknown derivatives numerically.

We can diagonalize $J(W) = PDP^{-1}$, where the diagonal matrix D is given by the following eigenvalues

$$\begin{aligned}\lambda_1 &= u \\ \lambda_2 &= u - \frac{\sqrt{pp_e + \rho^2 p_\rho}}{\rho} = u - c \\ \lambda_3 &= u + \frac{\sqrt{pp_e + \rho^2 p_\rho}}{\rho} = u + c\end{aligned}$$

where we have introduced the pseudo-speed of sound of the mixture defined by

$$c = \left[\frac{p}{\rho^2}\frac{\partial p}{\partial e} + \frac{\partial p}{\partial \rho}\right]^{\frac{1}{2}},$$

which was already introduced in Chapter 2.

The eigenvectors P_i, are given by

$$
\begin{aligned}
P_1 &= \begin{bmatrix} \frac{2p_e}{(2e+u^2)p_e-2\rho p_\rho} \\ \frac{2up_e}{(2e+u^2)p_e-2\rho p_\rho} \\ 1 \end{bmatrix} = \begin{bmatrix} \frac{p_e}{Ep_e-\rho p_\rho} \\ \frac{up_e}{Ep_e-\rho p_\rho} \\ 1 \end{bmatrix}, \\
P_2 &= \begin{bmatrix} \frac{2\rho}{2p+2e\rho+u^2\rho-2u\sqrt{pp_e+\rho^2 p_\rho}} \\ -\frac{2(-u\rho+\sqrt{pp_e+\rho^2 p_\rho})}{2p+2e\rho+u^2\rho-2u\sqrt{pp_e+\rho^2 p_\rho}} \\ 1 \end{bmatrix} = \begin{bmatrix} \frac{1}{H-uc} \\ \frac{u-c}{H-uc} \\ 1 \end{bmatrix}, \\
P_3 &= \begin{bmatrix} \frac{2\rho}{2p+2e\rho+u^2\rho+2u\sqrt{pp_e+\rho^2 p_\rho}} \\ \frac{2(u\rho+\sqrt{pp_e+\rho^2 p_\rho})}{2p+2e\rho+u^2\rho+2u\sqrt{pp_e+\rho^2 p_\rho}} \\ 1 \end{bmatrix} = \begin{bmatrix} \frac{1}{H+uc} \\ \frac{u+c}{H+uc} \\ 1 \end{bmatrix}.
\end{aligned}
$$

Another option is to write the jacobian matrix as a function of the derivatives of density respect to enthalpy $\left.\frac{\partial\rho}{\partial h}\right|_{p=const.}$ and pressure $\left.\frac{\partial\rho}{\partial p}\right|_{h=const.}$. In this case the derivatives of pressure respect to the conserved variables are written as functions of such density derivatives. Their expressions are

$$
\begin{aligned}
\frac{\partial p}{\partial w_1} &= \frac{2\rho_h + 2\rho - \rho_h u^2}{2(\rho_h + \rho\rho_p)}, \\
\frac{\partial p}{\partial w_2} &= \frac{\rho_h u}{\rho_h + \rho\rho_p}, \\
\frac{\partial p}{\partial w_3} &= -\frac{\rho_h}{\rho_h + \rho\rho_p}
\end{aligned}
$$

and after substituting them in the jacobian matrix (eq. 4.2.3)

$$
J(W) = \frac{\partial F(W)}{\partial W} = \begin{bmatrix} 0 & 1 & 0 \\ -u^2 + \frac{2\rho_h+2\rho-\rho_h u^2}{2(\rho_h+\rho\rho_p)} & 2u + \frac{\rho_h u}{\rho_h+\rho\rho_p} & -\frac{\rho_h}{\rho_h+\rho\rho_p} \\ -u(h+\frac{u^2}{2}) + u\frac{2\rho_h+2\rho-\rho_h u^2}{2(\rho_h+\rho\rho_p)} & h + \frac{u^2}{2} + u\frac{\rho_h u}{\rho_h+\rho\rho_p} & u - u\frac{\rho_h}{\rho_h+\rho\rho_p} \end{bmatrix}.
$$

The pseudo speed of sound can be re-defined as

$$
c = \left[\frac{\rho_h}{\rho} + \rho_p\right]^{-\frac{1}{2}}
$$

that is not the speed of sound of the mixture as its values are far from the experimental results shown in [**41**] and [**50**], but has dimension of velocity.

If we diagonalize this new jacobian matrix we obtain the same eigenvalues

$$\begin{aligned}\lambda_1 &= u,\\ \lambda_2 &= u-c,\\ \lambda_3 &= u+c\end{aligned}$$

and the eigenvectors expressed as functions of these new derivatives

$$P_1 = \begin{bmatrix} \frac{\rho_h}{H\rho_h+\rho} \\ \frac{u\rho_h}{H\rho_h+\rho} \\ 1 \end{bmatrix},$$

$$P_2 = \begin{bmatrix} \frac{1}{h+\frac{u}{2}(u-2c)} \\ \frac{2(u^2-1)}{2h(u+c)+u(u^2-2c^2-u)} \\ 1 \end{bmatrix} = \begin{bmatrix} \frac{1}{H-uc} \\ \frac{2(u^2-1)}{2h(u+c)+u(u^2-2c^2-u)} \\ 1 \end{bmatrix},$$

$$P_3 = \begin{bmatrix} \frac{1}{h+\frac{u}{2}(u+2c)} \\ \frac{2(u^2-1)}{2h(u-c)+u(u^2-2c^2+u)} \\ 1 \end{bmatrix} = \begin{bmatrix} \frac{1}{H+uc} \\ \frac{2(u^2-1)}{2h(u-c)+u(u^2-2c^2+u)} \\ 1 \end{bmatrix}.$$

Non Conservative Case

The system of equations 4.2.1 can be written in the following non conservative form

$$\begin{aligned}\frac{\partial\rho}{\partial t}+u\frac{\partial\rho}{\partial x}+\rho\frac{\partial u}{\partial x}&=0,\\ \rho\frac{\partial u}{\partial t}+\rho u\frac{\partial u}{\partial x}+\frac{\partial p}{\partial x}&=\phi_m,\\ \rho\frac{\partial h}{\partial t}+\rho u\frac{\partial u}{\partial x}+\rho u\frac{\partial h}{\partial x}+\rho u^2\frac{\partial u}{\partial x}-\frac{\partial p}{\partial t}&=\phi_e.\end{aligned}$$

Considering as primitive variables $V=[u,p,h]^t$ and that

$$\begin{aligned}\frac{\partial\rho}{\partial t}&=\frac{\partial\rho}{\partial h}\frac{\partial h}{\partial t}+\frac{\partial\rho}{\partial p}\frac{\partial p}{\partial t},\\ \frac{\partial\rho}{\partial x}&=\frac{\partial\rho}{\partial h}\frac{\partial h}{\partial x}+\frac{\partial\rho}{\partial p}\frac{\partial p}{\partial x}\end{aligned}$$

we can write our system (eq. 4.2.1) in the following vector form

$$AV_t+BV_x=S \tag{4.2.5}$$

where matrices A and B, with previous notation, are given by

$$A = \begin{bmatrix} 0 & \rho_p & \rho_h \\ \rho & 0 & 0 \\ \rho u & -2 & \rho \end{bmatrix}, \qquad B = \begin{bmatrix} \rho & \rho_p u & \rho_h u \\ \rho u & 1 & 0 \\ \rho u^2 & 0 & \rho u \end{bmatrix}.$$

Premultiplying by A^{-1}, system 4.2.5 can be transform in

$$V_t + CV_x = A^{-1}S$$

where C is

$$C = A^{-1}B = \begin{bmatrix} u & \frac{1}{\rho} & 0 \\ \rho c^2 & u & 0 \\ c^2 & 0 & u \end{bmatrix}.$$

If we diagonalize matrix $C = QDQ^{-1}$ results that the eigenvalues are again $u - c, u, u + c$ with the following matrix of eigenvectors

$$Q = \begin{bmatrix} -\frac{1}{c} & 0 & \frac{1}{c} \\ \rho & 0 & \rho \\ 1 & 1 & 1 \end{bmatrix}.$$

4.3. Mathematical Analysis of the Separated Two Phase Flow System

4.3.1. Introduction

The 1D one pressure separated two phase flow is characterized by the following system of six equations:

Mass equations

$$\frac{\partial}{\partial t}(\alpha\rho_v) + \frac{\partial}{\partial x}(\alpha\rho_v u_v) = 0,$$
$$\frac{\partial}{\partial t}((1-\alpha)\rho_l) + \frac{\partial}{\partial x}((1-\alpha)\rho_l u_l) = 0.$$

Momentum equations

$$\frac{\partial}{\partial t}(\alpha\rho_v u_v) + \frac{\partial}{\partial x}(\alpha\rho_v u_v^2) + \alpha\frac{\partial p}{\partial x} = 0,$$
$$\frac{\partial}{\partial t}((1-\alpha)\rho_l u_l) + \frac{\partial}{\partial x}((1-\alpha)\rho_l u_l^2) + (1-\alpha)\frac{\partial p}{\partial x} = 0.$$

Energy equations

$$\frac{\partial}{\partial t}(\alpha\rho_v E_v) + \frac{\partial}{\partial x}(\alpha\rho_v H_v u_v) + p\frac{\partial \alpha}{\partial x} = 0,$$
$$\frac{\partial}{\partial t}((1-\alpha)\rho_l E_l) + \frac{\partial}{\partial x}((1-\alpha)\rho_l H_l u_l) - p\frac{\partial \alpha}{\partial x} = 0.$$

We can write the system as function of the conserved variables

$$W = (\alpha\rho_v, (1-\alpha)\rho_l, \alpha\rho_v u_v, (1-\alpha)\rho_l u_l, \alpha\rho_v E_v, (1-\alpha)\rho_l E_l)^t$$

$$\frac{\partial W}{\partial t} + \frac{\partial F(W)}{\partial x} + C(W) + D(W) = 0, \tag{4.3.1}$$

where the source terms have not been considered as they are not necessary for the analysis of the eigenstructure and

$$F(W) = \begin{bmatrix} \alpha\rho_v u_v \\ (1-\alpha)\rho_l u_l \\ \alpha\rho_v u_v^2 \\ (1-\alpha)\rho_l u_l^2 \\ \alpha\rho_v u_v H_v \\ (1-\alpha)\rho_l u_l H_l \end{bmatrix}, \quad C(W) = \begin{bmatrix} 0 \\ 0 \\ \alpha\frac{\partial p}{\partial x} \\ (1-\alpha)\frac{\partial p}{\partial x} \\ 0 \\ 0 \end{bmatrix} \quad \text{and} \quad D(W) = \begin{bmatrix} 0 \\ 0 \\ 0 \\ 0 \\ p\frac{\partial \alpha}{\partial t} \\ -p\frac{\partial \alpha}{\partial t}. \end{bmatrix}$$

This is the system of equation with which we will work in our developments.

On the other hand the non conservative form of the system of equations is obtained by writing the system 4.3.1 in quasi-linear form:

$$A\frac{\partial V}{\partial t} + B\frac{\partial V}{\partial x} = 0, \tag{4.3.2}$$

$$\frac{\partial V}{\partial t} + A^{-1}B\frac{\partial V}{\partial x} = 0 \tag{4.3.3}$$

where $V = (\alpha, u_v, u_l, p, e_v, e_l)^t$ is the vector of primitive variables.

Instead of using the equations for conservation of energy some researchers prefer to use the entropy equations:

$$\frac{\partial}{\partial t}(\alpha\rho_v s_v) + \frac{\partial}{\partial x}(\alpha\rho_v s_v u_v) = 0,$$
$$\frac{\partial}{\partial t}((1-\alpha)\rho_l s_l) + \frac{\partial}{\partial x}((1-\alpha)\rho_l s_l u_l) = 0.$$

From the study of matrix $A^{-1}B$ we can check that there are two trivial eigenvalues for the energy or entropy equations, they are the velocities of each phase, $\lambda = u_v$ and

$\lambda = u_l$. To analyse the character of the system many investigators prefer to consider only the isentropic model since the equation of state for densities for phase k

$$\rho_k = \rho_k(p, s_k)$$

with the speed of sound given by

$$c_k^{-2} = \left(\frac{\partial \rho_k}{\partial p}\right)_{s_k}.$$

For the culculation of the eigenstructure of the system we shall introduce in the next section some of the methods more utilized in its study.

4.3.2. Analysis of the Eigenvalues

We have studied that in order to make the system conditional or unconditionally hyperbolic some terms are introduced, they are virtual mass terms or terms that take into account the pressure difference between interface and phase.

Once we have chosen the system of equations which characterizes properly our problem, it is necessary to select a numerical method that provide us approximate solutions of such a system. Firstly, we should have a perfect knowledge of the mathematical character of the system. To reach this end we will study its eigenstructure, in particular its jacobian matrix.

The regularizing terms, depending on their complexity, make the quest for the eigenstructure more or less difficult. For the evaluation of the eigenvalues we can apply approximate methods which is easier than determining them analytically. Hence, for determining the eigenvalues we can use any of the methods we describe in the sequel:

- Numerical methods, despite it is an easy way of calculating them these methods imply a high computational cost.
- Perturbation methods, based on the introduction of a small parameter, we can distinguish:
  - Perturbation of density method.
  - Series development of the eigenvalues.
- Analytical expressions obtained by means of mathematical packages, such as Mathematica or Maple.

4.3.2.1. Perturbation Analysis

An application of this method to two phase flow has been developed in [**16**] by Cortes. He spreads it to different configurations of two phase flow. The two phase flow system of equations is written in the form

$$\frac{\partial U}{\partial t} + \frac{\partial f(U)}{\partial x} + G(U)\frac{\partial U}{\partial x} = 0$$

taking into account a general expression of the pressure correction term

$$p - p_k^i \frac{\partial \alpha_k}{\partial x} = \theta_k(U)\frac{\partial U_2}{\partial x}$$

where U are the conserved variables.

By means of the definition of the characteristic densities

$$\widetilde{\rho}_v = \frac{\rho_v}{\rho_v^0} \qquad \widetilde{\rho}_l = \frac{\rho_l}{\rho_l^0}$$

and the perturbation parameter $\epsilon = \frac{\rho_l^0}{\rho_l^0}$, the system of equations is re-written as a function of such variables

$$\frac{\partial U}{\partial t} + A(U)\frac{\partial U}{\partial x} = 0.$$

Additionally the matrix A is divided in other three, such that

$$A(U) = \frac{1}{\epsilon}A_{-1}(U) + A_0(U) + \epsilon A_1(U).$$

Then, the method consist of studying the eigenstructure of A through the knowledge of the eigenstructure of matrix $\frac{1}{\epsilon}A_{-1}(U) + A_0(U)$ that has not derivatives of pressure.

4.3.2.2. Taylor Expansion of the Eigenvalues

We have seen that two eigenvalues are trivial and coincide with the velocities of the fluids, u_l and u_v, then we can apply this method to the resulting polynomial of fourth degree. We can write our polynomial of coefficients in x, depending on a parameter θ little enough, and that can be written as

$$P(x(\theta), \theta) = P_0(x) + \theta P_1(x) + \frac{\theta^2}{2}P_2(x)$$

where $P_0(x(\theta))$, $P_1(x(\theta))$ and $P_2(x(\theta))$ are three polynomials with real coefficients. The parameter more commonly used is $\theta = \frac{u_v - u_{ll}}{a_m} << 1$, with a_m the speed of sound of the two phase mixture.

Let us consider x_0, a root of $P_0(x)$. If there exist a $\theta_0 \in \Re^+$ such that

- it is a simple root, then there exist a function $x(\theta)$, derivable in θ, such that
$$x(\theta) = x_0 + \theta x_1 + o(\theta)$$
with
$$x_1 = -\frac{P_1(x_0)}{P_0'(x_0)}$$
and that $P(x(\theta), \theta) = 0$ for each $\theta \in [-\theta_0, \theta_0]$.
- it is a double root and $P_1(x_0) = 0$, then there exist two derivable functions $x(\theta_0)$ and $y(\theta_0)$ in θ
$$x(\theta) = x_0 + \theta x_1 + o(\theta) \qquad \text{and} \qquad y(\theta) = x_0 + \theta y_1 + o(\theta)$$
where x_1 and y_1 are roots of the polynomial
$$P_0''(x_0)x^2 + 2P_1'(x_0) + P_2(x_0) = 0$$
such that $P(x(\theta), \theta) = P(y(\theta), \theta) = 0$.

Some examples of the application of this method to the solutions of two phase problems can be found in [**47**], [**57**] or [**79**].

4.3.2.3. Analytical Expressions

We can obtain an analytical expression of the eigenvalues by writing the characteristic polynomial as

$$(u_v - \lambda)(u_l - \lambda)(\lambda^4 + C_3\lambda^3 + C_2\lambda^2 + C_1\lambda + C_0) = 0,$$

the roots of the fourth order polynomial can be obtained using the Mathematica's packages. Then, we just have to substitute coefficients C_i depending on the case we consider, conservative or non conservative.

Non Coservative Case

In this case for the six equations model and taking into account the interfacial pressure correction term p_i, coefficients C_i are:

$$\begin{aligned} C_0 &= u_l^2 u_v^2 + (k_1 + k_2)u_l^2 + k_3, \\ C_1 &= -2u_l^2 u_v - 2u_l u_v^2 - 2k_1 u_l - 2k_2 u_v, \\ C_2 &= u_l^2 + 4u_l u_v + u_v^2 + k_1 + k_2, \\ C_3 &= -2u_l - 2u_v, \end{aligned}$$

where

$$\begin{aligned} k_1 &= -\frac{p_i(1-\alpha)c_v^2 - \alpha\rho_v\rho_l^2c_v^2c_l^2}{\alpha\rho_l c_l^2 + (1-\alpha)\rho_v c_v^2}, \\ k_2 &= -\frac{p_i\alpha c_l^2 - (1-\alpha)\rho_v^2\rho_l c_v^2 c_l^2}{\alpha\rho_l c_l^2 + (1-\alpha)\rho_v c_v^2}, \\ k_3 &= \frac{p_i c_v^2 c_l^2}{\alpha\rho_l c_l^2 + (1-\alpha)\rho_v c_v^2} \end{aligned}$$

with c_v and c_l the speeds of sound of each phase, vapour and liquid respectively.

Conservative Case.

In this case we arrived to a similar polynomial whose coefficients are a bit more complicated, that is why we have preferred not to include them. Anyhow, as we will study later, by using other mechanisms we will be able to avoid the calculation of the eigenstructure in the solution of the system of equations.

4.3.3. Eigenvectors Analysis

Once the eigenvalues have been obtained, the next step is to determine the matrix of eigenvectors and its inverse. We will do that independently of the method used to calculate the eigenvalues and for the conservative and non conservative cases. In [**37**] and [**70**] can be found detailed expressions for the eigenvector, we refer to the first one for the general non conservative problem where virtual mass and pressure correction terms are considered and to the second for the conservative case.

Let us consider the system of equations in non conservative form, given by

$$\begin{aligned} A\frac{\partial V}{\partial t} + B\frac{\partial V}{\partial z} &= 0 \\ \frac{\partial V}{\partial t} + A^{-1}B\frac{\partial V}{\partial z} &= 0 \end{aligned} \tag{4.3.4}$$

to determine the matrix of eigenvectors we have to solve the system

$$CP = BP\Lambda \tag{4.3.5}$$

where Λ is the diagonal matrix and P the matrix of eigenvectors. For the eigenvector P_j this is equivalent to solve

$$(B - A\lambda_j)P_j = 0$$

where λ_j is the j eigenvalue, and P_j its corresponding eigenvector. So the system of equations we get is the following

$$\rho_v(u_v-\lambda_j)P_{1j}+\alpha\rho_v P_{2j}+\alpha\frac{\partial\rho_v}{\partial p}(u_v-\lambda_j)P_{4j}+\alpha\frac{\partial\rho_v}{\partial h_v}(u_v-\lambda_j)P_{5j}=0$$
$$-\rho_l(u_l-\lambda_j)P_{1j}+(1-\alpha)\rho_l P_{3j}+\alpha\frac{\partial\rho_l}{\partial p}(u_l-\lambda_j)P_{4j}+(1-\alpha)\frac{\partial\rho_v}{\partial h_v}(u_l-\lambda_j)P_{6j}=0$$
$$\alpha(u_v-\lambda_j)P_{2j}+(1-\alpha)\rho_l(\lambda_l-u_l)P_{3j}+P_{4j}=0$$
$$\alpha(\lambda_j-u_v)P_{4j}+(u_v-\lambda_j)P_{5j}=0$$
$$(1-\alpha)(u_l-\lambda)P_{4j}+(1-\alpha)\rho_l(u_l-\lambda)P_{6j}=0.$$

Solving for P_j, we have for its components

$$\begin{aligned}
P_{1j} &= 1-\frac{\alpha(u_v-\lambda_j)^2}{c_v^2}-\frac{(1-\alpha)(u_l-\lambda_j)^2}{c_l^2},\\
P_{2j} &= \frac{\rho_l}{\alpha}(u_v-\lambda_j)\left[(u_l-\lambda_j)^2(\frac{\alpha}{\rho_v c_v^2}+\frac{1-\alpha}{\rho_l c_l^2})-\frac{1}{\rho_l}\right],\\
P_{3j} &= -\frac{\rho_v}{1-\alpha}(u_l-\lambda_j)\left[(u_v-\lambda_j)^2(\frac{\alpha}{\rho_v c_v^2}+\frac{1-\alpha}{\rho_l c_l^2})-\frac{1}{\rho_v}\right],\\
P_{4j} &= \rho_v(u_v-\lambda_j)^2-\rho_l(u_l-\lambda_j)^2,\\
P_{5j} &= (u_v-\lambda_j)^2-\frac{\rho_l}{\rho_v}(u_l-\lambda_j)^2,\\
P_{6j} &= \frac{\rho_v}{\rho_l}(u_v-\lambda_j)^2-(u_l-\lambda_j)^2.
\end{aligned}$$

The vectors corresponding to the trivial eigenvalues u_v and u_l cannot be obtained using the previous system, although we can get them directly, being them

$$P_5=(0,0,0,0,1,0)^t$$

and

$$P_6=(0,0,0,0,0,1)^t$$

respectively.

The last step is the calculation of the inverse of the eigenvector matrix, it can be obtained numerically by using the ISML routines for example, in such a case our computing time will increase drastically, or we can also get an analytical expression in the following way. Taking into account 4.3.5, premultiplying by $P^{-1}B^{-1}$ and post-multiplying by P^{-1} we arrive at

$$P^{-1}A^{-1}B=\Lambda P^{-1}$$

by transposing the system

$$B^tA^{-t}P^{-t}=P^{-t}\Lambda$$

where the superscript $-t$ has been used to denote the transpose of the inverse. This system can be transform into the following problem

$$B(A^{-t}P^{-t}) = A^t(A^{-t}P^{-t})\Lambda$$

or what is the same, the calculation of the eigenvectors $Q = B^{-t}P^{-t}$ of the system

$$B^tQ = A^tQ\Lambda.$$

for whose eigenvectors, this system is equivalent to

$$(B^t - \lambda_i A^t)Q_i = 0. \tag{4.3.6}$$

Once we have matrix Q, the inverse of the eigenvectors matrix can be determined as

$$P^{-1} = Q^tA. \tag{4.3.7}$$

Conservative Case

In this case the procedure is very similar to the non conservative case. Its calculation together with the evaluation of the eigenvalues has allowed to contrast the behaviour of the numerical schemes studied.

4.4. Schemes Used to Solve the Separated Two Phase Flow System of Equations

4.4.1. Introduction

In the last decade some traditional upwind schemes applied to hyperbolic system of conservation laws have been extended to two phase flow, in this context new developments have appeared. In the case of the homogeneous model (3 equations) the approximations have been many, and due to the conservative form of the system the use of conservative schemes have been done without too many problems. On the other hand, despite the non conservative character of the two phase flow systems of four and six equations, some researchers have extended conservative schemes in order to guarantee a perfect resolution of discontinuities, among them we can stand out the works by Toumi [**77**] or Berger [**7**]. The utilization of non conservative schemes is more common, the work by Staëdtke et al. [**64**] or the one by Tiselj and Petelin on the RELAP system of equations [**71**] are good examples of this practice. In this thesis we have worked on the idea of the extension of conservative schemes to two phase flow.

If we take in consideration the vector form of the system of equations without source term

$$U_t + F(U)_x = 0,$$

in the conservative case we can solve it approximately by means of

$$U_i^{n+1} = U_i^n - \frac{\Delta t}{\Delta x}[F_{i+\frac{1}{2}} - F_{i-\frac{1}{2}}]$$

where the numerical flux is given by

$$F_{i+\frac{1}{2}} = F_i^+(U_i^n) + F_{i+1}^-(U_{i+1}^n).$$

Unlike centred schemes, upwind methods perform the discretization of the equations taking into account the direction of propagation of information in such a way that physical phenomena modelled by the equations are incorporated into the model. Upwind methods are usually classified in

- Flux Difference Splitting schemes, such as Godunov-type methods, the Roe and Osher's methods, etc., in them neighbouring cells interact through discrete, finite - amplitude waves that are found by solving exact or approximate Riemann problems.
- Flux Vector Splitting, which are techniques that distinguish between the influence of the forward and backward moving particles in the fluid. The Steger and Warming scheme or the van Leer scheme are examples of them.

The difference between these schemes is in how the numerical flux is defined, a complete introduction and review of many of such schemes can be found in books, now classics, by Leveque [**42**] or Toro [**76**], these schemes and other interesting methods will be briefly described in the following sections. Before introducing some recent application of upwind schemes to two phase flow, we must describe other relevant features of the Flux Difference and Flux Vector Splitting schemes.

4.4.2. Flux Difference Splitting versus Flux Vector Splitting Schemes

In the case of flux difference splitting schemes, the flux difference between the right and the left states is given by

$$F(u_R) - F(u_L) = (\Delta F)^+(u_L, u_R) + (\Delta F)^-(u_L, u_R).$$

These type of splitting are called flux difference splitting because the flux difference, $F(u_L) - F(u_R)$ is splitted into two parts, each associated with downstream and upstream travelling waves as we can see in figure 4.4.2, so

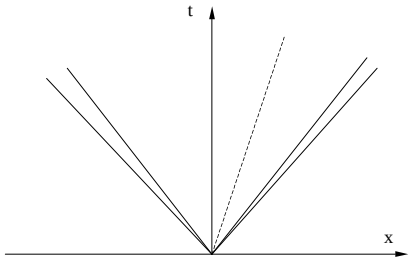

FIGURE 4.1. Structure of the solution based on travelling waves

$$\begin{aligned} f(u_L, u_R) &= F(u_L) + (\Delta F)^-(u_L, u_R) \\ &= F(u_R) - (\Delta F)^+(u_L, u_R) \\ &= \frac{1}{2}\{F(u_L) + F(u_R) - (\Delta F)^+(u_L, u_R) + (\Delta F)^-(u_L, u_R)\} \end{aligned}$$

On the other hand, the basic idea of the flux vector splitting schemes is to express the flux as a sum of two vectors

$$F(U) = F^+ - F^-$$

with the corresponding jacobian matrices

$$B^\pm = \frac{\partial F^\pm}{\partial U}$$

being for consistency $B^+ + B^- = A$ but $B^\pm \neq A^\pm$.

We observe that in these type of schemes the flux is expressed by

$$f(u_L, u_R) = F^+(u_L) + F^-(u_R).$$

A physical interpretation of this flux can be done just taking a look at figure 4.4.2 where the intercell flux is made out from two contributions, one from the forward component F_i^+ in the left cell and other from the right cell F_{i+1}^-.

The main advantage of FVS with respect to FDS is that the identification of upwind directions is accomplished with less effort than in Godunov-type methods, leading to simpler and more efficient schemes. In general they are less sophisticated and even do not involve to differeciate the flux vector to determine the numerical fluxes, being its main disadvantage to have a poorer resolution of discontinuities, particularly in the case of stationary contact and shear waves.

More recently, a new type of schemes has appeared, researchers call them hybrid flux splitting schemes. They appear as an attempt to improve FDS and FVS by

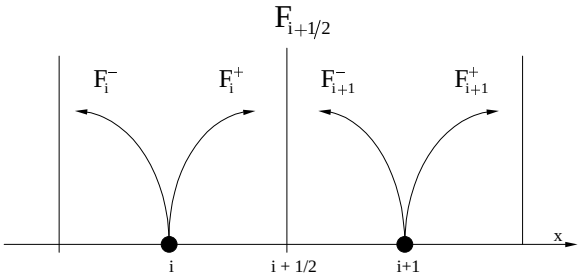

FIGURE 4.2. Splitting of the flux in cell i at time n

combining their advantages in a flux formulation, examples of them are AUSM [**45**], LDFSS [**22**] and HUS [**14**], they belong to this kind of schemes that have some of the features of FDS and FVS, basically:

(1) Robustness of flux vector splitting in capture of genuinely non linear waves, strong shocks and large rarefaction waves.
(2) Preserve the property met by the FVS methods to select only entropy satisfying approximate solutions.
(3) Offer the decisive ability of some flux difference splitting methods to exactly capture stationary contact discontinuities.

In particular, the AUSM schemes (sort for Advected Upstream Splitting Method) have been built upon the van Leer splitting [**82**], since its beginning the original AUSM [**45**] has suffered several improvements and some variants have been proposed. Their extension to two phase flow is going to be an important part of this work.

4.4.3. Roe's Approximate Riemann Solver

In order to overcome the problem of the non conservative terms of the two phase system, Toumi et al. in [**79**] and [**78**] linearize the non conservative products which provides them the possibility of constructing a linearized Riemann solver and a Roe averaged matrix. They study the isentropic two fluid model as much as the six equation models.

4.4.3.1. System of Equations

For the case of the six equations two fluid model, Toumi considers in [**78**] the following system of equations:

Mass equations

$$\frac{\partial}{\partial t}(\alpha_v\rho_v) + \frac{\partial}{\partial x}(\alpha_v\rho_v u_v) = \Gamma_v,$$
$$\frac{\partial}{\partial t}(\alpha_l\rho_l) + \frac{\partial}{\partial x}(\alpha_l\rho_l u_l) = \Gamma_l.$$

Momentum equation

$$\frac{\partial}{\partial t}(\alpha_v\rho_v u_v) + \frac{\partial}{\partial x}(\alpha_v\rho_v u_v^2) + \alpha_v\frac{\partial p}{\partial x} + I = \alpha_v\rho_v B + F_v^w + F^i,$$
$$\frac{\partial}{\partial t}(\alpha_l\rho_l u_l) + \frac{\partial}{\partial x}(\alpha_l\rho_l u_l^2) + \alpha_l\frac{\partial p}{\partial x} - I = \alpha_l\rho_l B + F_l^w - F^i.$$

Energy equations

$$\frac{\partial}{\partial t}(\alpha_v\rho_v E_v) + \frac{\partial}{\partial x}(\alpha_v\rho_v H_v u_v) + p\frac{\partial \alpha_v}{\partial t} = \alpha_v\rho_v u_v B + Q_v^w + Q_v^i - \Gamma_v h_v^*,$$
$$\frac{\partial}{\partial t}(\alpha_l\rho_l E_l) + \frac{\partial}{\partial x}(\alpha_l\rho_l H_l u_l) + p\frac{\partial \alpha_l}{\partial t} = \alpha_l\rho_l u_l B + Q_l^w + Q_l^i - \Gamma_l h_l^*.$$

To reach their linearized Riemann solver they take advantage of several hypothesis:

- Incompressible liquid phase with constant density
- For clarity in the development, they suppose the gas as perfect, although later they apply their solver to problems with change of phase such as blowdown tests.

4.4.3.2. Numerical Scheme

The numerical method applied in [**78**] is a first order upwind scheme that with their own notation is given by

$$W_j^{n+1} = W_j^n - \frac{\Delta t}{\Delta x}(F^+(U_{j-1}^n, U_j^n) - F^+(U_j^n, U_{j+1}^n))$$

with the positive and negative part of the flux given by

$$\begin{aligned} F^+(U_{j-1}^n, U_j^n) &= A^+(U_{j-1}^n, U_j^n)_\Phi(U_j^n - U_{j-1}^n) \\ F^+(U_j^n, U_{j+1}^n) &= A^-(U_j^n, U_{j+1}^n)_\Phi(U_{j+1}^n - U_j^n) \end{aligned}$$

where the matrix $A(v)$ is evaluated at an average state $\tilde{v}$ defined by $\tilde{\alpha}_k$, $\tilde{u}_k$, $\tilde{H}_k$ and $\tilde{p}_v^i$. To avoid complex eigenvalues they introduce the pressure correction term already presented in eq. 3.2, it is evaluated in the average state as well, this is

$$\tilde{I} = I(\tilde{v}) = \tilde{\alpha}_v\tilde{\delta}(\tilde{u}_v - \tilde{u}_l)^2\frac{\partial}{\partial x}(\alpha_l\rho_l).$$

4.4.4. Flux Schemes (VFFC)

In this section we introduce the flux schemes (VFFC), a kind of schemes developed by Ghidaglia et al. They are described in [**27**] and extensive reviews with some numerical results can be found in [**26**] and [**28**]. We must also mention their extension to two and three dimensions, done by Boucker in [**9**]. In the following we present some interesting characteristics of these type of schemes.

4.4.4.1. System of Equations

As we have already seen above the one dimensional system of equations can be written as

$$W_t + F_x(W) + C(W) + D(W) = S(W), \tag{4.4.1}$$

This system can be transformed, in the general case, into

$$\frac{\partial W}{\partial t} + \frac{\partial F(W)}{\partial x} + C'(W)\frac{\partial W}{\partial x} + D'(W)\frac{\partial W}{\partial t} = S(W) \tag{4.4.2}$$

where $C'(W)$ and $D'(W)$ are two matrices given by

$$C'(W) = \begin{bmatrix} 0 & 0 & 0 & 0 & 0 & 0 \\ 0 & 0 & 0 & 0 & 0 & 0 \\ -p & 0 & 0 & 0 & 0 & 0 \\ p & 0 & 0 & 0 & 0 & 0 \\ 0 & 0 & 0 & 0 & 0 & 0 \\ 0 & 0 & 0 & 0 & 0 & 0 \end{bmatrix} \quad \text{and} \quad D'(W) = \begin{bmatrix} 0 & 0 & 0 & 0 & 0 & 0 \\ 0 & 0 & 0 & 0 & 0 & 0 \\ 0 & 0 & 0 & 0 & 0 & 0 \\ 0 & 0 & 0 & 0 & 0 & 0 \\ p & 0 & 0 & 0 & 0 & 0 \\ -p & 0 & 0 & 0 & 0 & 0 \end{bmatrix}$$

and considering $(I + D'(W))^{-1}$, 4.4.2 can be reduced to

$$\frac{\partial W}{\partial t} + \frac{\partial F(W)}{\partial x} + C'(W)\frac{\partial W}{\partial x} = S(W) \tag{4.4.3}$$

with a new redefinition of each matrix and assuming the inversion of $(I + D'(W))^{-1}$. In the case of the analysis of separated two phase flow, to arrive to a simpler expression of $C'(W)$ they consider vapour as a perfect gas, liquid as incompressible and no change of phase is permitted. This allows them to write time derivatives as spatial derivatives just by taking into account the continuity equation of the liquid (see references cited

above). Thus from this point of view they yield the following matrix

$$C'(W) = \begin{bmatrix} 0 & 0 & 0 & 0 & 0 & 0 \\ 0 & 0 & 0 & 0 & 0 & 0 \\ 0 & \frac{p}{\rho_l} & 0 & 0 & 0 & 0 \\ 0 & -\frac{p}{\rho_l} & 0 & 0 & 0 & 0 \\ 0 & 0 & 0 & \frac{p}{\rho_l} & 0 & 0 \\ 0 & 0 & 0 & -\frac{p}{\rho_l} & 0 & 0 \end{bmatrix}.$$

4.4.4.2. Numerical Scheme

They propose the following explicit version for the flux schemes

$$W_j^{n+1} = W_j^n - \frac{\Delta t_n}{\Delta x}(I + E(W_j^n))(G_j^n(W_j^n, W_{j+1}^n) - G_j^n(W_{j-1}^n, W_{j+1}^n))$$

with $E(W_j^n) = C(W_j^n)J(W_j^n)^{-1}$ and the numerical flux

$$G(\mu; V, W) = \frac{F(V) + F(W)}{2} - U(\mu; V, W)\frac{F(V) - F(W)}{2}$$

where V and W are the left and right states respectively $U(\mu; V, W)$ is the sign of the matrix $A(W)$ that is defined as

$$U(\mu; V, W) = \text{sign}(A) = P\text{sign}(D)P^{-1}$$

and $\text{sign}(D) = diagonal(\text{sign}(\lambda_1)...\text{sign}(\lambda_6))$ with λ_i its eigenvalues.

We refer to Appendix A for an explanation of the sign of a matrix and the available methods for its evaluation.

To conclude we define matrix $A(W)$ as the result of considering that eq. 4.4.3 can be arranged, considering the jacobian matrix $J(W) = \frac{\partial F}{\partial W}$, as

$$\frac{\partial F(W)}{\partial t} + A(W)\frac{\partial F(W)}{\partial x} = 0$$

where $A(W) = J(W)(I + C(W)J(W)^{-1})$.

4.4.5. General Form of the VFFC Scheme

In this section we will describe a generalization of the VFFC scheme which is also suggested in [**80**]. We again consider the form of the six equation system presented in eq. 4.4.1

$$W_t + F_x(W) + C(W) + D(W) = S(W). \tag{4.4.4}$$

We can rewrite the system as equation 4.4.2 defining different $C'(W)$ and $D'(W)$

$$C(W) = C'(W)\frac{\partial W}{\partial x} = \begin{bmatrix} 0 & 0 & 0 & 0 & 0 & 0 \\ 0 & 0 & 0 & 0 & 0 & 0 \\ -p & 0 & 0 & 0 & 0 & 0 \\ p & 0 & 0 & 0 & 0 & 0 \\ 0 & 0 & 0 & 0 & 0 & 0 \\ 0 & 0 & 0 & 0 & 0 & 0 \end{bmatrix} \frac{\partial V}{\partial W}\frac{\partial W}{\partial x},$$

$$D(W) = D'(W)\frac{\partial W}{\partial t} = \begin{bmatrix} 0 & 0 & 0 & 0 & 0 & 0 \\ 0 & 0 & 0 & 0 & 0 & 0 \\ 0 & 0 & 0 & 0 & 0 & 0 \\ 0 & 0 & 0 & 0 & 0 & 0 \\ p & 0 & 0 & 0 & 0 & 0 \\ -p & 0 & 0 & 0 & 0 & 0 \end{bmatrix} \frac{\partial V}{\partial W}\frac{\partial W}{\partial t}.$$

Now we can write the system as 4.4.2 and grouping terms we have

$$(I + D'(W))\frac{\partial W}{\partial t} + (J(W) + C'(W))\frac{\partial W}{\partial x} = S(W)$$

premultiplying by $(I + D'(W))^{-1}$

$$\frac{\partial W}{\partial t} + (I + D'(W))^{-1}(J(W) + C'(W))\frac{\partial W}{\partial x} = (I + D'(w))^{-1}S(W). \tag{4.4.5}$$

4.4.5.1. Numerical Scheme for the General Form of the VFFC

For the evaluation of the numerical flux, let us consider that eq. 4.4.5 can be arranged as,

$$\frac{\partial F(W)}{\partial t} + A(W)\frac{\partial F(W)}{\partial x} = 0$$

where now $A(W) = J(W)(I + D(W))^{-1}(J(W) + C(W))J(W)^{-1}$.

In a similar manner that with the VFFC scheme we can propose the following explicit scheme for the approximate solution of system 4.4.5

$$W_j^{n+1} = W_j^n - \frac{\Delta t_n}{\Delta x}(I + D(W_j^n))^{-1}(I + E(W_j^n))(G_j^n(W_j^n, W_{j+1}^n) - G_j^n(W_{j-1}^n, W_{j+1}^n)) \\ +\Delta t_n(I + D(W_j^n))^{-1}(I + E(W_j^n))S_j^n$$

with $E(W_j^n) = C(W_j^n)J(W_j^n)^{-1}$ and the numerical flux

$$G(\mu; V, W) = \frac{F(V) + F(W)}{2} - U(\mu; V, W)\frac{F(V) - F(W)}{2}$$

where $U(\mu; V, W)$ is the sign of the new matrix $A(W)$. It is defined as

$$\text{sign}(A) = J(W)\text{sign}\left[(I + D(W))^{-1}(J(W) + C(W))\right]J^{-1}(W).$$

4.4.6. Städtke's Flux Vector Splitting

Presented by Städtke et al. in [**64**] and [**65**], its good capabilities have been widely demonstrated in a great variety of problems, recently in [**63**] for example. Its extension to two and three dimensions can be found in [**62**]. They prefer to consider the following system of six equations by using the equation for conservation of entropy instead of the energy equation. In the next section we are going to study this scheme a bit more thoroughly.

4.4.6.1. System of Equations

Thus in this case the system of equations is given by the following conservation laws

Mass equations

$$A\frac{\partial}{\partial t}(\alpha\rho_v) + \frac{\partial}{\partial x}(\alpha\rho_v u_v A) = A\sigma_v^M,$$
$$A\frac{\partial}{\partial t}((1-\alpha)\rho_l) + \frac{\partial}{\partial x}((1-\alpha)\rho_l u_l A) = A\sigma_l^M.$$

Momentum equations

$$A\frac{\partial}{\partial t}(\alpha\rho_v u_v) + \frac{\partial}{\partial x}(\alpha\rho_v u_v^2 A) + \alpha A\frac{\partial p}{\partial x} = AF_g^{int} + AF_g^{ext} + A\sigma_v^M u^{ext},$$
$$A\frac{\partial}{\partial t}((1-\alpha)\rho_l u_l) + \frac{\partial}{\partial x}((1-\alpha)\rho_l u_l^2 A) + (1-\alpha)A\frac{\partial p}{\partial x} = AF_f^{int} + AF_f^{ext} - A\Gamma u^{ext}.$$

Entropy equations

$$A\frac{\partial}{\partial t}(\alpha\rho_v s_v) + \frac{\partial}{\partial x}(\alpha\rho_v s_v u_v A) = A\frac{\sigma_v^Q}{T_v} + A\frac{F_v^{int}}{T_v}(u_v^{int} - u_v)$$
$$+A\frac{\sigma_v^M}{T_v}\left[h^{ex} - h_v + \frac{1}{2}(u^{ex} - u_v)^2\right] + A\sigma_v^M s_v,$$
$$A\frac{\partial}{\partial t}((1-\alpha)\rho_l s_l) + \frac{\partial}{\partial x}((1-\alpha)\rho_l s_l u_l A) = A\frac{\sigma_l^Q}{T_l} + A\frac{F_l^{int}}{T_l}(u_l^{int} - u_l)$$
$$+A\frac{\sigma_l^M}{T_l}\left[h^{ex} - h_l + \frac{1}{2}(u^{ex} - u_l)^2\right] + A\sigma_l^M s_l,$$

so the vector of conserved variables is $W = (\alpha\rho_v, (1-\alpha)\rho_l, \alpha\rho_v u_v, (1-\alpha)\rho_l u_l, \alpha\rho_v s_v, (1-\alpha)\rho_l s_l)^t$.

To guarantee hyperbolicity of the system they split the interfacial forces in the momentum equations into viscous and non viscous parts

$$F_k^{int} = F_k^v + F_k^{nv}$$

where F_k^v represents the interfacial drag forces that are described as $F_k^v = c_{drag}\rho_{cont}(u_v - u_l)$ and F_k^{nv} is a term that considers the virtual mass force and several space derivatives of void fraction and densities that allows to attain a fully hyperbolic system of equations.

This system can be written in non conservative form as

$$A\frac{\partial V}{\partial t} + B\frac{\partial V}{\partial x} = C$$

where $V = (\alpha, u_v, u_l, p, s_v, s_l)^t$ is the vector of primitive variables. If we premultiply by A^{-1} we have

$$\frac{\partial V}{\partial t} + G\frac{\partial V}{\partial x} = D \tag{4.4.6}$$

where $G = A^{-1}B$ and $D = A^{-1}C$.

We can diagonalize $G = T\Lambda T^{-1}$, and transform 4.4.6 in

$$\frac{\partial V}{\partial t} + T\Lambda T^{-1}\frac{\partial V}{\partial x} = D.$$

Now we are going to consider the matrix of change $J = \frac{\partial W}{\partial V}$, and we will operate our system in the following way

$$\begin{aligned} J^{-1}J\frac{\partial V}{\partial t} + T\Lambda T^{-1}J^{-1}J\frac{\partial V}{\partial x} &= D, \\ J^{-1}\frac{\partial W}{\partial t} + T\Lambda T^{-1}J^{-1}\frac{\partial W}{\partial x} &= D, \end{aligned}$$

so after premultiplying by J, we have this system

$$\frac{\partial W}{\partial t} + JT\Lambda T^{-1}J^{-1}\frac{\partial W}{\partial x} = E.$$

with $E = JD$

Finally they write the system as

$$\frac{\partial W}{\partial t} + \frac{\partial F}{\partial x} + H\frac{\partial F}{\partial x} = E$$

where $H = (JG - K)K^{-1}$ with $K = \frac{\partial F}{\partial V}$.

4.4.6.2. Numerical Scheme

They define the following numerical scheme

$$W_j^{n+1} = W_j^n - \frac{\Delta t}{\Delta x}(F_{j+\frac{1}{2}} - F_{j-\frac{1}{2}}) - \frac{\Delta t}{\Delta x}([H]^{nc})(F_{j+\frac{1}{2}} - F_{j-\frac{1}{2}}) + E_i^{n+1}\Delta t.$$

The numerical flux is derived by mean of the approximate solution of the Riemann problem between two adjacent cells. For this purpose, the basic equations 4.4.6 are transformed into

$$\frac{\partial F}{\partial t} + R\frac{\partial F}{\partial x} = E' \tag{4.4.7}$$

with the coefficient matrix $R = KGK^{-1}$ and $E' = KD$. This is basically what have been done in the general VFFC.

So the numerical flux is defined as

$$F_{j+\frac{1}{2}} = \sum_{k,\lambda_k>0} (\widetilde{R}_k)_{j+\frac{1}{2}}(F_k)_i + \sum_{k,\lambda_k<0} (\widetilde{R}_k)_{j+\frac{1}{2}}(F_k)_{i+1}.$$

Different averages can be chosen for the average state, the one suggested by Toumi et al. in [**80**] could be an option. More information regarding this flux can be found in the references cited above.

We have to remark that this formulation is similar to the generalization of the VFFC scheme, the difference resides in that VFFC is formulated in terms of the conserved variables and this is derived under a primitive variable formulation.

4.4.7. Other Recent Developments

Furthermore the schemes described above a lot of improvements have been done in numerical methods applied to two phase flow. In this section we are going to cite some of them.

As commented, Lee in [**41**] and [**40**] makes an interesting contribution in the field of the characterization of the speed of sound applying a flux splitting scheme to the solution of the two phase system of equations. Recently Saurel and Abgrall in [**58**] have studied the two pressure model adding a seventh equation for the evolution of the void fraction in order to close the system. Two numerical schemes have been applied to this system, a modified Godunov-Rusanov scheme and a Godunov-HLL scheme.

Regarding to non conservative schemes, we would like to stand out the work by Tiselj and Petelin in [**71**], [**72**], [**73**] and [**74**] where proposed a first and second order upwind scheme in order to solve a modified version of the two phase system of RELAP. They accomplished second order using extrapolation of variables (MUSCL approximation) and avoided oscillations by using slope limiters. It is fairly interesting their experiences with respect to the use of conserved or non conserved variables. They even study a very similar formulation to the general VFFC or the Städtke's flux vector splitting method. Hwang in his general paper [**37**] on the analysis of the eigenstructure of the two fluid model tackles some Toumi's experiments utilizing an explicit multi-step difference scheme of a linearized Riemann solver. Its second order version is derived by using the van Leer interpolation function.

Another important work is [**13**] by Coquel et al. where they introduce a splitting technique in which non conservative terms are discretized apart of the flux with different techniques. The method is based on a decomposition of the problem in other two:

(1) Solution of two classical and decoupled hydrodynamic systems using approximate Riemann solvers, kinetic solvers in particular where they include the source terms and
(2) Restoring the equality of pressures.

This kind of decoupling becomes an interesting point of view in the solution of the system of equations that was put in practice by Toro in [**75**] as well. In the next chapter we will take advantage of these techniques and experiences in order to extend some conservative schemes to two phase flow, before that we will introduce some of the advances done in the solution of the homogeneous two phase flow.

4.5. Schemes Used to Solve the Homogeneous Two Phase Flow System of Equations

As commented above the homogeneous model have been mostly studied using the non conservative form of the system. Among these applications we can stand out the Banerjee and Hancox's approach in which they use the method of characteristics [**5**]. In many cases, the studies on homogeneous flow are preliminary works which serve as initial applications of a scheme to two phase flow. Despite its scarce applicability to real problems, its simplicity makes it be the first candidate when anyone wants to study the potential of a scheme, even although it is not able to account for phenomena such as annular flow, gas with droplets or even more complicated regimes. Anyhow, many interesting applications or related development have appeared that are worthwhile to mention for their practical interest, this is the objective of the following sections.

4.5.1. Roe's Approximate Riemann Solver

Toumi developed in [**77**] a weak formulation of the Roe's approximate Riemann solver and he extended it to the four and six equations models in subsequent works as we has already studied. His model relies on the definition of a matrix using an averaged state at the intercell, which is similar to the one defined by Roe, that allows to linearized the Riemann problem. The jacobian matrix for the average state defined in [**77**] has the following form

$$A = \begin{bmatrix} 0 & 1 & 0 \\ \frac{\widetilde{\gamma}-3}{2}\widetilde{u}^2 + (\widetilde{\gamma}-1)\widetilde{\alpha} & -(\widetilde{\gamma}-3)\widetilde{u} & \widetilde{\gamma}-1 \\ -\widetilde{H} + \frac{\widetilde{\gamma}-1}{2}\widetilde{u}^2)\widetilde{u} + (\widetilde{\gamma}-1)\widetilde{u}\widetilde{\alpha} & \widetilde{H} - (\widetilde{\gamma}-1)\widetilde{u}^2 & \widetilde{\gamma}\widetilde{u} \end{bmatrix}.$$

Its eigenvalues are $\widetilde{u}-\widetilde{a}, \widetilde{u}$ and $\widetilde{u}-\widetilde{a}$ where $\widetilde{a}$ is an average speed of sound given by

$$\widetilde{a}^2 = (\widetilde{\gamma}-1)(\widetilde{H} - \frac{\widetilde{u}^2}{2} + \widetilde{\alpha}).$$

4.5.2. Flux Schemes (VFFC)

Ghidaglia et al. proposed in [**26**] the Flux Schemes which have been applied to the two fluid six equation model with success. In the same context they have also applied

it to the homogeneous model [**19**] considering change of phase, in this case the explicit flux scheme is given by

$$W_j^{n+1} = W_j^n - \frac{\Delta t_n}{\Delta x}(G_j^n(W_j^n, W_{j+1}^n) - G_j^n(W_{j-1}^n, W_{j+1}^n))$$

with

$$G(\mu; V, W) = \frac{F(V) + F(W)}{2} - U(\mu; V, W)\frac{F(V) - F(W)}{2}$$

where $U(\mu; V, W)$ is the sign of the matrix $J(W)$ which have been defined in Appendix A.

4.5.3. AUSM Scheme

This scheme will be widely described in the next chapter as it is one of the schemes we will extend to compressible and non steady two phase flow. It was developed by Liou initially in [**45**] and its application to homogeneous two phase flow was presented in [**49**]. More recently a comparison of this scheme with the Roe and the VFFC was presented in [**52**]. Basically it is based on a splitting of the flux into a convective part associated to the mass flux $\dot{m} = \rho u = \rho a M$ an a pressure part, so the numerical flux in the middle is given by

$$F_{\frac{1}{2}}(U_L, U_R) = F^c_{\frac{1}{2}} + P_{\frac{1}{2}} = \dot{m}\frac{1}{2}\Psi_{\frac{1}{2}} + \begin{pmatrix} 0 \\ p_{\frac{1}{2}} \\ 0 \end{pmatrix}$$

and a simple upwinding based on the sign of $\dot{m}_{\frac{1}{2}}$ is used to compute $\Psi_{\frac{1}{2}}$.

4.5.4. Flux Vector Splitting

In this section we will introduce another original development appeared recently. It consists of the application of Flux Vector Splitting Methods to homogeneous two phase flow. It has been done by Comino et al. in [**12**] where they manipulate the system of equations to arrive to the following non conservative version of the homogeneous system:

$$\frac{\partial \alpha}{\partial t} + \frac{(\rho k)_m}{\rho_{fg}}\frac{\partial p}{\partial t} + \frac{\partial G}{\partial z}\frac{1}{\rho_{fg}} = 0,$$

$$\frac{\partial G}{\partial t} + \frac{2G}{\rho_m}\frac{\partial G}{\partial z} + \left[1 - \frac{G^2}{\rho_m^2}(\rho k)_m\right]\frac{\partial p}{\partial z} - \frac{G^2\rho_{fg}}{\rho_m^2}\frac{\partial \alpha}{\partial z} = a,$$

$$\frac{\partial p}{\partial t} + \frac{G}{\rho_m}\frac{\partial p}{\partial z} + \frac{\rho_f\rho_g h_{fg}}{\rho_m d}\left\{\frac{\partial \alpha}{\partial t} + \frac{G}{\rho_m}\frac{\partial \alpha}{\partial z}\right\} = \frac{a}{b}.$$

After some manipulations, they solve the system of equation given by

$$\frac{\partial W}{\partial t} + D\frac{\partial W}{\partial z} = E$$

where $W = [G, p, \alpha]$. D and E are the result of operating in the previous system of equations.

The explicit scheme they propose is

$$W_j^{n+1} = W_j^n + E_j^n - \left[D_j^{+n}(W_j^n - W_{j-1}^n) + D_j^{-n}(W_{j+1}^n - W_j^n)\right]\frac{\Delta t}{\Delta z}$$

A complete derivation of the equations and matrices $D^{\pm}$ presented above can be found in [**12**].

We finish this chapter mentioning another interesting work by [**14**] that combines the study of homogenous two phase flow with the preconditioning methodology for low Mach number fluxes. Despite many others two phase applications have not been described we have highlighted some of the most relevant directions in the two phase flow field that researchers are following at the present moment.

Chapter 5

Development of Conservative Schemes for Two Phase Flow

5.1. Introduction

In this chapter we will study the application to two phase flow of advanced conservative schemes of the type

$$W_j^{n+1} = W_j^n - \frac{\Delta t}{\Delta x}\left[F_{j+\frac{1}{2}} - F_{j-\frac{1}{2}}\right] - \Delta t S_j^n. \tag{5.1.1}$$

Alternatively to the schemes that use the non conservative form of the equations, in the present thesis we will transform it into a conservative set of equations by means of the inclusion of non conservative terms in the source term. This will be one of the main ideas on which our work is based. In particular it will be concerned with the extension of TVD (Total Variation Diminishing, introduced in [**30**]), ATVD (Adapted TVD, introduced in [**24**]) and AUSM (Advected Upstream Splitting Method, introduced in [**45**]) schemes. In a first approximation we are going to study its extension to two phase mixtures, without considering change of phase and leaving it for further works.

In the first part we will focus on the study of the system of equations and its eigenstructure. Then we will introduce TVD schemes and its application to two phase flow. Then we will develop the ATVD schemes and we will explore their capabilities to analyse two phase flow problems. Finally we will analyse the AUSM schemes, namely AUSM+ and AUSMDV.

5.2. On the System of Six Equations in 1D Two Phase Flow

In previous sections, we have seen that the two phase flow system of six equations, in which the phases are considered independently and separated by the interface, can be written in non conservative form as follow

$$W_t + F_x(W) + C(W) + D(W) + S(W) = 0 \tag{5.2.1}$$

where W is the vector of conserved variables

$$W = \begin{bmatrix} \alpha\rho_v \\ (1-\alpha)\rho_l \\ \alpha\rho_v u_v \\ (1-\alpha)\rho_l u_l \\ \alpha\rho_v E_v \\ (1-\alpha)\rho_l E_l \end{bmatrix} = \begin{bmatrix} w_1 \\ w_2 \\ w_3 \\ w_4 \\ w_5 \\ w_6 \end{bmatrix} \tag{5.2.2}$$

with $E_k = e_k + \frac{u_k^2}{2}$.

$F(w)$ is the flux vector and is given by

$$F(w) = \begin{bmatrix} \alpha\rho_v u_v \\ (1-\alpha)\rho_l u_l \\ \alpha\rho_v u_v^2 + \alpha p \\ (1-\alpha)\rho_l u_l^2 + (1-\alpha)p \\ \alpha\rho_v H_v u_v \\ (1-\alpha)\rho_l H_l u_l \end{bmatrix}, \tag{5.2.3}$$

with $H_k = h_k + \frac{u_k^2}{2}$.

$C(W)$, $D(W)$ are the non conservative terms and $S(w)$ is the source term
(5.2.4)

$$C(W) = \begin{bmatrix} 0 \\ 0 \\ -p^i \frac{\partial \alpha}{\partial x} \\ p^i \frac{\partial \alpha}{\partial x} \\ 0 \\ 0 \end{bmatrix}, \qquad D(W) = \begin{bmatrix} 0 \\ 0 \\ 0 \\ 0 \\ p^i \frac{\partial \alpha}{\partial t} \\ -p^i \frac{\partial \alpha}{\partial t} \end{bmatrix}, \qquad S(W) = \begin{bmatrix} -\Gamma \\ \Gamma \\ -\alpha \rho_v g - \varphi_v \\ -(1-\alpha)\rho_l g - \varphi_l \\ -\alpha \rho_v g u_v - \psi_v \\ -(1-\alpha)\rho_l g u_l - \psi_l \end{bmatrix}$$

where p^i stands for the difference of pressure between each phase and the interface. As discussed in previous chapters, this term is included to make the system of equations hyperbolic, the approximation we will use is the one used in the CATHARE code, already presented in chapter 3 earlier

$$p^i = p - p_i = \sigma \frac{\alpha(1-\alpha)\rho_v \rho_l}{\alpha \rho_l + (1-\alpha)\rho_v}(u_v - u_l)^2.$$

On the other hand Γ, φ_k and ψ_k, take into account mass transfer through the interface, wall and interfacial frictions and heat transfer through the walls and between the phases. Depending on the problem, we will need closure relationships to characterize these terms. Anyhow, these terms will not have any influence in our development as we will not consider them in our study.

5.3. Jacobian Matrix of the System

The system of equation 5.2.1 can also be written in the following way

(5.3.1) $$W_t + F_x(W) + S(W) = 0$$

with the same definition of the vector of conserved variables, W and the flux vector, $F(W)$ but with a new definition of the source term $S(W)$

$$S(W) = \begin{bmatrix} 0 \\ 0 \\ -p^i \frac{\partial \alpha}{\partial x}\alpha - \rho_v g - \varphi_v \\ p^i \frac{\partial \alpha}{\partial x}(1-\alpha) - \rho_l g - \varphi_l \\ p^i \frac{\partial \alpha}{\partial t} - \alpha \rho_v g u_v - \psi_v \\ -p^i \frac{\partial \alpha}{\partial t} - (1-\alpha)\rho_l g u_l - \psi_l \end{bmatrix}.$$

For the above system (eq. 5.3.1) the jacobian matrix $J(W) = \frac{\partial F(W)}{\partial W}$ is given by

$$J(W) = \begin{bmatrix} 0 & 0 \\ 0 & 0 \\ -u_v^2 + p\frac{\partial \alpha}{\partial w_1} + \alpha\frac{\partial p}{\partial w_1} & p\frac{\partial \alpha}{\partial w_2} + \alpha\frac{\partial p}{\partial w_2} \\ -p\frac{\partial \alpha}{\partial w_1} + (1-\alpha)\frac{\partial p}{\partial w_1} & -u_l^2 - p\frac{\partial \alpha}{\partial w_2} + (1-\alpha)\frac{\partial p}{\partial w_2} \\ -u_v H_v + u_v\left(p\frac{\partial \alpha}{\partial w_1} + \alpha\frac{\partial p}{\partial w_1}\right) & u_v\left(p\frac{\partial \alpha}{\partial w_2} + \alpha\frac{\partial p}{\partial w_2}\right) \\ u_l\left(-p\frac{\partial \alpha}{\partial w_1} + (1-\alpha)\frac{\partial p}{\partial w_1}\right) & -H_l u_l + u_l\left(-p\frac{\partial \alpha}{\partial w_2} + (1-\alpha)\frac{\partial p}{\partial w_2}\right) \end{bmatrix}$$

$$\begin{bmatrix} 1 & 0 \\ 0 & 1 \\ 2u_v + p\frac{\partial \alpha}{\partial w_3} + \alpha\frac{\partial p}{\partial w_3} & p\frac{\partial \alpha}{\partial w_4} + \alpha\frac{\partial p}{\partial w_4} \\ -p\frac{\partial \alpha}{\partial w_3} + (1-\alpha)\frac{\partial p}{\partial w_3} & 2u_l - p\frac{\partial \alpha}{\partial w_4} + (1-\alpha)\frac{\partial p}{\partial w_4} \\ H_v + u_v\left(p\frac{\partial \alpha}{\partial w_3} + \alpha\frac{\partial p}{\partial w_3}\right) & u_v\left(p\frac{\partial \alpha}{\partial w_4} + \alpha\frac{\partial p}{\partial w_4}\right) \\ u_l\left(-p\frac{\partial \alpha}{\partial w_3} + (1-\alpha)\frac{\partial p}{\partial w_3}\right) & H_l + u_l\left(-p\frac{\partial \alpha}{\partial w_4} + (1-\alpha)\frac{\partial p}{\partial w_4}\right) \end{bmatrix}$$

$$\begin{bmatrix} 0 & 0 \\ 0 & 0 \\ p\frac{\partial \alpha}{\partial w_5} + \alpha\frac{\partial p}{\partial w_5} & p\frac{\partial \alpha}{\partial w_6} + \alpha\frac{\partial p}{\partial w_6} \\ -p\frac{\partial \alpha}{\partial w_5} + (1-\alpha)\frac{\partial p}{\partial w_5} & -p\frac{\partial \alpha}{\partial w_6} + (1-\alpha)\frac{\partial p}{\partial w_6} \\ u_v\left(1 + p\frac{\partial \alpha}{\partial w_5} + \alpha\frac{\partial p}{\partial w_5}\right) & u_v\left(p\frac{\partial \alpha}{\partial w_6} + \alpha\frac{\partial p}{\partial w_6}\right) \\ u_l\left(-p\frac{\partial \alpha}{\partial w_5} + (1-\alpha)\frac{\partial p}{\partial w_5}\right) & u_l\left(1 - p\frac{\partial \alpha}{\partial w_6} + (1-\alpha)\frac{\partial p}{\partial w_6}\right) \end{bmatrix}.$$

The derivatives of the pressure and the void fraction with respect to the conserved variables can be obtained from the derivatives of the conserved variables with respect to the primitives $\frac{\partial W}{\partial V}$, through the following inversion

$$\frac{\partial V}{\partial W} = \left(\frac{\partial W}{\partial V}\right)^{-1},$$

where

$$\frac{\partial W}{\partial V} = \begin{bmatrix} \rho_v & 0 & 0 & \alpha\frac{\partial \rho_v}{\partial p} \\ -\rho_l & 0 & 0 & (1-\alpha)\frac{\partial \rho_l}{\partial p} \\ \rho_v u_v & \alpha\rho_v & 0 & \alpha u_v \frac{\partial \rho_v}{\partial p} \\ -\rho_l u_l & 0 & (1-\alpha)\rho_l & (1-\alpha)u_l\frac{\partial \rho_l}{\partial p} \\ \rho_v(H_v - p) & \alpha\rho_v u_v & 0 & \alpha H_v \frac{\partial \rho_v}{\partial p} - \alpha \\ -\rho_l(H_l - p) & 0 & (1-\alpha)\rho_l u_l & (1-\alpha)H_l\frac{\partial \rho_l}{\partial p} - (1-\alpha) \end{bmatrix}$$

$$\begin{bmatrix} \alpha\frac{\partial \rho_v}{\partial p} & 0 \\ 0 & (1-\alpha)\frac{\partial \rho_l}{\partial h_l} \\ \alpha u_v \frac{\partial \rho_v}{\partial p} & 0 \\ 0 & (1-\alpha)u_l\frac{\partial \rho_l}{\partial h_l} \\ \alpha H_v \frac{\partial \rho_v}{\partial p} + \alpha\rho_v & 0 \\ 0 & (1-\alpha)H_l\frac{\partial \rho_l}{\partial h_l} + (1-\alpha)\rho_l \end{bmatrix},$$

and finally

$$\begin{aligned} \frac{\partial \alpha}{\partial w_1} &= \frac{(1-\alpha)}{d}\rho_l c_l^{-2}(\rho_v + \frac{\partial \rho_v}{\partial h_v}(H_v - u_v^2)) \\ \frac{\partial \alpha}{\partial w_2} &= -\frac{\alpha}{d}\rho_v c_v^{-2}(\rho_l + \frac{\partial \rho_l}{\partial h_l}(H_l - u_l^2)) \\ \frac{\partial \alpha}{\partial w_3} &= \frac{(1-\alpha)}{d}\rho_l u_v c_l^{-2}\frac{\partial \rho_v}{\partial h_v} \\ \frac{\partial \alpha}{\partial w_4} &= -\frac{\alpha}{d}\rho_v u_l c_v^{-2}\frac{\partial \rho_l}{\partial h_l} \\ \frac{\partial \alpha}{\partial w_5} &= -\frac{(1-\alpha)}{d}\frac{\partial \rho_v}{\partial h_v}\rho_l c_l^{-2} \\ \frac{\partial \alpha}{\partial w_6} &= \frac{\alpha}{d}\frac{\partial \rho_l}{\partial h_l}\rho_v c_v^{-2} \end{aligned}$$

and

$$\begin{aligned}
\frac{\partial p}{\partial w_1} &= (\frac{\partial \rho_l}{\partial h_l}p - \rho_l^2)(\rho_v + \frac{\partial \rho_v}{\partial h_v}(H_v - u_v^2))\frac{1}{d} \\
\frac{\partial p}{\partial w_2} &= (\frac{\partial \rho_v}{\partial h_v}p - \rho_v^2)(\rho_l + \frac{\partial \rho_l}{\partial h_l}(H_l - u_l^2))\frac{1}{d} \\
\frac{\partial p}{\partial w_3} &= \frac{\partial \rho_v}{\partial h_v}(\frac{\partial \rho_l}{\partial h_l}p - \rho_l^2)u_v\frac{1}{d} \\
\frac{\partial p}{\partial w_4} &= \frac{\partial \rho_l}{\partial h_l}(\frac{\partial \rho_v}{\partial h_v}p - \rho_v^2)u_l\frac{1}{d} \\
\frac{\partial p}{\partial w_5} &= \frac{\partial \rho_v}{\partial h_v}(\frac{\partial \rho_l}{\partial h_l}p - \rho_l^2)\frac{1}{d} \\
\frac{\partial p}{\partial w_6} &= \frac{\partial \rho_l}{\partial h_l}(\frac{\partial \rho_v}{\partial h_v}p - \rho_v^2)\frac{1}{d}
\end{aligned}$$

where

$$d = \frac{\partial \rho_l}{\partial h_l}\left[\frac{\partial \rho_v}{\partial h_v}p + \rho_v(\alpha p\frac{\partial \rho_v}{\partial p} + (1-\alpha)\rho_v\right] + \rho_l\left[\alpha\rho_l\rho_v c_v^{-2} - (1-\alpha)\frac{\partial \rho_l}{\partial p}(\frac{\partial \rho_v}{\partial h_v}p + \rho_v^2)\right].$$

with the speeds of sound of each phase given by

$$c_k^2 = \frac{1}{\frac{\partial \rho_k}{\partial p} + \frac{1}{\rho_k}\frac{\partial \rho_k}{\partial h_k}}.$$

Through this procedure we are able to calculate the jacobian matrix of the system, for the conserved and primitive variables.

In the following and with the system of six equations, we will only consider water and air mixtures. Since we are mainly involved with the numerical performance of the scheme than with the perfect representation of the behaviour of the fluids, we have utilized much simpler equations of state (stiffened gas and perfect gas). So we have yielded the following expressions for the derivatives of density

$$\begin{aligned}
\frac{\partial \rho_v}{\partial p} &= \frac{\rho_v}{p} \\
\frac{\partial \rho_v}{\partial h_v} &= -\frac{\rho_v}{h_v} \\
\frac{\partial \rho_l}{\partial p} &= \frac{\rho_v}{p + p_\infty} \\
\frac{\partial \rho_l}{\partial h_l} &= -\frac{\rho_l}{h_l}.
\end{aligned}$$

5.4. Lax and Wendroff Schemes

The Lax and Wendroff can be applied to find solutions of the system 5.3.1. It is a centred scheme in which the numerical flux is defined by

$$F_{i+\frac{1}{2}} = \frac{1}{2}\{F_{i+1} + F_i - \frac{\Delta t}{\Delta x} J_{j+\frac{1}{2}}(F_{i+1} - F_i)\}.$$

The source term is discretized by means of the following approximations:

- Spatial derivatives by using a centred discretization

$$\left(p\frac{\partial \alpha}{\partial x}\right)_j^n \simeq p_j \frac{\alpha_{j+1}^n - \alpha_{j-1}^n}{2\Delta x}.$$

- Time derivatives by means of a backward discretization in time

$$\left(p\frac{\partial \alpha}{\partial t}\right)_j^n \simeq p_j \frac{\alpha_j^n - \alpha_j^{n-1}}{\Delta t^n}.$$

- Gravity terms as

$$\alpha_k \rho_k g \simeq (\alpha_k \rho_k)_j^n g,$$
$$\alpha_k \rho_k u_k g \simeq (\alpha_k \rho_k u_k)_j^n g.$$

The scheme is second order accurate in space and time and a complete description of it can be found in [**35**]. It is not monotone and produce spurious oscillations in the presence of discontinuities. We have applied it to the benchmark tests described in Appendix B, in particular

- Faucet test.
- Toumi's shock tube.
- Sedimentation test.
- Oscillating manometer test.

The scheme is not able to yield satisfactory numerical solutions for any of them, as an example in figure 5.1 we show the result for the faucet problem, the picture represents the evolution of the solutions obtained for the void fraction at the first computations. With it, we demonstrate the bad characterization of discontinuities that this scheme presents.

The source term has a big influence in the solution as it has been studied in [**24**] for the Euler system of equations. A new version of the Lax and Wendroff scheme was introduced to tackle this problem. It is an adapted version for the analysis of the system of equations that appears when we study inviscid fluids flowing in conducts with variable cross section. This version was called Adapted Lax and Wendroff (ALW)

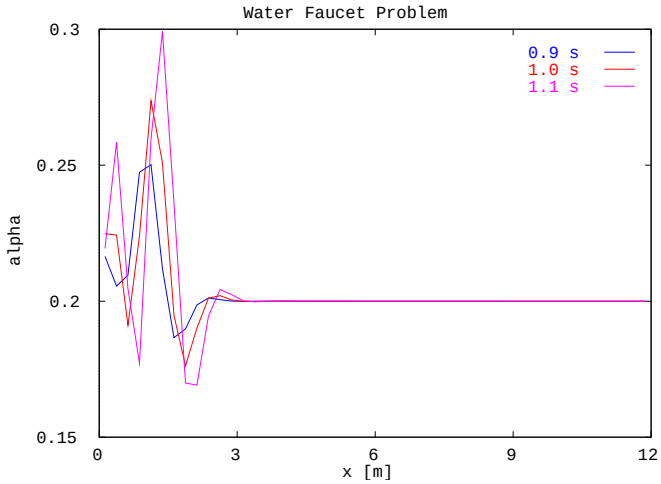

FIGURE 5.1. Results obtained for the Lax and Wendroff scheme. $\sigma = 3$, $CFL = 0.9$ and 50 cells

scheme. Following such a formulation, we have defined

$$B(W(x,t) = \int_{x_1}^{x} S'(z,W)dW, x \in [x_1, x_N]$$

which allows us to write the system of equation given by eq. 5.3.1 as

$$W_t + G(W)_x + S''(W) = 0$$

where $G(W) = F(W) + B(W)$. In this case the source term has been divided in two parts, S'(W) which contains the spatial derivatives of the void fraction and S"(W) which includes time derivatives of the void fraction and gravity terms.

To get approximate solutions of this system we consider the ALW conservative scheme

$$W_j^{n+1} = W_j^n - \frac{\Delta t}{\Delta x}\left[G_{j+\frac{1}{2}}^{n+\frac{1}{2}} - G_{j-\frac{1}{2}}^{n+\frac{1}{2}}\right] - \frac{\Delta t}{\Delta x}\left[B_{j-\frac{1}{2},j} + B_{j,j+\frac{1}{2}}\right] - \Delta t S_j^{''n}$$

the source term $S_j^{''n}$ only includes the approximation of the time derivatives of α and the gravity terms. On the other hand the ALW numerical flux is given by

$$G_{j+\frac{1}{2}}^{n+\frac{1}{2}} = \frac{1}{2}\left[\hat{F}_{j+\frac{1}{2}} - \frac{\Delta t}{\Delta x}\left(\frac{\partial F}{\partial W} + \frac{\partial B}{\partial W}\right)_{j+\frac{1}{2}}^{n}(F_{j+1} - F_j + B_{j,j+\frac{1}{2}} + B_{j+\frac{1}{2},j+1})\right]$$

where $B_{j,j+1}$ represents $\int_{x_j}^{x_{j+1}} S'(z,W)dz$ and the numerical fluxes have been evaluated verifying the steady state equation

$$\left[\frac{\partial F}{\partial x} + \frac{\partial B}{\partial x}\right]_{j+\frac{1}{2}} = 0, \qquad \forall j.$$

It lead us to

$$\begin{aligned}\frac{\hat{F}^L_{j+\frac{1}{2}} - F_j}{\frac{\Delta x}{2}} &= -\frac{B_{j+\frac{1}{2}} - B_j}{\frac{\Delta x}{2}},\\ \frac{F_{j+1} - \hat{F}^R_{j+\frac{1}{2}}}{\frac{\Delta x}{2}} &= -\frac{B_{j+1} - B_{j+\frac{1}{2}}}{\frac{\Delta x}{2}}.\end{aligned}$$

By taking out $\hat{F}^L_{j+\frac{1}{2}}$ and $\hat{F}^R_{j+\frac{1}{2}}$ from the previous expressions and approximating $\hat{F}_{j+\frac{1}{2}}$ with $\frac{\hat{F}^L_{j+\frac{1}{2}} + \hat{F}^R_{j+\frac{1}{2}}}{2}$ the numerical flux at the intercell is given by

$$\begin{aligned}G_{j+\frac{1}{2}} = \frac{1}{2}[&F_{j+1} + F_j - B_{j,j+\frac{1}{2}} + B_{j+\frac{1}{2},j+1}\\ &- \frac{\Delta t}{\Delta x}\left(\frac{\partial F}{\partial W} + \frac{\partial B}{\partial W}\right)^n_{j+\frac{1}{2}} (F_{j+1} - F_j + B_{j,j+\frac{1}{2}} + B_{j+\frac{1}{2},j+1})].\end{aligned}$$

A detailed derivation of these expressions can be found in [**24**]. In order to conclude with its extension to two phase flow, just remains to describe the expressions of terms of type $B_{j,j+1}$. Only the spatial derivatives of the void fraction have been included in these terms. The other source terms (gravity, time derivatives, etc.) are part of the S term. In general they are approximated by

$$\begin{aligned}B_{j,j+\frac{1}{2}} &= \int_{x_i}^{x_{i+\frac{1}{2}}} p\frac{\partial \alpha}{\partial z} dz \simeq p_{j+\frac{1}{2}}\left(\alpha_{j+\frac{1}{2}} - \alpha_j\right),\\ B_{j+\frac{1}{2},j+1} &= \int_{x_{i+\frac{1}{2}}}^{x_i} p\frac{\partial \alpha}{\partial z} dz \simeq p_{j+\frac{1}{2}}\left(\alpha_{j+1} - \alpha_{j+\frac{1}{2}}\right).\end{aligned}$$

The results obtained with this scheme are still unsatisfactory and it is necessary to use very small CFL to arrive to poor representations of the exact solution. An example of that is figure 5.2 where we have represented the results of the faucet test with $\sigma = 3$, 50 cells and $CFL = 0.01$, we can see some improvements with respect to the Lax and Wendroff scheme, although it is still a bit oscillatory. Perhaps, due to this small *CFL*, we have been able to produce sufficient numerical dissipation and get these solutions.

Other tests have been studied with this scheme as well (sedimentation and oscillating manometer), but only with the Toumi's shock tube we have obtained some result. We observe again a bad representation of the wave fronts (figure 5.3). Void fraction and pressure present some oscillations which are more dramatic in the pressure plot. We remark that it has been necessary to go to a very low CFL to arrive to these poor results.

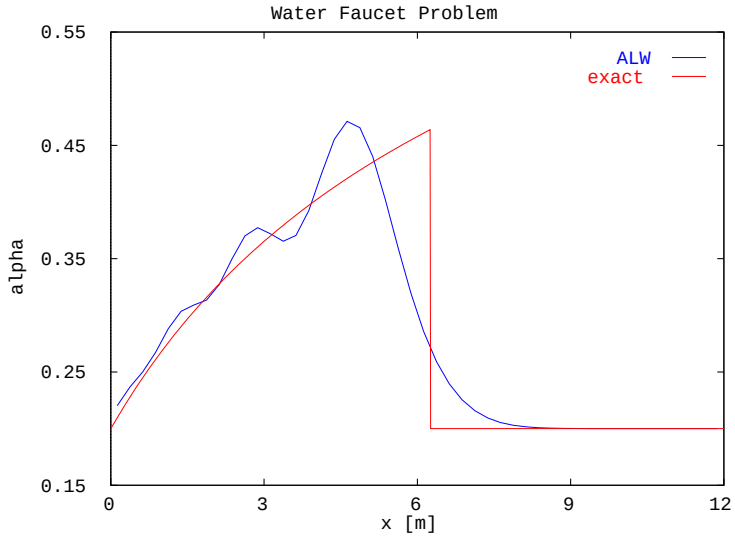

FIGURE 5.2. Void fraction obtained with the ALW scheme

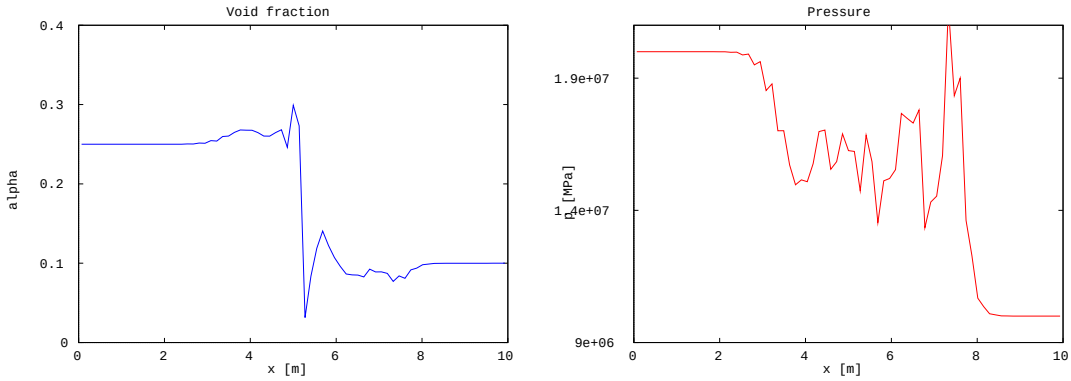

FIGURE 5.3. Results obtained with the ALW scheme for the shock tube problem

5.5. TVD Schemes

5.5.1. Introduction

In this section we study the extension of TVD schemes to two phase flow. We recall that Total Variation Stable methods are those whose total variation, given by

$$TV(u^n) = \sum_{i=-\infty}^{\infty} \left| u_{i+1}^n - u_i^n \right|,$$

does not increase in time. They are commonly called Total Variation Diminishing (TVD) methods and as mentioned above the following property holds

$$TV(u^{n+1}) \leq TV(u^n), \qquad \forall n.$$

The TVD property is important because guarantees convergence and the scheme does not produce false oscillations.

5.5.2. First Order TVD Scheme

To get approximate solutions of the system of equations (5.3.1) we propose the scheme given by

$$W_j^{n+1} = W_j^n - \frac{\Delta t}{\Delta x}\left[F_{j+\frac{1}{2}} - F_{j-\frac{1}{2}}\right] - \Delta t S_j^n,$$

where the flux in the middle is defined by

$$F_{j+\frac{1}{2}} = \frac{1}{2}\left[F_{j+1} + F_j - P_{j+\frac{1}{2}} h(D_{j+\frac{1}{2}}) P^{-1}_{j+\frac{1}{2}} \left(F_{j+1} - F_j\right)\right]$$

with

$D_{j+\frac{1}{2}}$: the diagonal matrix of eigenvalues λ_i of the jacobian matrix J, defined in equation 5.3 and evaluated in the point $x_{j+\frac{1}{2}}$.

$P_{j+\frac{1}{2}}$: The matrix of right eigenvectors of J also evaluated at the intercell.

$P^{-1}_{j+\frac{1}{2}}$: The inverse of the previous matrix.

$h(D_{j+\frac{1}{2}}) = diag(\text{sign}(\lambda_1), \ldots, \text{sign}(\lambda_6))$. "sign" is the sign function given by

$$\text{sign}(\lambda) = \begin{cases} 1 & \text{if } \lambda \geq 0, \\ -1 & \text{otherwise.} \end{cases}$$

The difinition of the numerical flux allows to introduce the concept of "the sign of a matrix". In the case of the jacobian matrix, we define its sign as

$$\text{sign}(J) = P h(D) P^{-1}.$$

We will use for its evaluation the algorithm described in appendix A which avoids the matrix diagonalization in the calculation of its sign. This reduces the calculation time considerably as we have checked.

In the homogeneous case the scheme is first order and TVD under the CFL condition

$$\frac{\Delta t}{\Delta x} \max |\mu^k| \leq 1.$$

The discretization of the derivatives of the void fraction have been done following the same principle we used with Lax and Wendroff schemes. The terms of the form

$p\frac{\partial \alpha}{\partial x}$ have been discretized by means of a central discretization in space and terms of the type $p\frac{\partial \alpha}{\partial t}$ with a backward discretization leaving the scheme explicit. Then, at node j and time level n we have again

$$\left(p\frac{\partial \alpha}{\partial x}\right)_j^n \simeq p_j \frac{\alpha_{j+1}^n - \alpha_{j-1}^n}{2\Delta x},$$

$$\left(p\frac{\partial \alpha}{\partial t}\right)_j^n \simeq p_j \frac{\alpha_j^n - \alpha_j^{n-1}}{\Delta t^n}.$$

5.5.2.1. Numerical Results

In the next section we are going to anylise the behaviour of this scheme under certain benchmarks.

Water Faucet Test

The results of the faucet test are shown for different number of cells in figure 5.4. For 50 cells, it is observed in the figure that the scheme presents some dissipation in the discontinuity. They are less consistent when the number of cells is increased. Despite we recover a bit the discontinuity, oscillations increase with the number of cells.

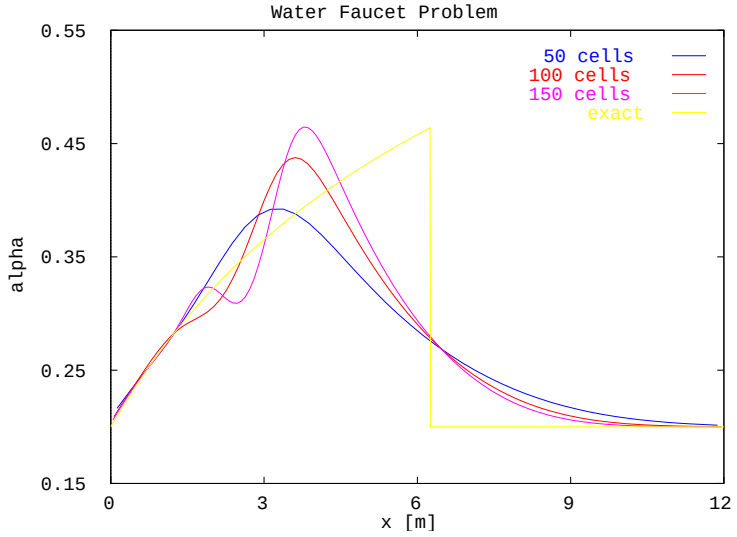

FIGURE 5.4. Void fraction for different number of cells

We have observed that the bad behaviour of this scheme in the solution of the faucet test can be corrected by making a backward approximation for the spatial derivative of the void fraction

$$\left(p\frac{\partial\alpha}{\partial x}\right)_j^n \simeq p_j\frac{\alpha_j^n-\alpha_{j-1}^n}{\Delta x}.$$

To justify this behaviour we are going to consider the analytical solution of the faucet test which (also studied in appendix B). To reach to an exact solution it is necessary to consider only the liquid phase and neglect the effect of pressure in the momentum equation. In the case of the centred discretization the contributions of the pressure terms do not cancel each other which yields a departure from the analytical solution as is shown in figure 5.4. An opposite effect occurs when we consider the backward discretization, resulting a better approximation to the solution as is shown in figure 5.5, here we have depicted the solutions for the faucet test with different mesh points (50, 100 and 150), with $CFL = 0.9$ and $sigma = 3$. In spite of the improvements, we shall remark that a loss of monotonicity is detected on the left of the discontinuity as the number of cells increases.

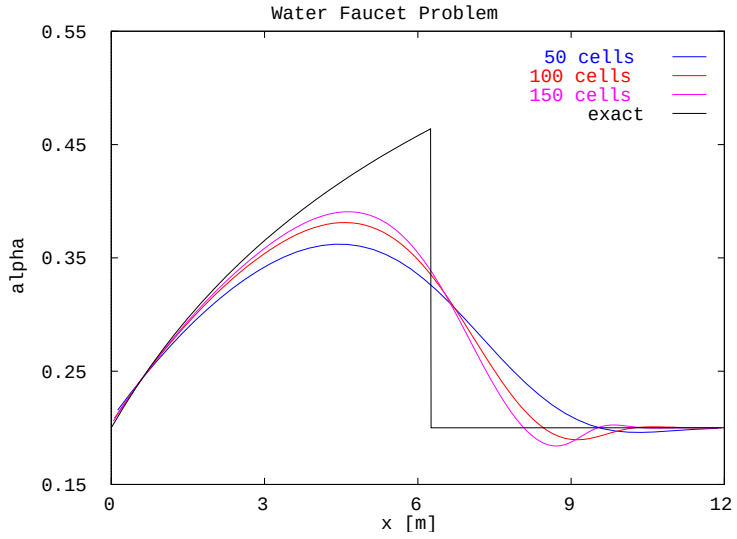

FIGURE 5.5. Grid convergence study for the TVD scheme with backward discretization of the spatial derivatives of void fraction

Toumi's Shock Tube

This benchmark consists of a two-fluid shock tube problem whose initial and boundary conditions are described in appendix B. In figure 5.6 we show the results corresponding to different grid points.

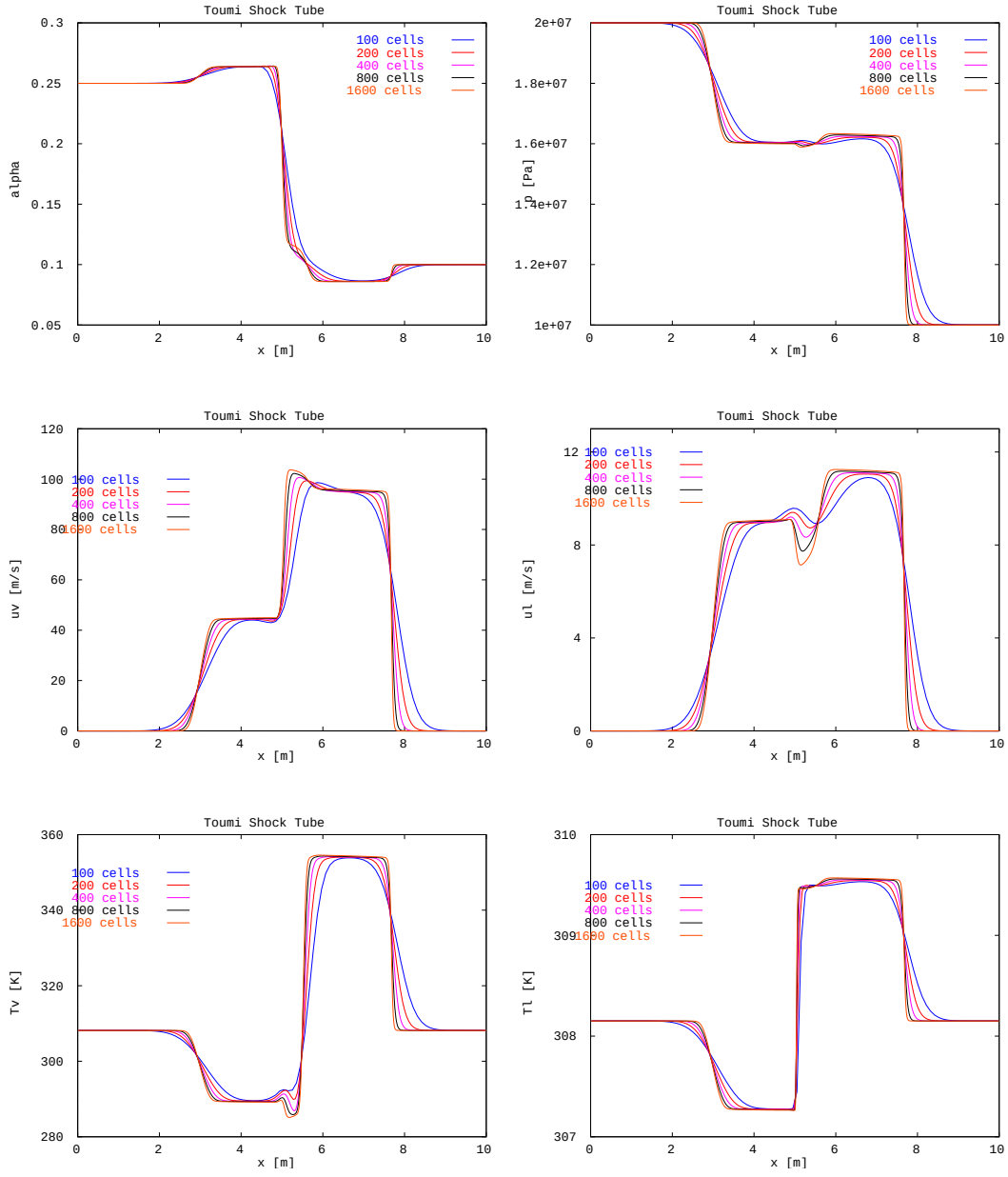

FIGURE 5.6. Toumi's shock tube, 1^{st} order TVD, central discretization for the spatial derivatives: Grid convergence study with the TVD scheme, $\sigma = 3.0$. From top to bottom, left to right, void fraction, pressure, gas velocity, liquid velocity, gas temperature, liquid temperature.

We can observe clearly the convergence to the exact solution as the number of cells increases. Calculations have been done with $CFL = 0.1$ and $\sigma = 3.0$ for different number of cells. In the case we use a backward discretization, things do not go as well as with the centred approximation figure 5.7.

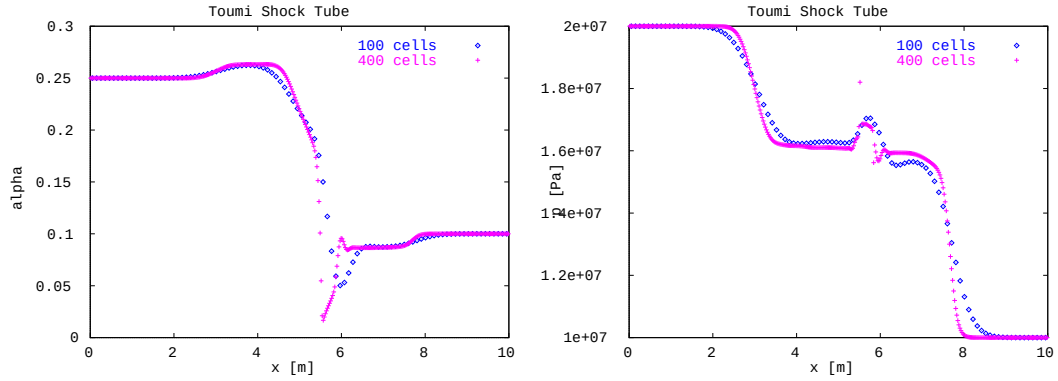

FIGURE 5.7. Toumi's shock tube, $1^s t$ order TVD, backward discretization for the spatial derivatives. Left: void fraction, right: pressure

As studied above, the interfacial pressure correction term affects to the eigenstructure of the system and it is characterized by the value of the parameter σ. In figure 5.8 we show this influence on the gas velocity and temperature for several values of σ.

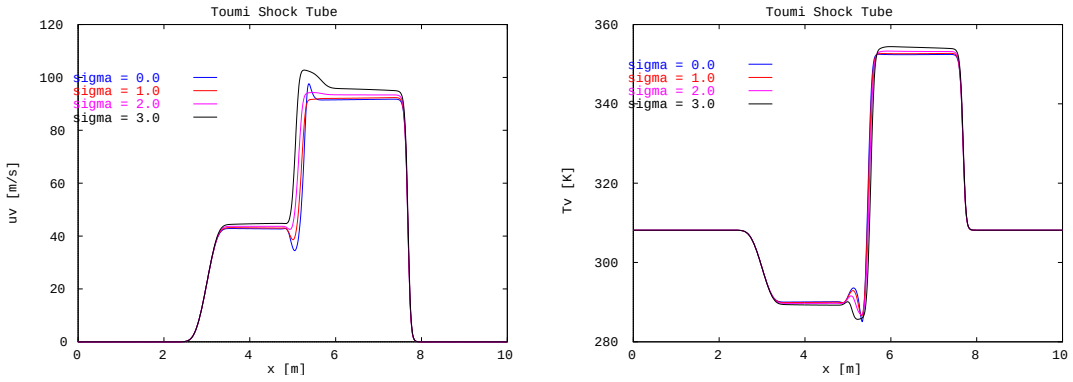

FIGURE 5.8. Effect of interfacial pressure correction terms on the structure of the solution in the shock tube problem

As commented in [**72**], the effect of this sort of terms in the solution is negligible when we study problems involving heat transfer and friction. In this way, we will

consider the values of $\sigma = 2$ or 3 which provide enough hyperbolicity to the scheme and yield fairly good results.

Sedimentation Test

In this test a column of a homogeneous mixture of water and air is separated under the action of gravity. In figure 5.9 we show the results produced by the TVD scheme, we find that we have to decrease too much the CFL number as much as in the shock tube test, about 0.1, to get a good solution of the problem. To illustrate the results we have also depicted in figure 5.10 the evolution of the void fraction profile. Going to lower $CFL = 0.01$ we are able to reach steady state with better accuracy. All the figures show a bit oscillatory behaviour near the discontinuity, beside the discontinuity produced between the states of $\alpha = 0$ and $\alpha = 1$.

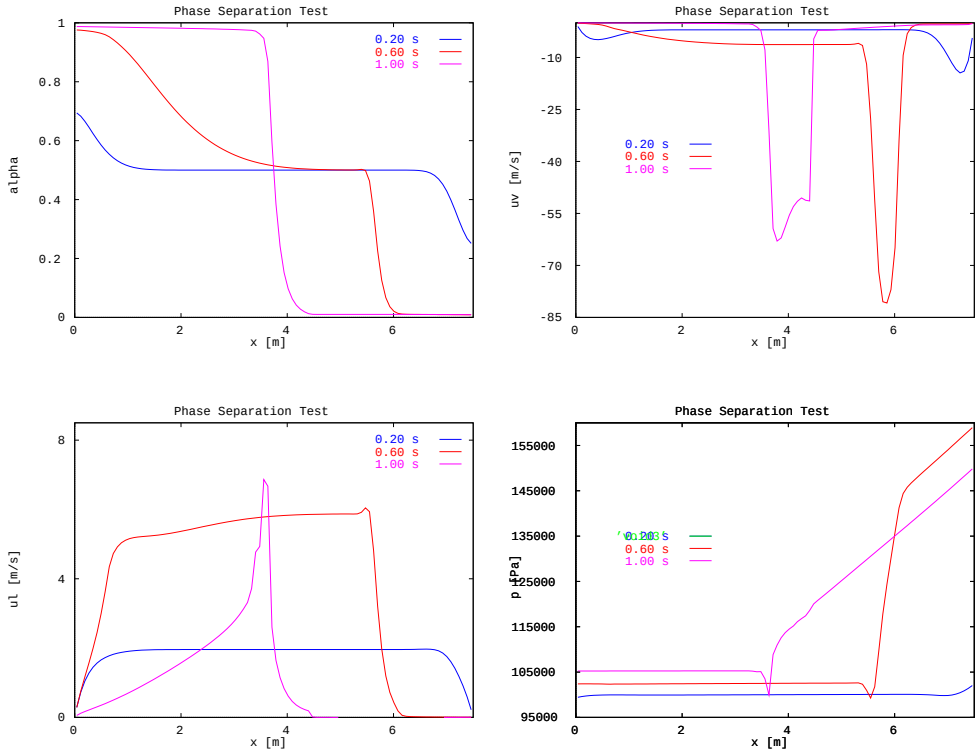

FIGURE 5.9. Phase separation test, 1^{st} order TVD. $\sigma = 2.0$ and $CFL = 0.1$. From top to bottom, left to right, void fraction, gas velocity, liquid velocity, pressure

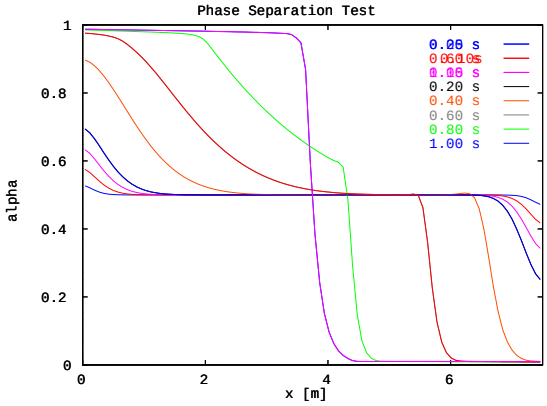

FIGURE 5.10. Evolution of void fraction for the phase separation test

With respect to the oscillating manometer, we shall notice that we have not been able to solve the problem by using the different versions of TVD schemes.

5.5.3. Second Order TVD Scheme

In this section we are going to study the second order version of the TVD scheme. Second order has been accomplished by means of the MUSCL strategy. In this case we have followed the formulation of the Hancock's method described in [**76**]. It consists of the following steps:

(1) Data reconstruction, in which we make a lineal approximation of the values of the primitive variables

$$V_j^L = V_j^n - \frac{1}{2}\Delta x \frac{\partial V}{\partial x},$$
$$V_j^R = V_j^n + \frac{1}{2}\Delta x \frac{\partial V}{\partial x}.$$

To avoid spurious oscillations the spatial derivatives of the primitives can be limited by using any of the limiters described in [**35**].

(2) Time evolution of $\frac{\Delta t}{2}$ of W_j^L and W_j^R,

$$\overline{W}_j^{L,R} = W_j^{L,R} - \frac{\Delta t}{2\Delta x}[F(W_j^R) - F(W_j^L)].$$

(3) Approximate solution of the piece-wise constant data Riemann problem,

$$W_t + F(W)_x + S(W) = 0,$$

$$W(x,0) = \begin{cases} \overline{W}_j^R, & \text{if } x < 0. \\ \overline{W}_{j+1}^L, & \text{if } x > 0. \end{cases}$$

In this step we will use our approximate TVD flux in order to determine the numerical flux in the middle,

$$F_{j+\frac{1}{2}} = F^{TVD}(\overline{W}_j^R, \overline{W}_{j+1}^L).$$

In order to illustrate the behaviour of this second order TVD scheme we have included some numerical results.

Faucet Problem

We show in figure 5.11 the results corresponding to the second order version of the TVD scheme, the results are basically the same. Independently of the discretization of the spatial derivative we consider (centred or backward) we get a oscillatory behaviour. Despite the increase in the precision we have not been able to improve the results obtained for the first order version (figure 5.4).

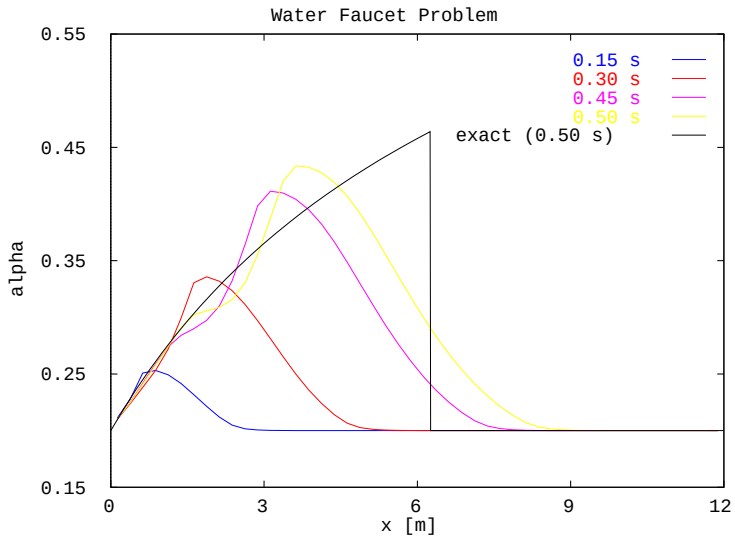

FIGURE 5.11. Void fraction for different instants, 2nd order

Toumi's shock tube

As we have done for the first order approximation we have included the evolution of the solution as the mesh points increase, this is shown in figure 5.12. For the calculations we have also used $CFL = 0.1$ and $\sigma = 3.0$. The scheme is too oscillatory, even after using slope limiters to reduce the oscillations produced by the second order.

5.5.4. Adapted TVD Scheme

5.5.4.1. ATVD and Separated Two Phase Flow

As ALW, the adapted TVD scheme (ATVD for sort) was introduced by Gascón in [**24**]. Using the same definitions utilized in the ALW scheme, our system of equations may be transformed into

$$W_t + G_x(W) + S''(W) = 0$$

where

$$G(W) = F(W) + \int_0^x S'(w)dx.$$

$S'(w)$ and $S''(w)$ include the source terms depending on the case.

The extension of the ATVD numerical scheme to two phase flow is given by

$$W_j^{n+1} = W_j^n - \frac{\Delta t}{\Delta x}\left[G_{j+\frac{1}{2}} - G_{j-\frac{1}{2}}\right] - \frac{\Delta t}{\Delta x}\left[B_{j-\frac{1}{2},j} + B_{j,j+\frac{1}{2}}\right] - \Delta t S_j^{''n},$$

with the numerical flux given by

$$G_{j+\frac{1}{2}} = \frac{1}{2}\left\{F_j + F_{j+1} - B_{j,j+\frac{1}{2}} + B_{j+\frac{1}{2},j+1} - P_{j+\frac{1}{2}} h(\overline{D}_{j+\frac{1}{2}}) Q_{j+\frac{1}{2}}\left[F_{j+1} - F_j + B_{j,j+1}\right]\right\}.$$

Two options for the function $h(\overline{D}_{j+\frac{1}{2}})$ have been studied

$$h(\overline{D}_{j+\frac{1}{2}}) = diag\left(sign(\alpha^k_{j+\frac{1}{2}})\right) h(\overline{D}_{j+\frac{1}{2}}) \qquad = diag\left(sign(\alpha^k_{j+\frac{1}{2}} + \beta^k_{j+\frac{1}{2}})\right).$$

The parameters $\alpha_{j+\frac{1}{2}}$ and $\beta_{j+\frac{1}{2}}$ are defined by

$$\alpha_{j+\frac{1}{2}} = \frac{\Delta t}{\Delta x}\frac{\delta f_{j+\frac{1}{2}}}{\delta u_{j+\frac{1}{2}}},$$

$$\beta_{j+\frac{1}{2}} = \frac{\Delta t}{\Delta x}\frac{\delta b_{j+\frac{1}{2}}}{\delta u_{j+\frac{1}{2}}}$$

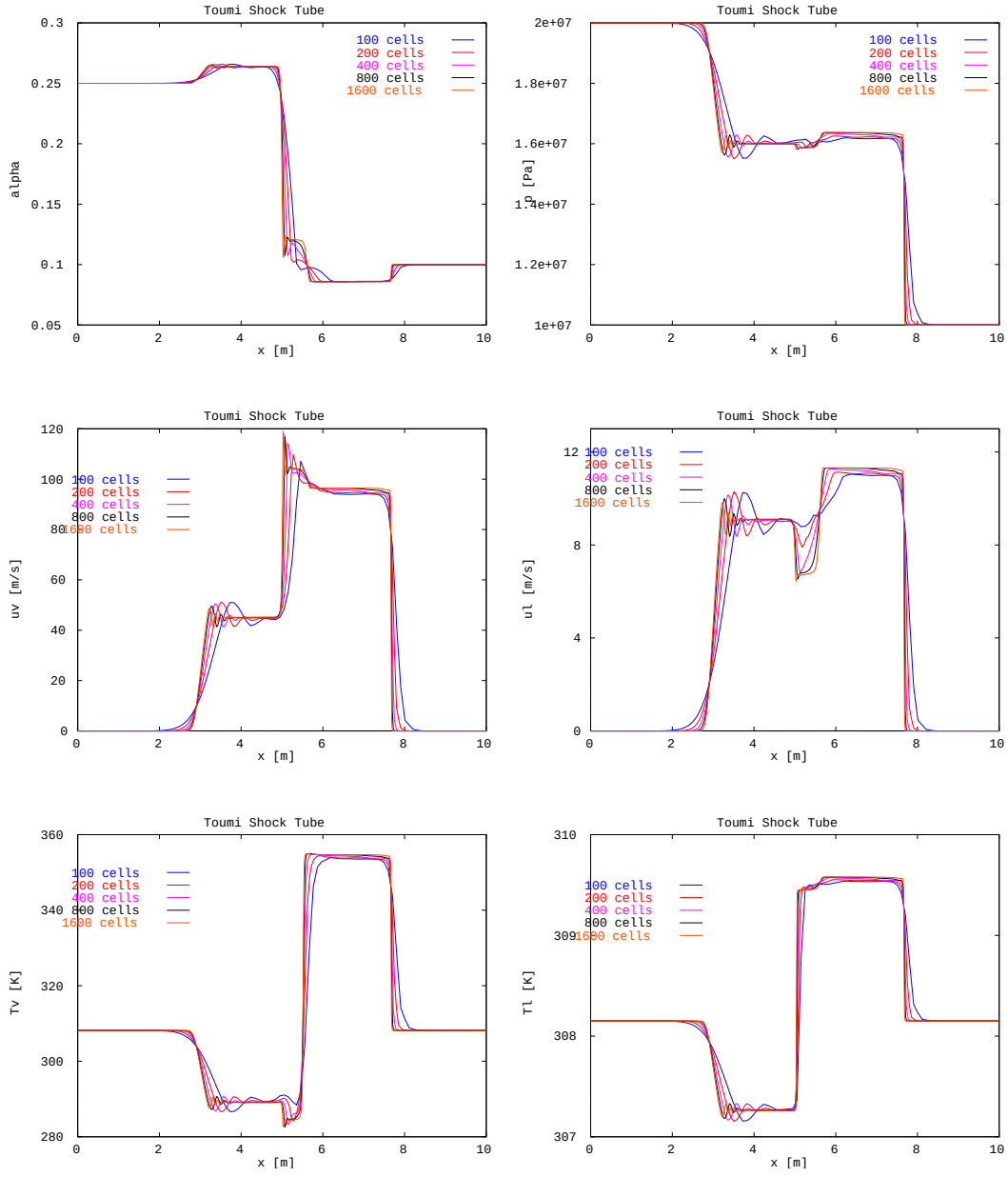

FIGURE 5.12. Toumi's shock tube, 2^{nd} order TVD: Grid convergence study with the TVD scheme, $\sigma = 3.0$. From top to bottom, left to right, void fraction, pressure, gas velocity, liquid velocity, gas temperature, liquid temperature.

with

$$\delta f_{j+\frac{1}{2}} = P^{-1}_{j+\frac{1}{2}} \left(F_{j+1} - F_j\right),$$
$$\delta u_{j+\frac{1}{2}} = P^{-1}_{j+\frac{1}{2}} \left(W_{j+1} - W_j\right),$$
$$\delta b_{j+\frac{1}{2}} = P^{-1}_{j+\frac{1}{2}} \left(B_{j+1} - B_j\right).$$

For the calculation of the parameters in the middle we have used a particularization of Roe averages to two phase flow. We have followed the criteria of [**79**], so we have considered,

$$\overline{u}_k = \frac{\sqrt{(\rho_k\alpha_k)^R}u_k^R + \sqrt{(\rho_k\alpha_k)^L}u_k^L}{\sqrt{(\rho_k\alpha_k)^R} + \sqrt{(\rho_k\alpha_k)^L}},$$
$$\overline{H}_k = \frac{\sqrt{(\rho_k\alpha_k)^R}H_k^R + \sqrt{(\rho_k\alpha_k)^L}H_k^L}{\sqrt{(\rho_k\alpha_k)^R} + \sqrt{(\rho_k\alpha_k)^L}},$$
$$\overline{\alpha} = 1 - 2\frac{(1-\alpha^L)(1-\alpha^R)}{(1-\alpha^L) + (1-\alpha^R)},$$
$$\overline{p} = \frac{p^L(1-\alpha^L) + p^R(1-\alpha^R)}{(1-\alpha^L) + (1-\alpha^R)}.$$

We have not detected important improvements between this approximation and the one obtained by using simple averages, for the phase k we would have

$$\overline{u}_k = \frac{u_k^L + u_k^R}{2}, \qquad \overline{H}_k = \frac{H_k^L + H_k^R}{2}, \qquad \overline{u}_k = \frac{\alpha_k^L + \alpha_k^R}{2} \quad \text{or} \quad \overline{p}_k = \frac{p_k^L + p_k^R}{2}.$$

5.5.4.2. ATVD and Homogeneous Two Phase Flow

In this section we fix the preliminaries to apply the First Order Adapted TVD Scheme to the homogeneous two phase flow model. Its interest resides in that the system of equations can be written in conservative form. If we consider ducts with constant cross section we will not have to leave terms with derivatives in the source terms. In this case the system of equations is given by

$$W_t + JW_z + S = 0 \tag{5.5.1}$$

where the source term is function of W and z. However, in the following the S term is considered only z dependent. The general dependence of S with z and W has been studied in [**24**], being the main difficulty, the evaluation of the derivatives of the source term respect to W.

The system of equations 5.5.1 can be transformed into a system of three scalar equations along the characteristic lines. Thereby we get

$$U_t + DU_z + P^{-1}C = 0 \tag{5.5.2}$$

where we have followed a standard procedure by introducing the characteristic variables

$$U = P^{-1}W.$$

D and P are the diagonal matrix of eigenvalues of J and P the right eigenvectors.

We can write equation 5.5.2 as follow

$$U_t + DU_z + S'_z = 0$$

where $S'(W) = P^{-1}C(W) = P^{-1}B_z$.

Finally, with $G^U = DU + S'$, we can write the system as homogeneous

$$U_t + G^U_z = 0. \tag{5.5.3}$$

We will use a first order TVD scheme to approximate solutions of 5.5.3

$$U^{n+1}_j = U^n_j - \lambda(G^U_{j+\frac{1}{2}} - G^U_{j-\frac{1}{2}})$$

where

$$G^U_{j+\frac{1}{2}} = \frac{1}{2}\left[G^U_j + G^U_{j+1} - h(D_{j+\frac{1}{2}})(G^U_{j+1} - G^U_j)\right]$$

and $h(D) = \text{sign}(D)$.

After some transformations we arrive at the following scheme that approximates solutions of 5.5.1

$$W^{n+1}_j = W^n_j - \lambda\left[G^*_{j+\frac{1}{2}} - G^*_{j-\frac{1}{2}}\right] - \lambda\left[B_{j-\frac{1}{2},j} + B_{j,j+\frac{1}{2}}\right]$$

where

$$\begin{aligned} G^*_{j+\frac{1}{2}} &= \frac{1}{2}\Big\{F_j + F_{j+1} + B_{j+\frac{1}{2},j+1} - B_{j,j+\frac{1}{2}} \\ &\quad -P_{j+\frac{1}{2}}h(D_{j+\frac{1}{2}})P^{-1}_{j+\frac{1}{2}}(F_{j+1} - F_j + B_{j,j+1})\Big\}. \end{aligned}$$

We need to determine the thermodynamic variables in order to close the problem. The calculation process is described as follow. The density and the internal energy is determined directly from the knowledge of the conserved variables $\rho = w_1$ and $e = \frac{w_3}{w_1} - \frac{w_2}{w_1}$, but we have to calculate the pressure. To do that we suppose the phases are in thermal equilibrium (homogeneous equilibrium model) and we have

$$e = xe_g + (1-x)e_f \rightarrow f_1(p, e, , x) = 0 \tag{5.5.4}$$

for the density

$$\rho = \alpha\rho_g + (1-\alpha)\rho_f \rightarrow f_2(p,\rho,x) = 0 \tag{5.5.5}$$

and for the void fraction

$$\alpha = \frac{1}{1+\left(\frac{1-x}{x}\frac{\rho_g}{\rho_f}\right)} \rightarrow f_3(p,\alpha,x) = 0 \tag{5.5.6}$$

by substituting 5.5.6 in 5.5.5, we get a relationship for the quality, x, that with 5.5.4 gives

$$e - \frac{\rho_g(\rho_f-\rho)}{\rho(\rho_f-\rho_g)}(e_g-e_f) - e_f = 0 \tag{5.5.7}$$

this is a function

$$f(p,\rho,e) = 0$$

as

$$\begin{aligned} e_g &= e_g(p) \qquad e_f = e_f(p) \\ \rho_g &= \rho_g(p) \qquad \rho_f = \rho_f(p) \end{aligned}$$

this will allow to get the pressure from 5.5.7 as an implicit function of density and internal energy.

We shall remark that the calculation of the primitive variables from the conserved variables in separated two phase flow has been left to the appendix A. Their expressions have been derived rigurously.

5.5.4.3. Numerical Results

We have studied the behaviour of this scheme by using the tests described in Appendix B. In the case of separated two phase flow, we have analysed the following tests:

- Water faucet.
- Toumi's shock tube.
- Sedimentation.
- Oscillating manometer.

Regarding homogeneous two phase flow we have considered the boiling tube test.

Faucet flow test

We have studied the influence in the solution provided by the ATVD scheme when the *CFL* number or the value of σ change. These results are shown in figures 5.13 In the first case we have fixed $\sigma = 2$ and in the other $CFL = 0.9$. For both cases we have chosen a 50 point mesh.

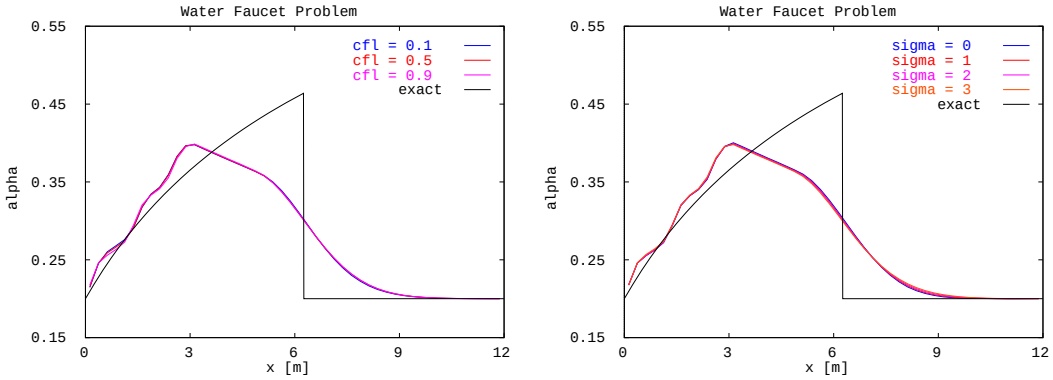

FIGURE 5.13. Left:Influence of the CFL number on the ATVD scheme. Right: Influence of the σ parameter on the ATVD scheme

We can notice in figure 5.14 how we approach the analytical solution as the number of mesh points increases. The scheme presents some oscillations as it reaches the discontinuity. This example corresponds to $\sigma = 2$ and $CFL = 0.9$.

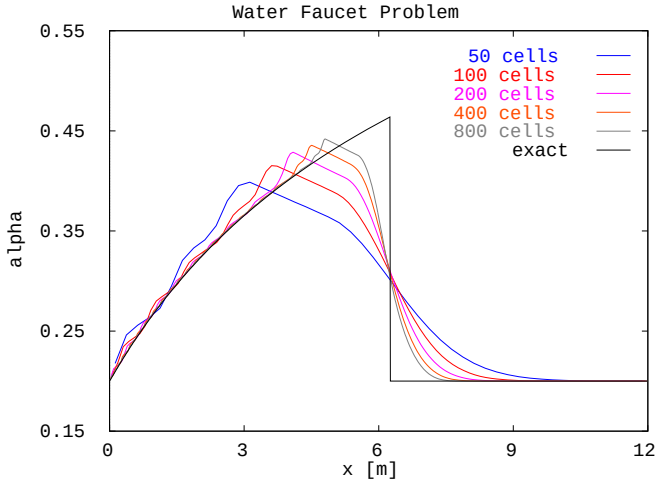

FIGURE 5.14. Grid convergence study for the ATVD scheme

These results have been obtained for the case in which the function h only depends on $\alpha_{j+\frac{1}{2}}$ and $\beta_{j+\frac{1}{2}}$. When we consider h only α-dependent we cannot obtain any satisfactorious results.

The analysis of the faucet test with the ATVD scheme is concluded by making the calculation for a mesh of 1600 points. Although the approach to the exact solution is

higher, many oscillations have appeared in the rest of the variables with the exception of the liquid velocity, this is shown in figure 5.15.

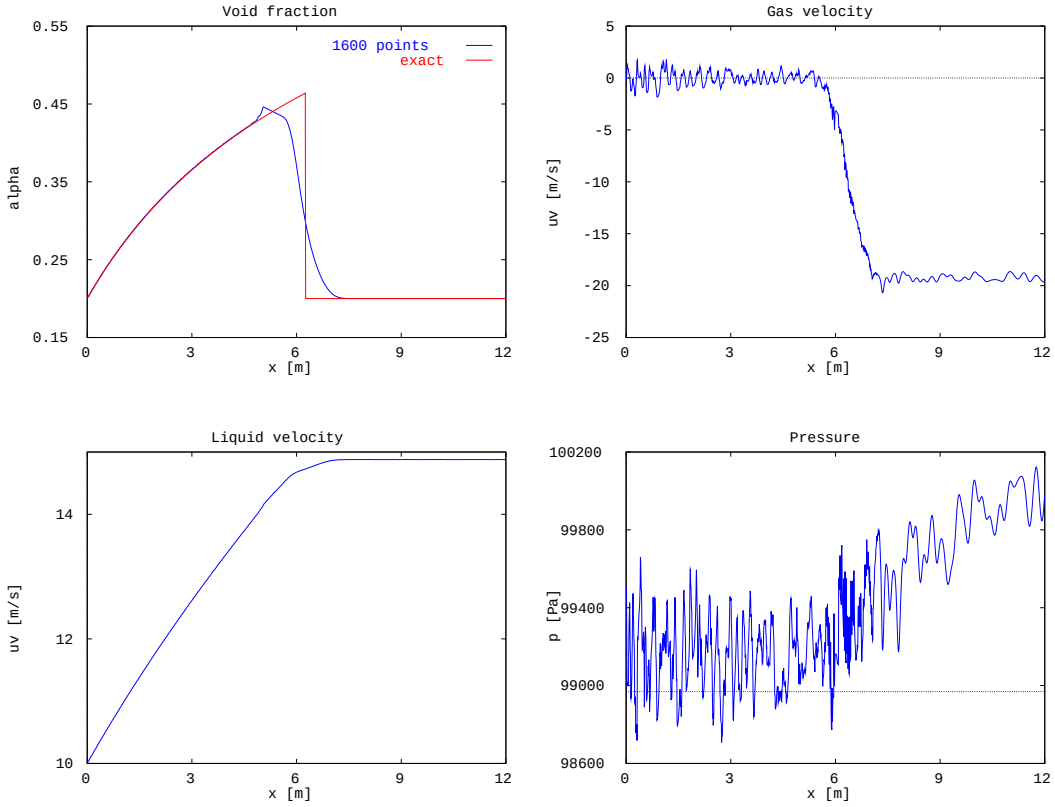

FIGURE 5.15. Faucet test, ATVD: Profiles of void fraction, gas velocity, liquid velocity and pressure

Toumi's Shock Tube

In the case in which $h(\overline{D}_{j+\frac{1}{2}})) = h(\alpha_{j+\frac{1}{2}} + \beta_{j+\frac{1}{2}}$ we have not obtained good results. They have been collected in figure 5.16, they are the results obtained for the shock tube with $\sigma = 2$ and $CFL = 0.1$. We observe the appearance of too many oscillations.

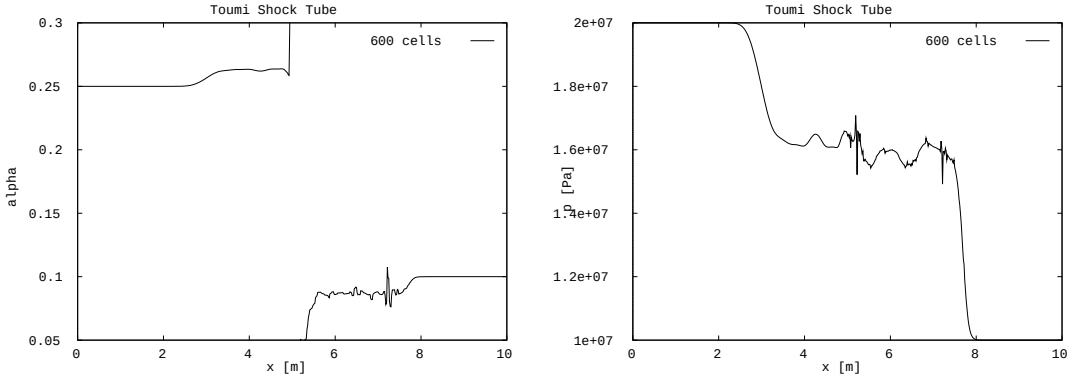

FIGURE 5.16. Results for the ATVD scheme considering $\beta_{j+\frac{1}{2}}$ in function $h(D_{j+\frac{1}{2}})$

Unlike the faucet test if we do not consider the influence of the term $\beta_{j+\frac{1}{2}}$ in $h(\overline{D}_{j+\frac{1}{2}})$ and leave it as

$$h(\overline{D}_{j+\frac{1}{2}}) = h(\alpha_{j+\frac{1}{2}})$$

we get better results as figure 5.17 showes. They have been obtained considering $\sigma = 2$ and $CFL = 0.1$.

The scheme has not been able to model neither the separation test nor the oscillating manometer test. We have observed different behaviours of the scheme depending on whether it includes or not the derivatives of the source terms in the h function. This does not allow to conclude any satisfactorious results with respect to the ATVD.

Boiling Tube

We have utilized the ATVD to solve the homogeneous system of equations which models the two phase mixture in this benchmark. The test consist of a tube with constant cross section heated by a source of heat whose characteristics are described with the initial and the boundary conditions have been described in Appendix B. We can see the profiles of the variables more representative in figure 5.18.

Those results have been obtained for a 50 points mesh and CFL = 1. In this case, since the source term has been considered constant the ATVD scheme is reduced to the VFFC scheme. We have found some problems with the boundary conditions,

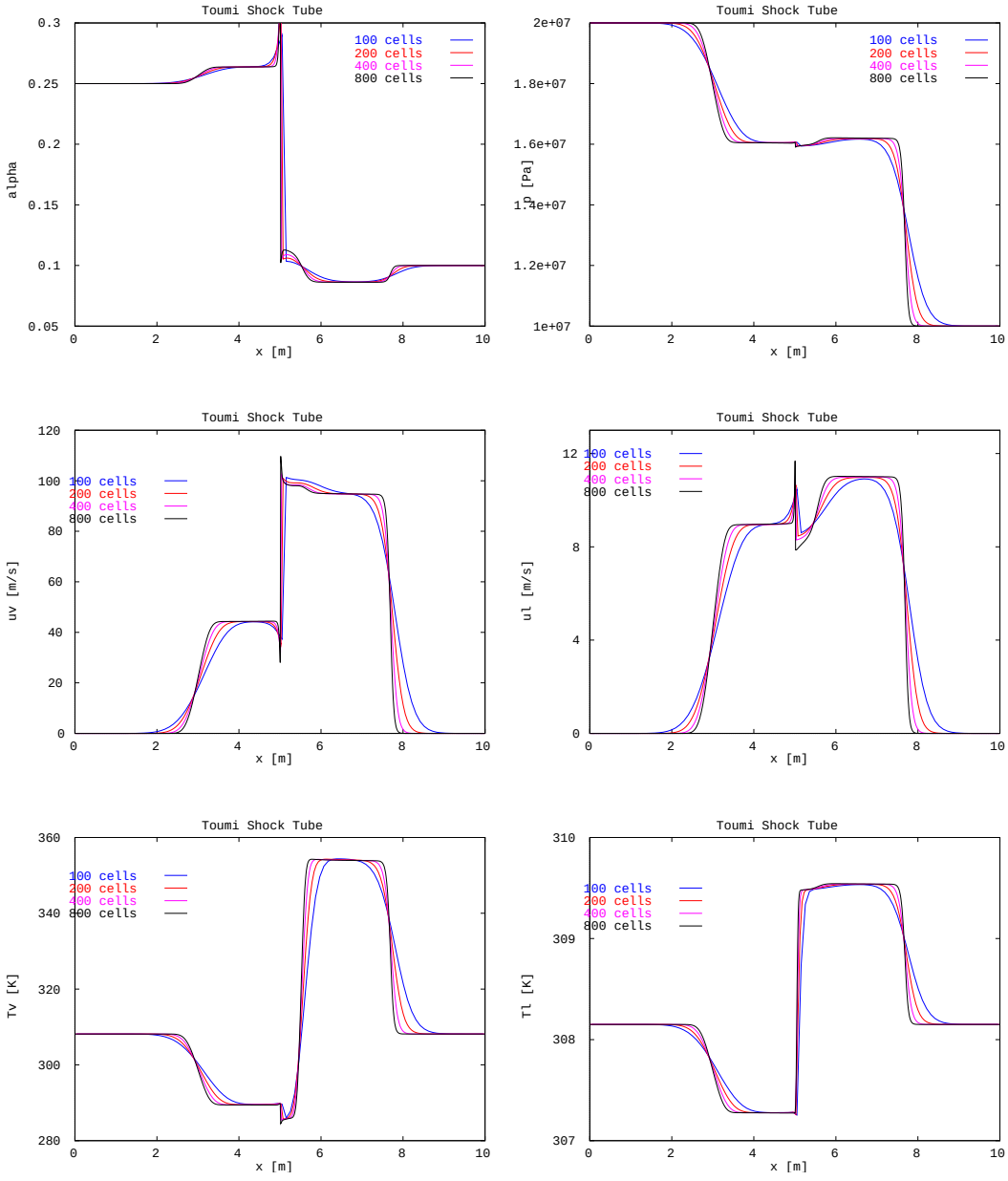

FIGURE 5.17. Toumi's shock tube, 1^{st} order ATVD: Grid convergence study with the TVD scheme, $\sigma = 2.0$. From top to bottom, left to right, void fraction, pressure,gas velocity, liquid velocity, gas temperature, liquid temperature.

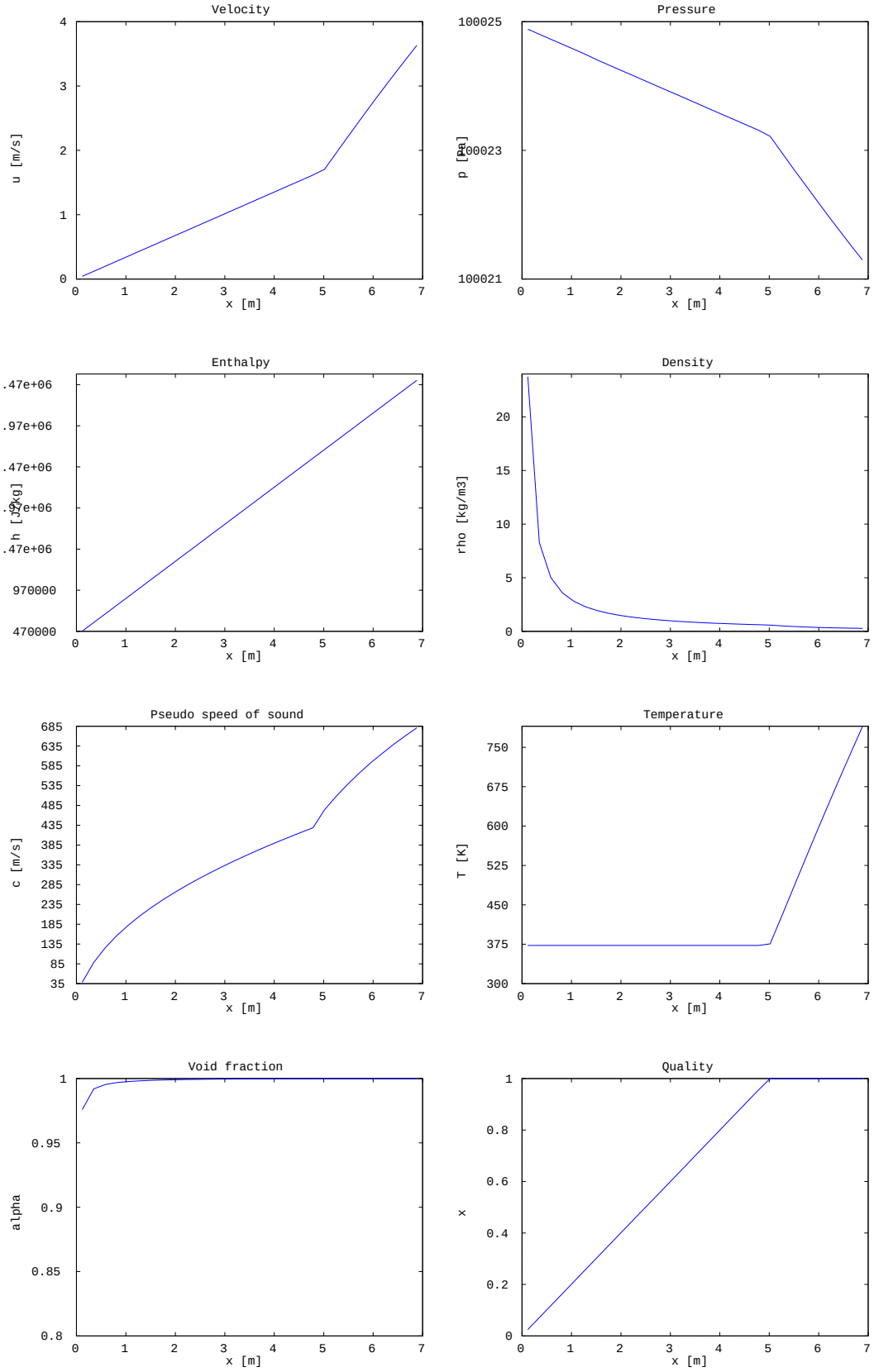

FIGURE 5.18. Boiling tube with ATVD, from top to botton, left to right: velocity, pressure, enthalpy, density, speed of sound, temperature, void fraction and quality

perhaps due to the fact that the characteristic time is too large. The discontinuity of the variables in the transition from two phase flow to single phase flow have been modelled very well as can be seen in the figures.

5.5.5. Decoupling of the System of Equations

In this section we study the possibility of analysing the conservation laws of each phase separately. In this sense some works can be found in the literature. We can cite the analysis done by Toro in [**75**], where a reactive medium, formed by a gas and a solid, is modelled separately by considering the homogeneous system of equations of each phase. Another recent contribution is the work of [**13**]. The authors study the same system of equations we are studying here, they use kinetic schemes for the solution of some two phase problems by considering the phases flowing alone in channels with constant cross section equal to α or $(1-\alpha)$ and depending on whether we have vapour or liquid.

The following ideas will be utilized in the extension of the AUSM schemes to two phase flow. We will analyse the phases independently, getting the numerical fluxes for each phase and later adding to them the discretizations of the derivatives of the void fraction and the gravitational terms.

In our development we will introduce some of the new advances done in the study of hyperbolic conservation laws, in particular, in the characterization of inviscid fluids flowing in pipes with variable cross section. This is, the application of the already extended ATVD schemes to the system of equations of each phase as though they were flowing independently in ducts with cross sections α and $(1-\alpha)$.

In this case we will have the same system of equations we have been studying but for each phase. The system for the phase k is given by

$$\begin{aligned}
\frac{\partial}{\partial t}(\alpha_k\rho_k) + \frac{\partial}{\partial x}(\alpha_k\rho_k u_k) &= 0 \\
\frac{\partial}{\partial t}(\alpha_k\rho_k u_k) + \frac{\partial}{\partial x}(\alpha_k\rho_k u_k^2 + \alpha_k p) - p^i\frac{\partial \alpha_k}{\partial x} &= \alpha_k\rho_k g \\
\frac{\partial}{\partial t}(\alpha_k\rho_k E_k) + \frac{\partial}{\partial x}(\alpha_k\rho_k H_k u_k) - p^i\frac{\partial \alpha_k}{\partial t} &= \alpha_k\rho_k u_k g
\end{aligned}$$

In vector form we have that the system is

$$W_t + F_x + S = 0. \tag{5.5.8}$$

In this occasion the vector of conserved variables, the flux vector and the source term are given by

(5.5.9)

$$W = \begin{bmatrix} \alpha_k\rho_k \\ \alpha_k\rho_k u_k \\ \alpha_k\rho_k E_k \end{bmatrix}, \qquad F = \begin{bmatrix} \alpha_k\rho_k u_k \\ \alpha_k\rho_k u_k^2 + \alpha_k p \\ \alpha_k\rho_k H_k u_k \end{bmatrix} \qquad \text{and} \qquad S = \begin{bmatrix} 0 \\ p^i \frac{\partial \alpha_k}{\partial x} - \alpha_k\rho_k g \\ -p^i \frac{\partial \alpha_k}{\partial t} - \alpha_k\rho_k u_k g \end{bmatrix}.$$

The jacobian matrix of such a flux vector is given by

$$J = \frac{\partial F}{\partial W} = \begin{bmatrix} 0 & 1 & 0 \\ -u^2 + \frac{c^2(2\rho_h h + 2\rho - \rho_h u^2}{2\rho} & 2u + \frac{c^2\rho_h u}{\rho} & -\frac{c^2\rho_h}{\rho} \\ -u(h + \frac{u^2}{2}) + \frac{c^2 u(2\rho_h h + 2\rho - \rho_h u^2}{2\rho} & h + \frac{u^2}{2} + \frac{c^2\rho_h u^2}{\rho} & (1 - \frac{c^2\rho_h}{\rho})u \end{bmatrix},$$

If we analyse its eigenstructure we have the following set of eigenvalues

$$\begin{aligned} \lambda_1 &= u - c, \\ \lambda_2 &= u, \\ \lambda_3 &= u + c \end{aligned}$$

and their corresponding eigenvectors

$$P_1 = \begin{bmatrix} \frac{2\rho_h}{2\rho_h h + 2\rho + \rho_h u^2} \\ \frac{2\rho_h u}{2\rho_h h + 2\rho + \rho_h u^2} \\ 1 \end{bmatrix},$$

$$P_2 = \begin{bmatrix} \frac{2}{2h - 2cu + u^2} \\ \frac{2}{2h - 2cu + u^2} \\ 1 \end{bmatrix},$$

$$P_3 = \begin{bmatrix} \frac{2}{2h + 2cu + u^2} \\ \frac{2(c+u)}{2h + 2cu + u^2} \\ 1 \end{bmatrix}.$$

In order to get approximate solutions of our system we will use a scheme of the form

$$W_j^{n+1} = W_j^n - \frac{\Delta t}{\Delta x}\left[F_{j+\frac{1}{2}} - F_{j-\frac{1}{2}}\right] - \Delta t S_j^n$$

using the decoupled systems of equations for obtaining the flux at the intercells, solving for it two different Riemann problems that will involve different schemes for each fluid (in this case ATVD).

- For the gas or vapour phase we will utilize the ATVD scheme described above. We will introduce the spatial derivatives of void fraction in the flux vector in the same form we did before, using for its evaluation the same discretization as well. So that, we will have for the gas that the numerical flux is

$$F_{j+\frac{1}{2}} = \frac{1}{2}\left[F_{j+1} + F_j - B_{j,j+\frac{1}{2}} + B_{j+\frac{1}{2},j+1} - h(D_{j+\frac{1}{2}})(F_{j+1} - F_j + B_{j,j+\frac{1}{2}} + B_{j+\frac{1}{2},j+1})\right]$$

with the function $h(D_{j+\frac{1}{2}})$ given by the sign of the jacobian of the vapour system of equations

$$h(D_{j+\frac{1}{2}}) = \text{sign}(J_{j+\frac{1}{2}})) = P\text{sign}(D_{j+\frac{1}{2}})P^{-1}$$

- For the liquid we have tested the approach described above but the results have not been satisfactory. Another more simplified model has been considered for the liquid. It is based on the consideration that pressure does not change between two adjacent cells, this allows a better approximation to the analytical solution of Faucet test (see Appendix) and good solutions for the Toumi's shock tube as we will show below. Such a model provides a fairly different jacobian matrix. So, if we consider the flux vector given in eq. 5.5.9 the corresponding jacobian matrix is

$$J = \begin{bmatrix} 0 & 1 & 0 \\ -u_l^2 - p\frac{\partial\alpha}{\partial w_1} & 2u_l - p\frac{\partial\alpha}{\partial w_2} & -p\frac{\partial\alpha}{\partial w_3} \\ -u_l(H_l + p\frac{\partial\alpha}{\partial w_1}) & H_l - u_l p\frac{\partial\alpha}{\partial w_2} & u_l(1 - p\frac{\partial\alpha}{\partial w_1}) \end{bmatrix},$$

as the derivatives of pressure are all equal to zero.

If we choose as primitive variables α, u_l and T_l, the derivatives of α with respect to the conserved variables are

$$\frac{\partial\alpha}{\partial w_1} = -\rho_l, \qquad \frac{\partial\alpha}{\partial w_2} = 0 \qquad and \qquad \frac{\partial\alpha}{\partial w_3} = -\frac{\rho_l}{T_l}.$$

The eigenstructure of this jacobian matrix is given by the eigenvalues

$$\begin{aligned} \lambda_1 &= u - c^*, \\ \lambda_2 &= u, \\ \lambda_3 &= u + c^* \end{aligned}$$

where c^* is a pseudo speed of sound with dimension of velocity and given by

$$c^* = \sqrt{\frac{1}{\frac{\rho_l}{p} - \frac{1}{h_l}}}.$$

Their respective eigenvectors are

$$P_1 = \begin{bmatrix} \frac{1}{h_l + \frac{u_l}{2}(ul - 2c^*)} \\ -\frac{2(\frac{h_l p}{c^*} - pu_l)(\frac{h_l p}{c^*} - pu_l + h_l \rho_l u_l)}{-p(p - h_l \rho_l)u_l^3 + \frac{h_l p}{c^*}(-2h_l p + 2h_l^2 \rho_l - 3pu_l^2 + h_l \rho_l u_l^2)} \\ 1 \end{bmatrix},$$

$$P_2 = \begin{bmatrix} \frac{2}{u_l^2} \\ \frac{2}{u_l} \\ 1 \end{bmatrix},$$

$$P_3 = \begin{bmatrix} \frac{1}{h_l + \frac{u_l}{2}(ul + 2c^*)} \\ \frac{2(\frac{h_l p}{c^*} - pu_l)(\frac{h_l p}{c^*} - pu_l + h_l \rho_l u_l)}{p(p - h_l \rho_l)u_l^3 + \frac{h_l p}{c^*}(-2h_l p + 2h_l^2 \rho_l - 3pu_l^2 + h_l \rho_l u_l^2)} \\ 1 \end{bmatrix}.$$

5.5.5.1. Numerical Results

In this section we are going to analyse the results obtained using a decoupled version of the Adapted TVD scheme .

Water Faucet Test

In figure 5.19 we show the evolution of void fraction until steady state is reached. We notice a very good behaviour of the scheme with respect to previous schemes. In this case, the discontinuity appears a bit smeared since we have first order and the mesh has few points. This effect is reduced by increasing the number of cells. The results have been obtained by using $CFL = 0.9$ and $\sigma = 2$.

We have also tested the effect in the solutions produced when the mesh is refined. We have run three different cases, with meshes of 50, 100 and 200 points. The results obtained have been compared with the exact solution in figure 5.20. The Courant number have been put to $CFL = 0.9$ and the parameter $\sigma = 2$. We notice how the characterization of the discontinuity is better as the number of cells increases.

Toumi's Shock Tube

In the case of the shock tube test we have yielded the evolution of the different variables of interest as the mesh points increases. These results have been depicted in figure 5.21. Some spurious oscillations appear in the void fraction and in the velocities when the number of cells is too high (1600 points).

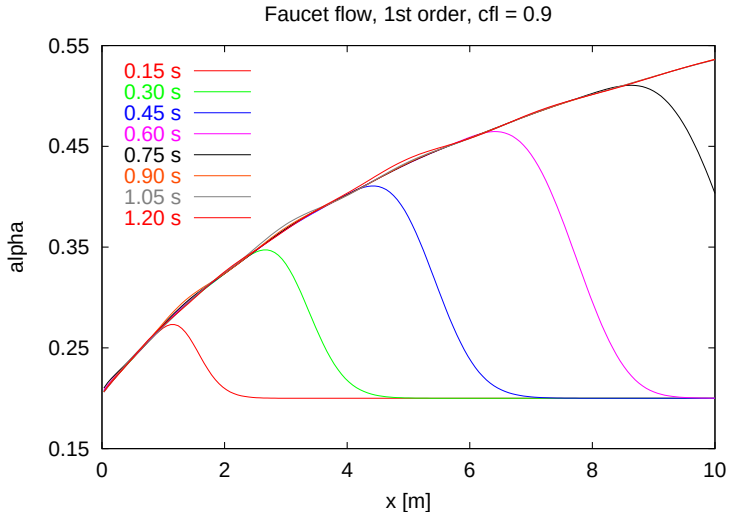

FIGURE 5.19. Evolution of void fraction with time.

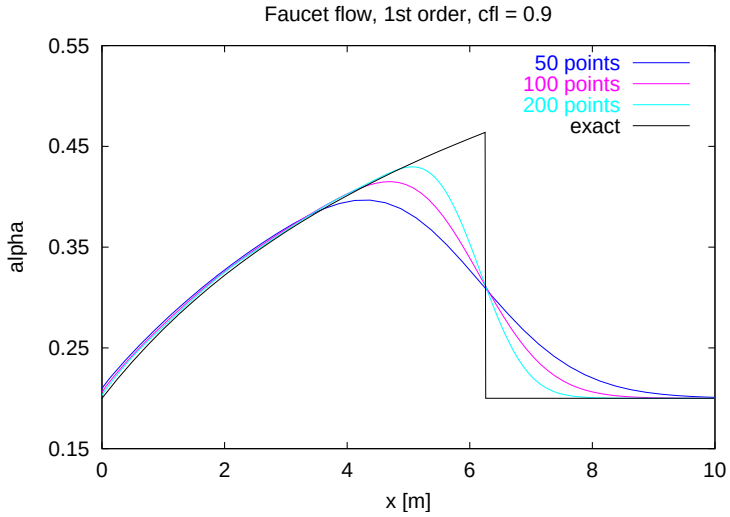

FIGURE 5.20. Void fraction for different number of cells.

On the other hand, we have not succeded using this scheme to solve the system of equation for the other tests (sedimentation and oscillating manometer). Furthermore, we remark that its applicability is reduced to problems in which the liquid phase can be modelled with that simplified model.

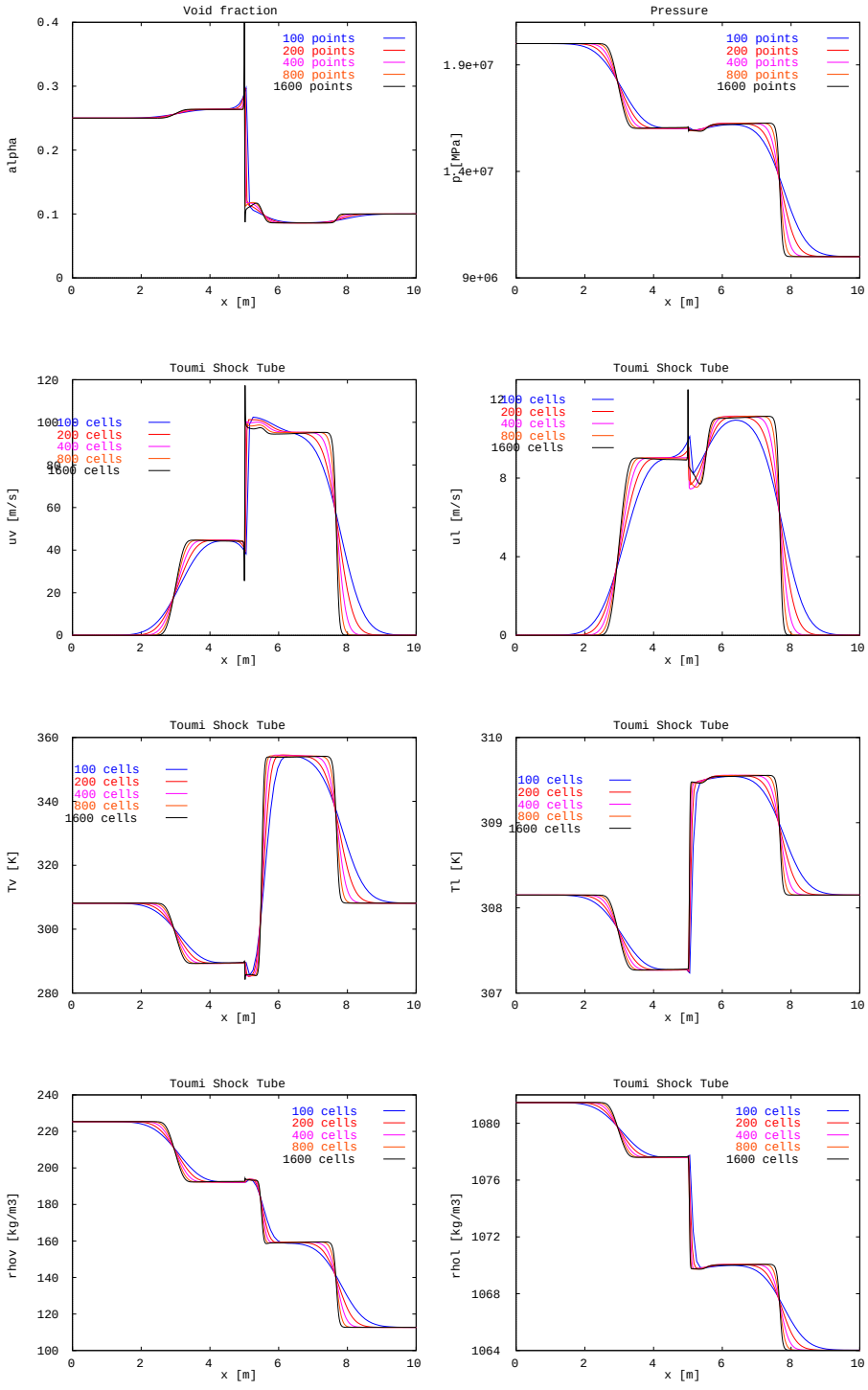

FIGURE 5.21. Toumi's shock tube, 1^{st} order ATVD2: Grid convergence study with the ATVD scheme, $\sigma = 2.0$. From top to bottom, left to right, void fraction, pressure, gas velocity, liquid velocity, gas temperature, liquid temperature, gas density and liquid density.

5.6. Extension of the AUSM+ Scheme to Two Phase Flow

5.6.1. Introduction

The AUSM family of schemes was introduced by Liou in [**45**] due to the deficiencies of Godunov type schemes and its approximation schemes such as Roe and Osher and Solomon schemes (shock instability in multidimensions). He solves them by considering the mass flux as an essential element in constructing a robust and accurate numerical flux. As mentioned above, one of their main characteristics is that the utilization of theses schemes do not imply differentiation as the majority of the flux difference schemes and therefore we do not have to determine the eigenstructure of the system. This property is also very helpful when studying different models for the fluids it only affects strongly to the eigenstructure that we do not need to calculate with the AUSM schemes.

In a search of a scheme with the accuracy of flux difference splitting and the efficiency of flux vector splitting Liou presents in [**43**] the AUSM+ scheme as a new improved version of the AUSM with the following features:

- Exact resolution of a stationary normal shocks and contact discontinuities.
- Positivity preserving property.
- Free of oscillations at the slowly moving shock.
- Algorithmic simplicity and easy extension to treat other hyperbolic systems.
- Improvement in accuracy over its predecessor AUSM and other popular schemes.
- Simplicity and easy generalization to other conservation laws.

We are going to introduce the AUSM schemes, for which we will consider approximations to the initial value problem given by

$$\begin{aligned} \frac{\partial W}{\partial t} + \frac{\partial F}{\partial x} &= 0, \quad t > 0, \quad -\infty \leq x \leq \infty \\ W(x,0) &= W_0(x) \end{aligned}$$

where $W = (\rho, \rho u, \rho E)^t$.

These approximations are defined by the following explicit scheme

$$W_j^{n+1} = W_j^n - \lambda \left[F^n_{j+\frac{1}{2}} - F^n_{j-\frac{1}{2}} \right], \quad n \in N,\ j \in Z$$

where $\lambda = \frac{\Delta t}{\Delta x}$, and the definition of the flux is done by means of a distinction of a convective and a pressure parts such that

$$F = F^{(c)} + P.$$

where $F^{(c)} = \dot{m}\Psi$, $\dot{m} = \rho M a$, $\Psi = \begin{pmatrix} 1 \\ u \\ h_t \end{pmatrix}$ and $P = \begin{pmatrix} 0 \\ p \\ 0 \end{pmatrix}$

Hence the numerical flux is defined as

$$F_{i+\frac{1}{2}} = F^c_{i+\frac{1}{2}} + F^p_{i+\frac{1}{2}}$$

with

$F^c_{i+\frac{1}{2}}$: the numerical convective flux and

$F^p_{i+\frac{1}{2}}$: the numerical pressure flux.

For the Euler equations, the numerical flux at the interface is given by

$$F^c_{i+\frac{1}{2}} = \dot{m}_{\frac{1}{2}}(u_L, u_R)\psi_{\frac{1}{2}}(u_L, u_R)$$

where the left and right states are denoted by L (left) and R (right)

$$\psi_{\frac{1}{2}}(u_L, u_R) = \begin{cases} \Psi_L, & \text{if } \dot{m}_{\frac{1}{2}} \geq 0 \\ \Psi_R, & \text{otherwise.} \end{cases}$$

The pressure flux comprises only one variable

$$F^p_{\frac{1}{2}} = (0, p_{\frac{1}{2}}(u_L, u_R), 0)^t$$

Thus the scheme is completed by the definition of the interface variables. The difference among the AUSM schemes resides in the definition of the coefficients $\dot{m}_{\frac{1}{2}}$ and $p_{\frac{1}{2}}$. Their definitions are based on some polynomials, functions of the Mach number (M).

For the definition of $\dot{m}_{\frac{1}{2}}$we have

$$M^{\pm}_{(1)}(M) = \frac{1}{2}(M \pm |M|),$$

$$M^{\pm}_{(2)}(M) = \begin{cases} M^{\pm}_{(1)}(M), & \text{if } |M| \geq 1, \\ \pm\frac{1}{4}(M \pm 1)^2, & \text{otherwise,} \end{cases}$$

$$M^{\pm}_{(4,\beta)}(M) = \begin{cases} M^{\pm}_{(1)}(M), & \text{if } |M| \geq 1, \\ M^{\pm}_{(2)}(M)\left[1 \mp 16\beta M^{\mp}_{(2)}(M)\right], & \text{otherwise} \end{cases}$$

and for the pressure

$$P^{\pm}_{(3)}(M) = \begin{cases} \frac{M^{\pm}_{(1)}(M)}{M}, & \text{if } |M| \geq 1, \\ \pm M^{\pm}_{(2)}(M)(2 \mp M), & \text{otherwise.} \end{cases}$$

$$P^{\pm}_{(5,\alpha)}(M) \begin{cases} \frac{M^{\pm}_{(1)}(M)}{M}, & \text{if } |M| \geq 1, \\ \pm M^{\pm}_{(2)}(M) \left[(2 \mp M) - 16\alpha M^{\mp}_{(2)}(M) \right], & \text{otherwise} \end{cases}$$

with $\alpha = \frac{3}{16}, \beta = \frac{1}{8}$.

These definitions are completed with the numerical speed of sound, $a_{\frac{1}{2}} = a(u_L, u_R)$, the Mach numbers used in the above polynomials, $p_{\frac{1}{2}}$ and $\dot{m}_{\frac{1}{2}}$ which are defined as

$$M_L(u_L, u_R) = \frac{u_L}{a_{\frac{1}{2}}}, \text{ and } M_R(u_L, u_R) = \frac{u_R}{a_{\frac{1}{2}}},$$
$$p_{\frac{1}{2}}(u_L, u_R) = P^{+}_{(5,\alpha)}(M)p_L + P^{-}_{(5,\alpha)}(M)p_R,$$
$$\dot{m}_{\frac{1}{2}}(u_L, u_R) = a_{\frac{1}{2}}(\rho_L M^{+}_{\frac{1}{2}} + \rho_R M^{-}_{\frac{1}{2}}).$$

In this work two of these AUSM schemes have been considered, the AUSM+ [**43**] as it represents an improvement of the previous AUSM, and the AUSMDV [**49**] because it improves the robustness of AUSM in dealing with the collision of strong shocks. A complete description of the family of AUSM can be found in [**44**]. Depending on the scheme, we have the following definitions of $M^{\pm}_{\frac{1}{2}}$

AUSM+:

$$\begin{aligned} M_{\frac{1}{2}}(M_L, M_R) &= M^{+}_{(4,\beta)}(M_L) + M^{-}_{(4,\beta)}(M_R), \\ M^{\pm}_{\frac{1}{2}} &= \frac{1}{2}(M_{\frac{1}{2}} \pm \left| M_{\frac{1}{2}} \right|). \end{aligned}$$

AUSMDV:

$$\begin{aligned} M^{+}_{\frac{1}{2}}(M_L, \omega^{+}_{\frac{1}{2}}) &= \omega^{+}_{\frac{1}{2}} M^{+}_{(4,\beta)}(M_L) + (1 - \omega^{+}_{\frac{1}{2}}) M^{+}_{(1)}(M_L), \\ M^{-}_{\frac{1}{2}}(M_R, \omega^{-}_{\frac{1}{2}}) &= \omega^{-}_{\frac{1}{2}} M^{-}_{(4,\beta)}(M_R) + (1 - \omega^{-}_{\frac{1}{2}}) M^{-}_{(1)}(M_R), \end{aligned}$$

with $\omega^{\pm}_{\frac{1}{2}} = \omega^{\pm}(u_L, u_R)$ and $0 \leq \omega^{\pm} \leq 2$.

In the following sections we tackle the extension of these schemes, AUSM+ and AUSMDV, to the system of equations that appears in two phase flow. Afterwards some numerical results are included in order to illustrate their behaviour under the resolution of some difficult benchmarks.

5.6.2. Definition of the AUSM+ and AUSMDV Numerical Fluxes in Two Phase Flow

The AUSM+ finite difference method can compete with Roe's Approximate Riemann Solvers and VFFC method in order to solve the above system of equations. Some experiences have been done in applying this scheme to two phase flow, the homogeneous case is studied in [**52**] and the isentropic case (four equation model) in [**51**]. They are presented as schemes that are able to capture shocks and contact discontinuities with minimal numerical dissipation and oscillations. Their idea consists of a splitting of the flux term in two, a convective and a pressure term. Here, we present its extension to the six equation model in two phase flow.

If we consider the system of equations 5.2.1, the flux vector 5.2.2 can be splitted in the following way

$$F(W) = F^c(E) + F^p(W)$$

where

$$F^c(W) = \begin{bmatrix} \alpha\rho_v u_v \\ (1-\alpha)\rho_l u_l \\ \alpha\rho_v u_v^2 \\ (1-\alpha)\rho_l u_l^2 \\ \alpha\rho_v H_v u_v \\ (1-\alpha)\rho_l H_l u_l \end{bmatrix} = \begin{bmatrix} \dot{m}_v \\ \dot{m}_l \\ \dot{m}_v u_v \\ \dot{m}_l u_l \\ \dot{m}_v H_v \\ \dot{m}_l H_l \end{bmatrix}, \qquad F^p(W) = \begin{bmatrix} 0 \\ 0 \\ \alpha p \\ (1-\alpha)p \\ 0 \\ 0 \end{bmatrix}.$$

Our scheme will have the form

$$W_i^{n+1} = W_i^n - \frac{\Delta t}{\Delta x}\left[F_{i+\frac{1}{2}}(W_i^n, W_i^{n+1}) - F_{i-\frac{1}{2}}(W_i^{n-1}, W_i^n)\right] - \Delta t S_i^n. \tag{5.6.1}$$

We must notice that the non conservative terms has been included in the source term as well, hence the numerical flux at the interface is

$$F_{i+\frac{1}{2}} = F^c_{i+\frac{1}{2}} + F^p_{i+\frac{1}{2}} \tag{5.6.2}$$

the convective part may be written for the j^{th} component of $F_{i+\frac{1}{2}}$ as:

$$F^c_{j,i+\frac{1}{2}} = \dot{m}_{k,i+\frac{1}{2}} \left[F_j^c\right]_{i,i+1}$$

where $k = v, l$ depends on whether the phase is vapour (v) or liquid (l), j odd or even respectively

$$\left[F_j^c\right]_{i,i+1} = \begin{cases} F^c_{j,i} & \text{if } \dot{m}_{k,i+\frac{1}{2}} \geq 0 \\ F^c_{j,i+1} & \text{if} \dot{m}_{k,i+\frac{1}{2}} < 0 \end{cases}.$$

$\dot{m}_{k,i+\frac{1}{2}}$ has been defined for the two phase flow case as

$$\dot{m}_{k,i+\frac{1}{2}} = a_{k,i+\frac{1}{2}}(\rho_{k,i}M^{+}_{k,i+\frac{1}{2}} + \rho_{k,i+1}M^{-}_{k,i+\frac{1}{2}})$$

with

$$a_{k,i+\frac{1}{2}} = \sqrt{a_{k,i}a_{k,i+1}},$$
$$M^{\pm}_{k,i+\frac{1}{2}} = \frac{1}{2}\left(M_{k,i+\frac{1}{2}} \pm \left|M_{k,i+\frac{1}{2}}\right|\right),$$
$$M_{k,i+\frac{1}{2}} = M^{+}_{k,\beta}(M_{k,i}) + M^{-}_{k,\beta}(M_{k,i}),$$

and

$$M^{\pm}_{k,\beta} = \begin{cases} \frac{1}{2}(M_k \pm |M_k|) & \text{if } |M_k| \geq 1 \\ \pm\frac{1}{4}(M_k \pm 1)^2\left[1 \mp 16\beta \mp \frac{1}{4}(M_k \mp 1)^2\right] & \text{otherwise} \end{cases}$$

where $\alpha = \frac{3}{8}$ and $\beta = \frac{1}{8}$.

The pressure term, F^p at the interface is

$$F^{p}_{i+\frac{1}{2}} = \begin{bmatrix} 0 \\ 0 \\ p_{v,\frac{1}{2}} \\ p_{l,\frac{1}{2}} \\ 0 \\ 0 \end{bmatrix}$$

where

$$p_{k,\frac{1}{2}} = P^{+}_{k,\alpha}(M_{k,i})\alpha_{k,i}p_i + P^{-}_{k,\alpha}(M_{k,i+1})\alpha_{k,i+1}p_{i+1}$$

with $\alpha_v = \alpha$, $\alpha_l = 1 - \alpha$ and

$$P^{\pm}_{k,\alpha} = \begin{cases} \frac{1}{2}\frac{(M \pm |M|)}{M} & \text{if } |M| \geq 1, \\ \pm\frac{1}{4}(M \pm 1)^2\left[1 \mp 16\beta \mp \frac{1}{4}(M \mp 1)^2\right] & \text{otherwise.} \end{cases}$$

AUSMDV differs of AUSM+ in the definition of $\dot{m}_{k,i+\frac{1}{2}}$, this is

$$M^{\pm}_{k,i+\frac{1}{2}} = \left(\omega^{\pm}_{\frac{1}{2}}M^{\pm}_{k,\beta}(M_{k,i}) + (1 - \omega^{\pm}_{\frac{1}{2}})\frac{1}{2}(M_k \pm |M_k|)\right)$$

where

$$\omega^{\pm}_{\frac{1}{2}} = \frac{2f_{i,i+1}}{f_i + f_{i+1}}.$$

Two possible definition of the blended function, f have been tested

$$f = \frac{p}{\alpha_k\rho_k} \qquad \text{and} \qquad f = \frac{1}{\alpha_k\rho_k}.$$

The usage of the second version is recommended in [**49**] as the first one leads to shock instabilities.

Non conservative terms in 5.2.1 have been discretized with the same criteria used above, a central discretization has been used for

$$p\frac{\partial \alpha}{\partial x} \approx p_i^n \frac{\alpha_{i+1}^n - \alpha_{i-1}^n}{2\Delta x}$$

and a backward one for

$$p\frac{\partial \alpha}{\partial t} \approx p_i^n \frac{\alpha_i^n - \alpha_i^{n-1}}{\Delta t^{n-1}}.$$

5.6.3. Higher Order Extension

In order to get second order accuracy and preserve monotonicity, Liou suggests in [**43**] the usage of variable extrapolation, based on the MUSCL strategy. We have tested three algorithms in order to get second order in space and time.

1st option, it consists of the following steps widely explained in [**35**]:
1st step. Propagation of the conserved variables over a time step of $\frac{\Delta t}{2}$, this defines intermediate values for the conserved variables, and hence for the primitive ones, using the first order scheme, eq. 5.6.1 over $\frac{\Delta t}{2}$

$$W_j^{n+\frac{1}{2}} = W_j^n - \frac{\Delta t}{2\Delta x}(F_{j+\frac{1}{2}} - F_{j-\frac{1}{2}}) - \frac{\Delta t}{2}\Delta S^n$$

with $f_{j+\frac{1}{2}}$ the above AUSM+ flux (eq. 5.6.2).

2nd step. Definition of the interface variables as second order extrapolations to the intermediate values W, this step does not have to be conservative so we could utilize conserved or primitive variables, we have preferred using primitive variables following recomendations of Saurel in [**58**], he recomends their utilization in order to preserve a uniform solution by regarding pressure and velocity at the end of the predictor step, this has been the reason that has made us consider primitive variables instead conserved variables, so we can calculate from $W_j^{n+\frac{1}{2}}$, $V_j^{n+\frac{1}{2}}$

$$\begin{aligned} V_{j+\frac{1}{2}}^L &= \overline{V}_j + \frac{1}{2}\psi(\frac{V_{j+2} - V_{j+1}}{\Delta x}, \frac{V_j - V_{j-1}}{\Delta x})\Delta x \\ V_{j+\frac{1}{2}}^R &= \overline{V}_{j+1} - \frac{1}{2}\psi(\frac{V_{j+1} - V_j}{\Delta x}, \frac{V_j - V_{j-1}}{\Delta x})\Delta x, \end{aligned} \tag{5.6.3}$$

where monotonicity has been preserved using limiters ψ, in [**35**] can be found a summary of the most important limiters. Four of them has been tested,

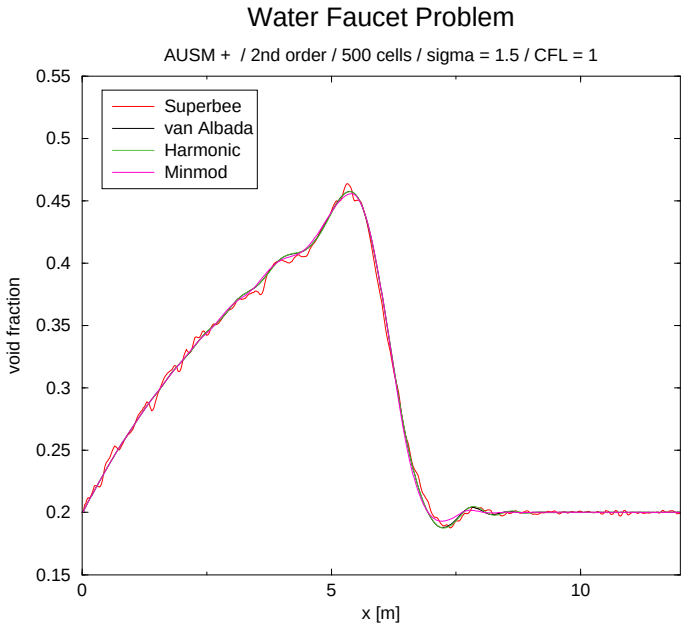

FIGURE 5.22. Second order approach using different limiters

- *superbee*

$$\psi(x,y) = \frac{1}{2}(1+\mathrm{sgn}(xy))\max[0,\min(2\frac{x}{y},1),\min(\frac{x}{y},2)].$$

- *minmod*

$$\psi(x,y) = \frac{1}{2}(1+\mathrm{sgn}(xy))\frac{1}{2}(\mathrm{sgn}(x)+\mathrm{sgn}(y))\min(|x|,|y|).$$

- *van Albada*

$$\psi(x,y) = \frac{1}{2}(1+\mathrm{sgn}(xy))\frac{xy(x+y)}{x^2+y^2}.$$

- *harmonic*

$$\psi(x,y) = \frac{1}{2}(1+\mathrm{sgn}(xy))\frac{2xy}{x+y}.$$

In figure 5.22 we show the results obtained for each limiter, we can observe similar behaviours with all of them except for the superbee which presents some oscillations.

3^{rd} step. Definition of the second order AUSM+ numerical flux

$$F^{(2)}_{i+\frac{1}{2}} = F_{j+\frac{1}{2}}(V^L_{j+\frac{1}{2}}, V^R_{j+\frac{1}{2}})$$

and finally the conserved variables in $n+1$ are updated

$$W_j^{n+1} = W_j^n - \frac{\Delta t}{\Delta x}(F^{(2)}_{j+\frac{1}{2}} - F^{(2)}_{j-\frac{1}{2}}) - \Delta t S^n. \tag{5.6.4}$$

This algorithm is similar to the one presented by van Leer in [**82**], but he assumes some initial values for the conserved variables before step 1

$$W^n_{j\pm\frac{1}{2}}(x) = W_j^n \pm \frac{(\delta W)_j^n}{2}, \qquad x_{j-\frac{1}{2}} < x < x_{j+\frac{1}{2}}$$

with

$$(\delta W)_j^n = ave(W^n_{j+1} - W_j^n, W_j^n - W^n_{j-1}).$$

2nd option. On the other hand we have considered the problem of second order approximation by limiting also the prediction step. Using in this case the primitive variables in the following way

$$V_j^{n+\frac{1}{2}} = V_j^n + \frac{\Delta t}{2}\left(\frac{\partial V}{\partial t}\right)_j \tag{5.6.5}$$

since we can write the system of equation 5.2.1 in non conservative form as

$$B\frac{\partial V}{\partial t} + C\frac{\partial V}{\partial x} = S$$

we have premultiplied by B^{-1}

$$\frac{\partial V}{\partial t} + A\frac{\partial V}{\partial x} = B^{-1}S$$

where $A = B^{-1}C$. Then equation 5.6.5 has been written as

$$V_j^{n+\frac{1}{2}} = V_j^n - \frac{\Delta t}{2}A(V_j)\left(\frac{\partial V}{\partial x}\right)_j + \frac{\Delta t}{2}B^{-1}(V_j)S$$

and then, the derivative $\left(\frac{\partial V}{\partial x}\right)_j$ has been limited by the minmod limiter, due to the good results obtained previously. We must evaluate the matrix A at each mesh point, in this case A is a bit complex.

Now we determine the AUSM+ fluxes at the interfaces, for which we determine the primitives variables at the left and the right side using the same approximation than in the first option (equations 5.6.3), finally we follow the *3^{rd} step* of the previous method to get the approach 5.6.4.

3rd option. An alternative option has been considered, doing some manipulations in the propagation step

$$W_j^{n+\frac{1}{2}} = W_j^n - \frac{\Delta t}{2}\frac{\partial W}{\partial t}$$

and as

$$\frac{\partial W}{\partial t} = -\frac{\partial F}{\partial x} + S = -\frac{\partial F}{\partial V}\frac{\partial V}{\partial x} + S$$

and therefore

$$W_j^{n+\frac{1}{2}} = W_j^n - \frac{\Delta t}{2} A(V_j) \left(\frac{\partial V}{\partial x}\right)_j + \frac{\Delta t}{2} S$$

where $A(V_j) = \frac{\partial F}{\partial V}$.

In figure 5.23 we represent the results obtained for the Faucet test, in particular for the first and third options. They show the same behaviour so that we have not included the second because as it gives similar results than option 3. We prefer the third option since it yields an easier matrix A than in the 2^{nd} option.

Taking into account the equations of state defined above, it is

$$A = \frac{\partial F}{\partial V} = \begin{bmatrix} \rho_v u_v & \alpha\rho_v & 0 \\ -\rho_l u_l & 0 & (1-\alpha)\rho_l \\ p + \rho_v u_v^2 & 2\alpha\rho_v u_v & 0 \\ -p - \rho_l u_l^2 & 0 & 2(1-\alpha)\rho_l u_l \\ \rho_v u_v H_v & \alpha\rho_v(H_v + u_v^2) & 0 \\ -\rho_l u_l H_l & 0 & (1-\alpha)\rho_l(H_l + u_l^2) \end{bmatrix}$$

$$\begin{bmatrix} \frac{\alpha\rho_v u_v}{p} & -\frac{\alpha\rho_v u_v}{T_v} & 0 \\ \frac{(1-\alpha)\rho_l u_l}{p-p_\infty} & 0 & -\frac{\alpha\rho_l u_l}{T_l} \\ \alpha(1 + \frac{\rho_v u_v^2}{p}) & -\frac{\alpha\rho_v u_v^2}{T_v} & 0 \\ (1-\alpha)(1 + \frac{\rho_l u_l^2}{p+p_\infty}) & 0 & -\frac{\alpha\rho_l u_l^2}{T_l} \\ \alpha\frac{\gamma_v}{\gamma_v - 1} u_v(\frac{u_v^2}{2c_{pv}T_v} + 1) & -\frac{\alpha\rho_v u_v^3}{2T_v} & 0 \\ (1-\alpha)\frac{\gamma_l}{\gamma_l - 1} u_l(\frac{u_l^2}{2c_{pl}T_l} + 1) & 0 & -\frac{\alpha\rho_l u_l^3}{2T_l} \end{bmatrix}.$$

It is important remark that in option 2 and 3 the source terms have not been considered at the prediction step although results are similar as it is shown in figure 5.24.

5.6.4. AUSM Schemes and Low Mach Number Flows

In [**49**], Liou states that two effects on the solution appears as the flow speed approaches to zero:

- A drastic slowdown or level off of convergence rate and

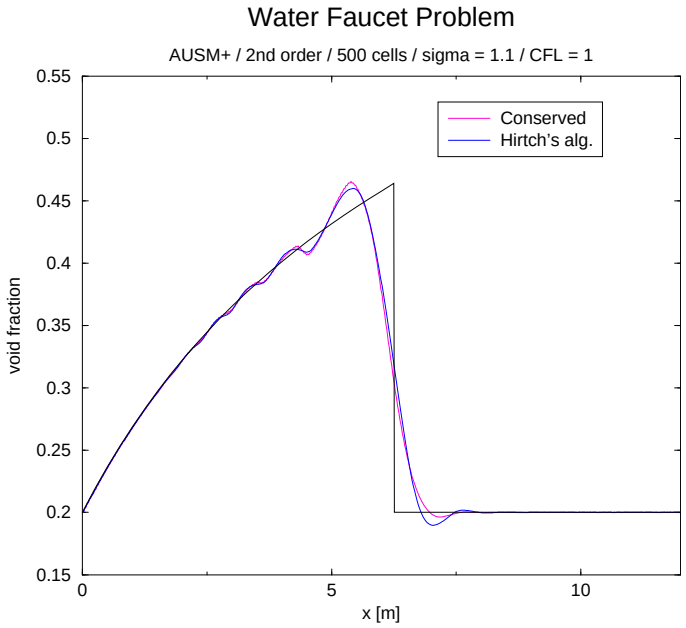

FIGURE 5.23. Comparison for 1st, 2nd and 3rd options, using minmod limiter

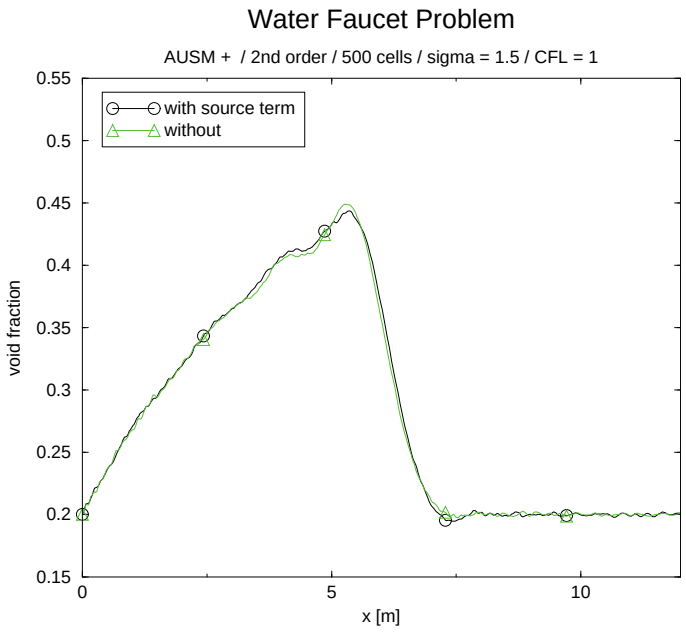

FIGURE 5.24. Comparison between results obtained considering or not the source terms in the prediction step

- An inaccurate or even incorrect solution.

The way of dealing with these problems is by introducing preconditioning techniques.

The inaccuracies in the upwind schemes are primarily due to incorrect scaling of the signal speed as M goes to zero. This introduces numerical dissipation, so the numerical fluxes need to be modified to correct this situation. The preconditioning alters the eigenvalues of the hyperbolic systems so that the wave speeds become more or less equalized. To do that a modified speed of sound is introduced that enables this effect.

With respect to the AUSM+ scheme, it is necessary remark that the mass flux would be the same we have in the initial definition of the AUSM+ but with a "scaled speed of sound" that will give smaller dissipation. Regarding the AUSMDV scheme the pressure difference also needs to be re-scaled properly. In the case of AUSM+, where we have not pressure diffusion terms we will add one to maintain pressure velocity coupling low Mach flows.

We have tried to introduce preconditioning following [**23**]:
Firstly we define

$$U_{ref}^2 = \min(a^2, \max(\left|\overrightarrow{V}\right|^2, k\left|\overrightarrow{V}_\infty\right|^2$$

with $\overrightarrow{V}_\infty$: the average incoming velocity (a value $k = 0.25$ was chosen in this analysis).
Based on it, a reference Mach number is defined

$$M_{ref}^2 = \frac{U_{ref}^2}{a}.$$

For the preconditioned AUSM+ and AUSMDV, we have to re-difine $\dot{m}_{\frac{1}{2}}$ and $a_{\frac{1}{2}}$.
Preconditioned Mach number

$$\widetilde{M}_{i,i+1} = \frac{1}{f_{\frac{1}{2}}} M_{i,i+1} = \frac{u_{i,i+1}}{\widetilde{a}_{\frac{1}{2}}}$$

with the preconditioned speed of sound

$$\widetilde{a}_{\frac{1}{2}} = f_{\frac{1}{2}} a_{\frac{1}{2}}$$

and

$$f_{\frac{1}{2}} = f(M, M_{ref}) = \frac{\sqrt{(1 - M_{ref_{\frac{1}{2}}}^2)^2 M_{\frac{1}{2}}^2 + 4M_{ref_{\frac{1}{2}}}^2}}{1 - M_{ref_{\frac{1}{2}}}^2}.$$

and taking into account [**49**] it is bounded by

$$1 \geq f \geq \begin{cases} |M| & \text{if } 1 >> M^2 >> M^2_{ref} \\ 2M_{ref} & \text{if } 1 >> M^2_{ref} >> M^2 \end{cases}$$

We have called $M_{\frac{1}{2}} = \frac{u_i}{a_{\frac{1}{2}}}$.

The Mach numbers at left and right states are

$$\begin{aligned} \overline{M}_i &= \frac{1}{2}[(1+M^2_{ref_{\frac{1}{2}}})\widetilde{M}_i + (1-M^2_{ref_{\frac{1}{2}}})\widetilde{M}_{i+1}] \\ \overline{M}_i &= \frac{1}{2}[(1+M^2_{ref_{\frac{1}{2}}})\widetilde{M}_{i+1} + (1-M^2_{ref_{\frac{1}{2}}})\widetilde{M}_i]. \end{aligned}$$

After defining these terms we have to derive the preconditioned mass fluxes, they will depend on either we choose AUSMDV or AUSM+, by using $(\overline{M}_i, \overline{M}_{i+1})$, we add to the usual AUSM mass flux the contribution from pressure diffusion

$$\dot{m}_{\frac{1}{2}} = \begin{cases} \dot{m}_{AUSMDV} \\ \dot{m}_{AUSM+} \end{cases} + \dot{m}_p$$

where

$$\dot{m}_p = \widetilde{a}_{\frac{1}{2}}(\frac{1}{M^{*2}} - 1)[M^+_{4,\beta}(\overline{M}_L) - M^+_{(1)}(\overline{M}_L) - M^-_{4,\beta}(\overline{M}_R) + M^-_{(1)}(\overline{M}_R)]\frac{p_L - p_R}{\frac{p_L}{\rho_L} + \frac{p_R}{\rho_R}}.$$

For the AUSM+ the mass flux is calculated by means of

$$\dot{m}_{\frac{1}{2}} = (\rho u)_{\frac{1}{2}} = (\rho u)_{\frac{1}{2}AUSM+} + \widetilde{a}_{\frac{1}{2}}(\frac{1}{M^2_{ref_{\frac{1}{2}}}} - 1)[M^+_{4,\beta}(\overline{M}_i)$$

$$-M^+_{(1)}(\overline{M}_i) - M^-_{4,\beta}(\overline{M}_{i+1}) + M^-_{(1)}(\overline{M}_{i+1})]\frac{p_i - p_{i+1}}{\frac{p_i}{\rho_i} + \frac{p_{i+1}}{\rho_{i+1}}}$$

For the AUSMDV the interface mass flux is defined by using the expressions in [**23**].

$$\dot{m}_{\frac{1}{2}} = (\rho u)_{\frac{1}{2}} = a_{\frac{1}{2}}(\rho_i m^+_{\frac{1}{2}} + \rho_{i+1} m^-_{\frac{1}{2}}).$$

Taking into account [**23**] and [**49**], preconditioning of two phase flow is advised in order to improve the results at low Mach numbers. Despite the low Mach numbers we have found, preconditioning has not been necessary in some of the tests studied which that we describe below, namely the Faucet test and the Toumi's shock tube. In the phase separation problem and in the oscillating manometer test we have found some numerical diffusion in the solution, it has been avoided by adding a term related to

the preconditioned version of the mass flux when the fluid is incompressible (see [**23**] for details)

$$\dot{m}_{\frac{1}{2}} = (\rho u)_{\frac{1}{2}} + C(u_{\frac{1}{2}}, U_{ref}) \frac{\sqrt{u_{\frac{1}{2}}^2 + 4U_{ref}^2}}{U_{ref}^2}(p_i - p_{i+1})$$

this is

$$\dot{m}_{\frac{1}{2}} = (\rho u)_{\frac{1}{2}} + 0.001(p_i - p_{i+1}).$$

However, this has not been enough in the manometer test. For the four equations model a perfect representation of the fluxes was achieved (see [**51**], perhaps because the diffusion is mostly introduced by the energy equations. Numerical diffusion would have been eliminated by using AUSM schemes plus a better preconditioning formulations as is recommended in[**23**]. This has been left for a further research.

5.6.5. Numerical Results

In this section we describe the behaviour of AUSM+ and AUSMDV under some numerical tests. We study as much their first order approximation as the second order one which has been done using the MUSCL approximation accompanied by a minmod slope limiter.

5.6.5.1. Water Faucet Test

We begin showing the results obtained with the first order approximation scheme, in figure 5.25, we show the results of the simulations for different number of cells and for $t = 0.5$ seconds, in figure 5.26 is also shown the evolution of void fraction until steady state is reached for a 200 cell mesh

It is possible check that some oscillations appears when a higher number of cells is considered (1500 cells in figure 5.25), this has been avoided adding the term defined in eq. 5.2, that makes the system hyperbolic.

In fig. 5.27 we see how oscillations are smeared as σ grows, in figure 5.28 is represented void fraction for a mesh of 3000 cells and $\sigma = 3$.

In figures **??** and **??** we can find plotted some of the primitives variables for different values of σ, which shows the influence of such a parameter in the value of the variables, some differences can be detected in pressures but not in the rest of the variables, this is due to, in this pressure particular problem, it has practically no influence over the other variables.

With second order approximation we have not found any additional improvement in the case of the algorithms explained above, we have in figure 5.29 the influence

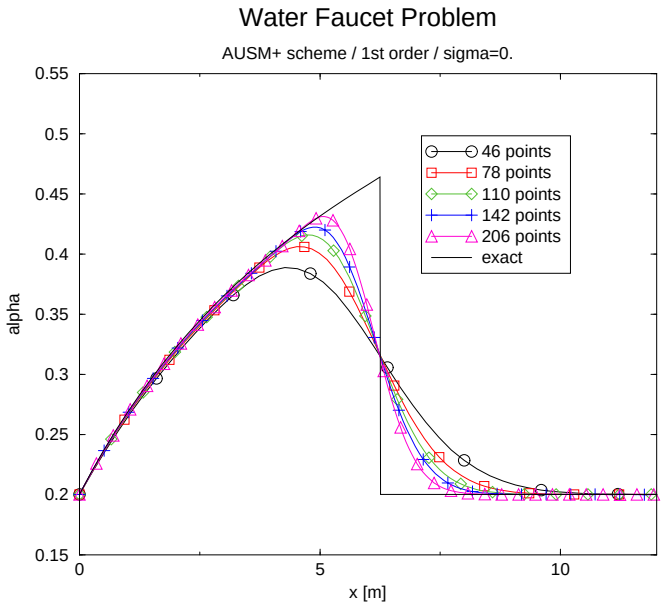

FIGURE 5.25. Influence of discretization (from 46 to 206 cells)

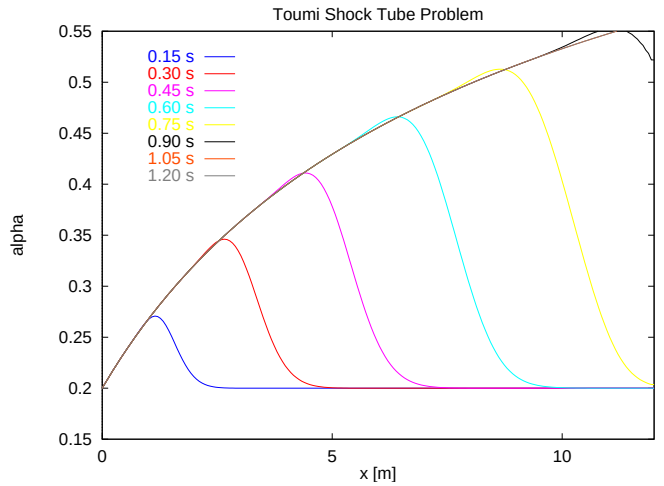

FIGURE 5.26. Evolution of void fraction for a 200 cells mesh

of the mesh chosen in the results and in figure 5.30 we also observe how oscillations decrease as the model become hyperbolic (σ increases).

The effect of using AUSMDV scheme has been checked with this test, in figure we can see how the AUSM+ provides better results in the case of second order (in

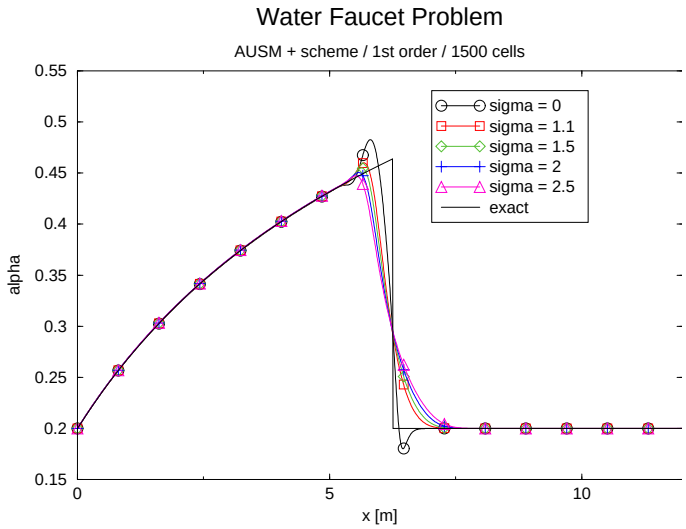

FIGURE 5.27. Computation with 1500 cells and different values of σ

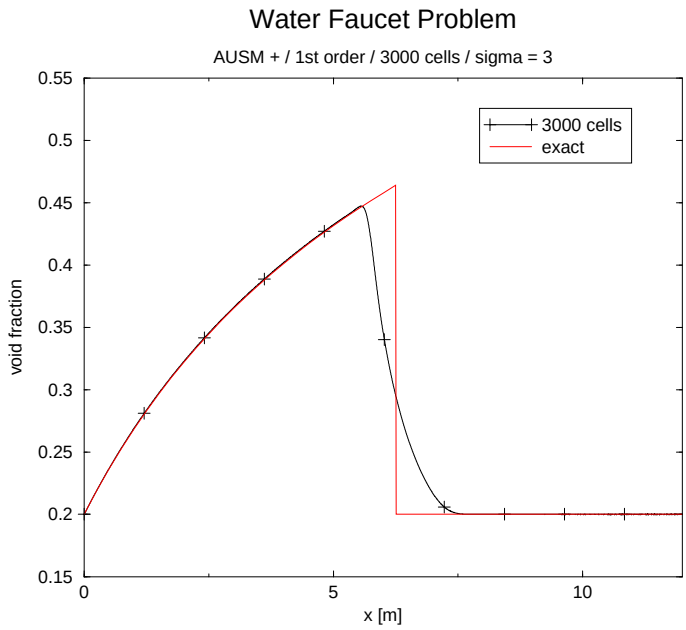

FIGURE 5.28. Computation with 3000 cells and $\sigma = 3$, compared with the exact solution

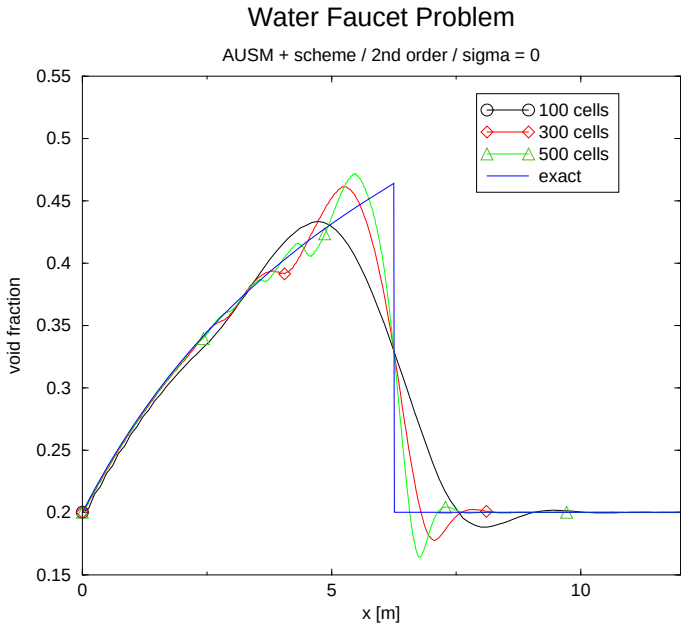

FIGURE 5.29. Influence of discretization, $\sigma = 0$

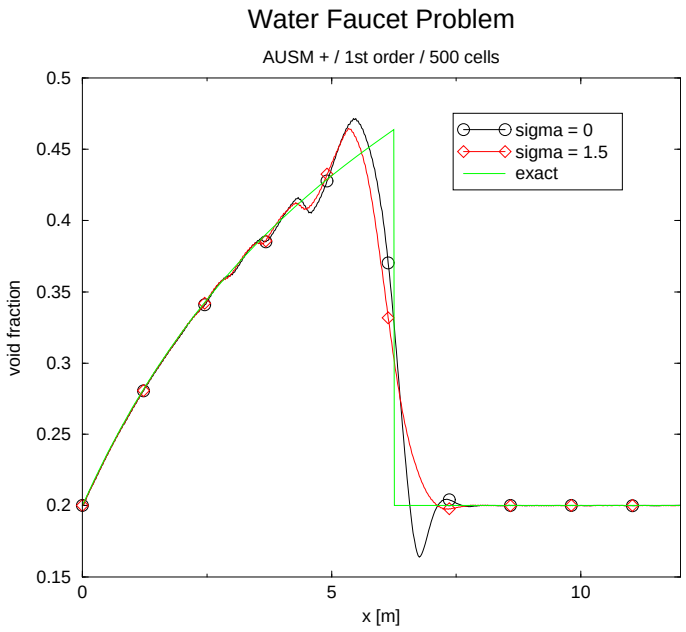

FIGURE 5.30. Computation with 500 cells and various values of σ

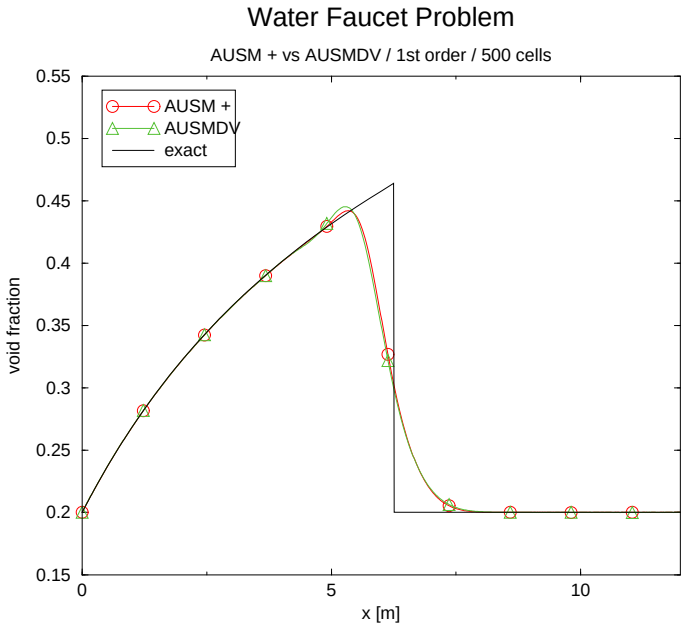

FIGURE 5.31. Comparison of ausm+ and ausmdv in Ransom test with first order precision

first order similar results figure), on the other hand AUSMDV gives better results in problems with shocks, as we will see below but needs a CFL number lower or iqual to 0.3.

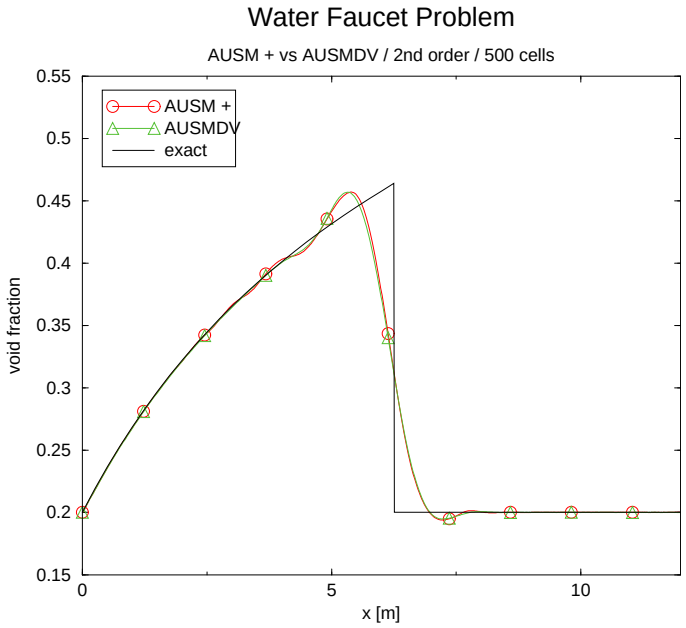

FIGURE 5.32. Comparison of ausm+ and ausmdv in Ransom test with second order precision

5.6.5.2. Toumi's Shock Tube

In figures 5.33, 5.34, 5.35 and 5.36, is shown the evolution of the profiles of the primitives variables α, u_v, u_l, p, $,T_v$ and T_l, as the number of point mesh increases (100, 200, 400, 800 and 1600). They correspond to different versions of the AUSM schemes, fist order AUSM+, second order AUSM+, first order AUSMDV and second order AUSMDV respectively. All of the cases have been calculated with $\sigma = 2$ and CFL $= 0.1$, the results correspond to a time of 0.005 seconds.

We have compared all these schemes in figure 5.37, it corresponds to a mesh of 1600 points, again with $\sigma = 2$ and $CFL = 1$.

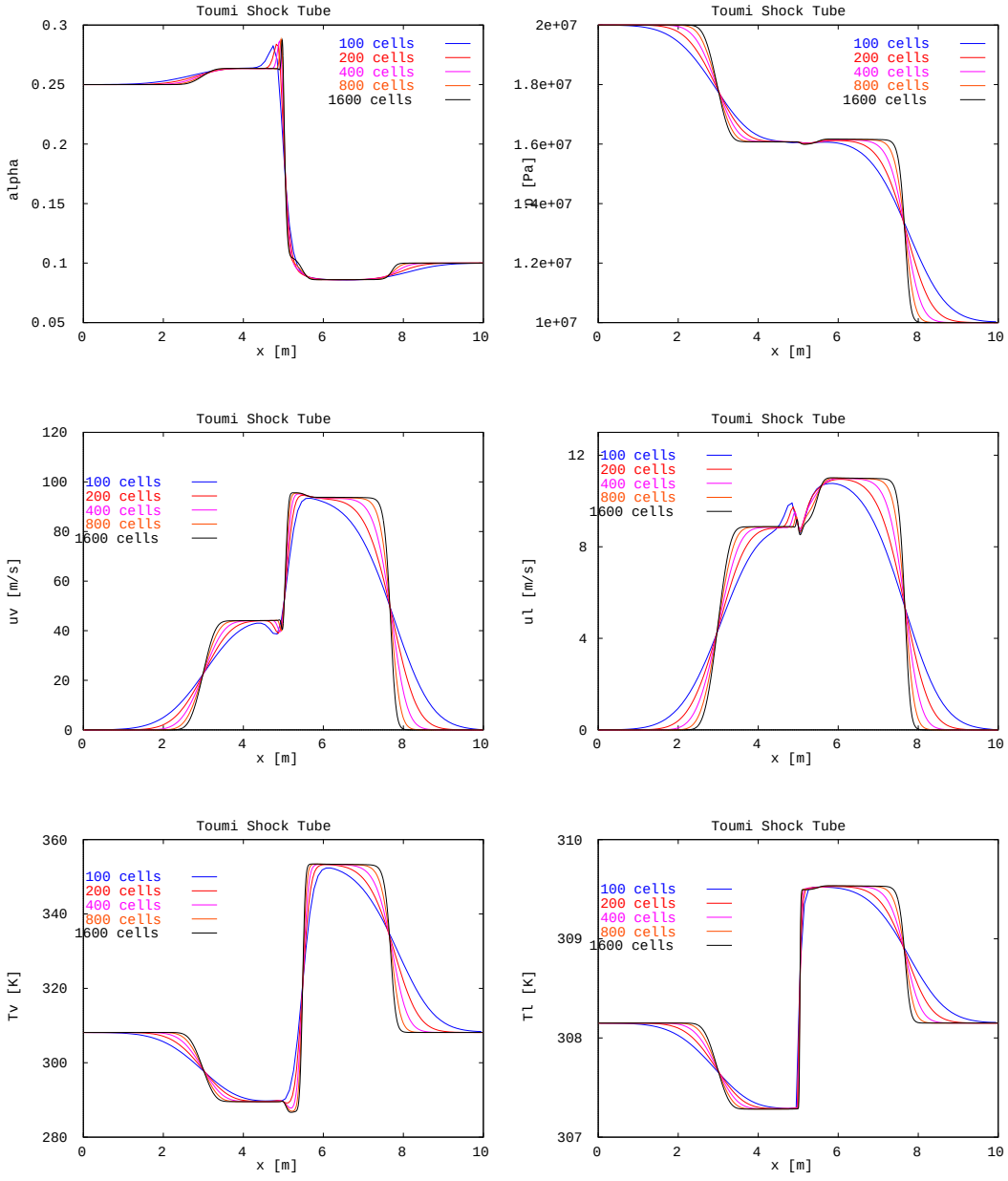

FIGURE 5.33. Toumi's shock tube, 1^{st} order AUSM+: Grid convergence study with the AUSM+ scheme, $\sigma = 2.0$. From top to bottom, left to right, void fraction, pressure, gas velocity, liquid velocity, gas temperature, liquid temperature.

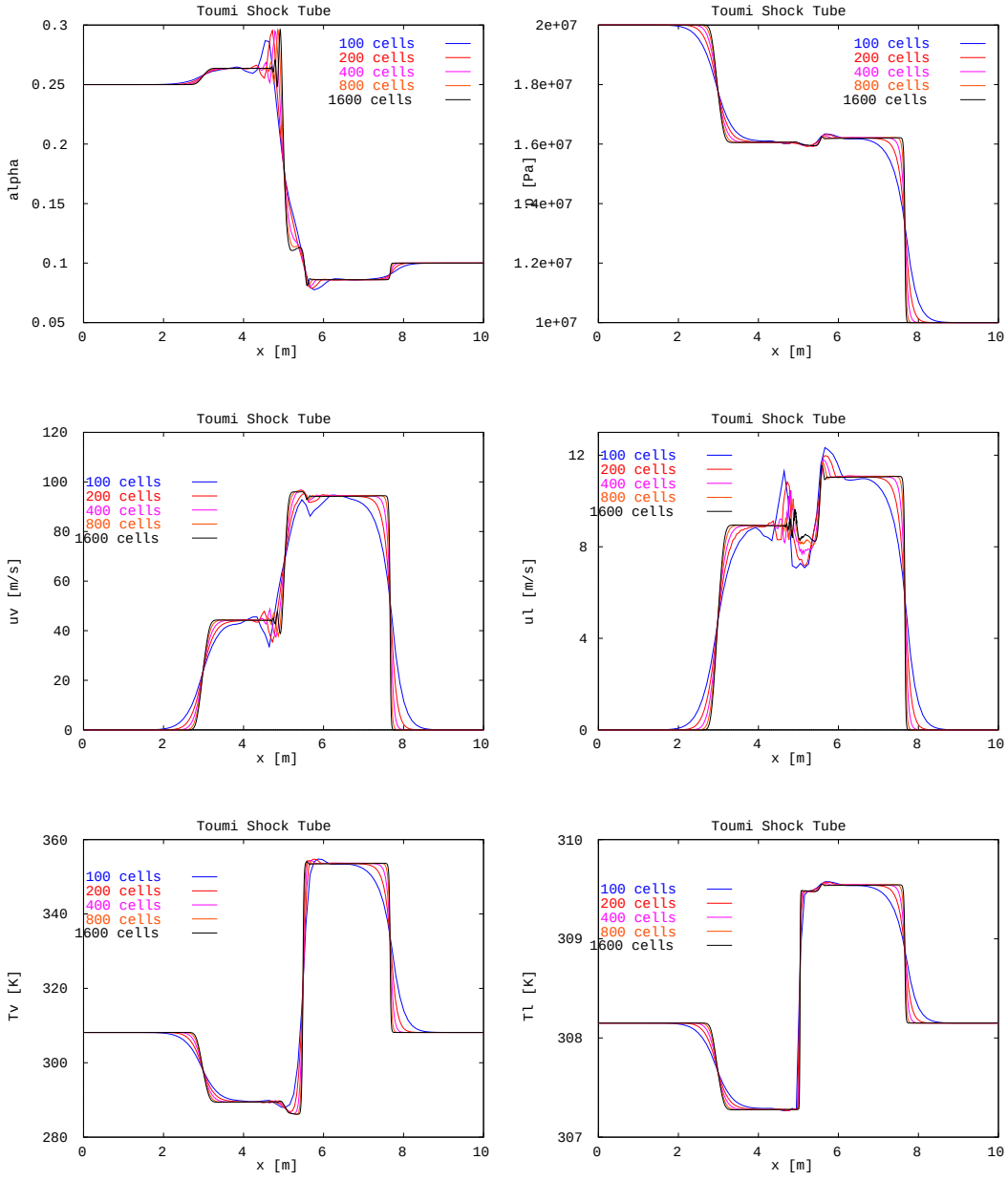

FIGURE 5.34. Toumi's shock tube, 2^{nd} order AUSM+: Grid convergence study with the AUSM+ scheme, $\sigma = 2.0$. From top to bottom, left to right, void fraction, pressure, gas velocity, liquid velocity, gas temperature, liquid temperature.

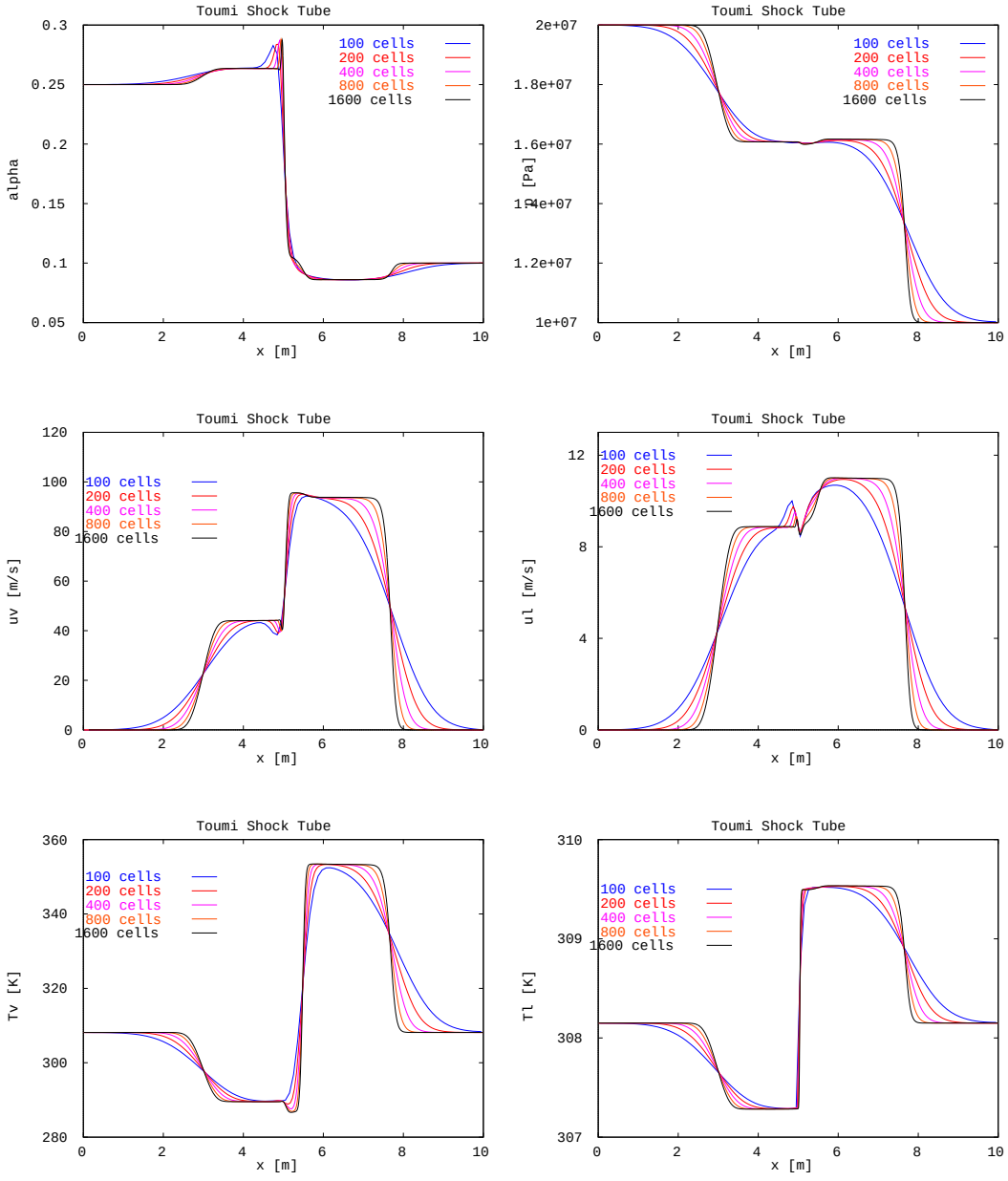

FIGURE 5.35. Toumi's shock tube, 1^{st} order AUSMDV: Grid convergence study with the AUSMDV scheme, $\sigma = 2.0$. From top to bottom, left to right, void fraction, pressure, gas velocity, liquid velocity, gas temperature, liquid temperature.

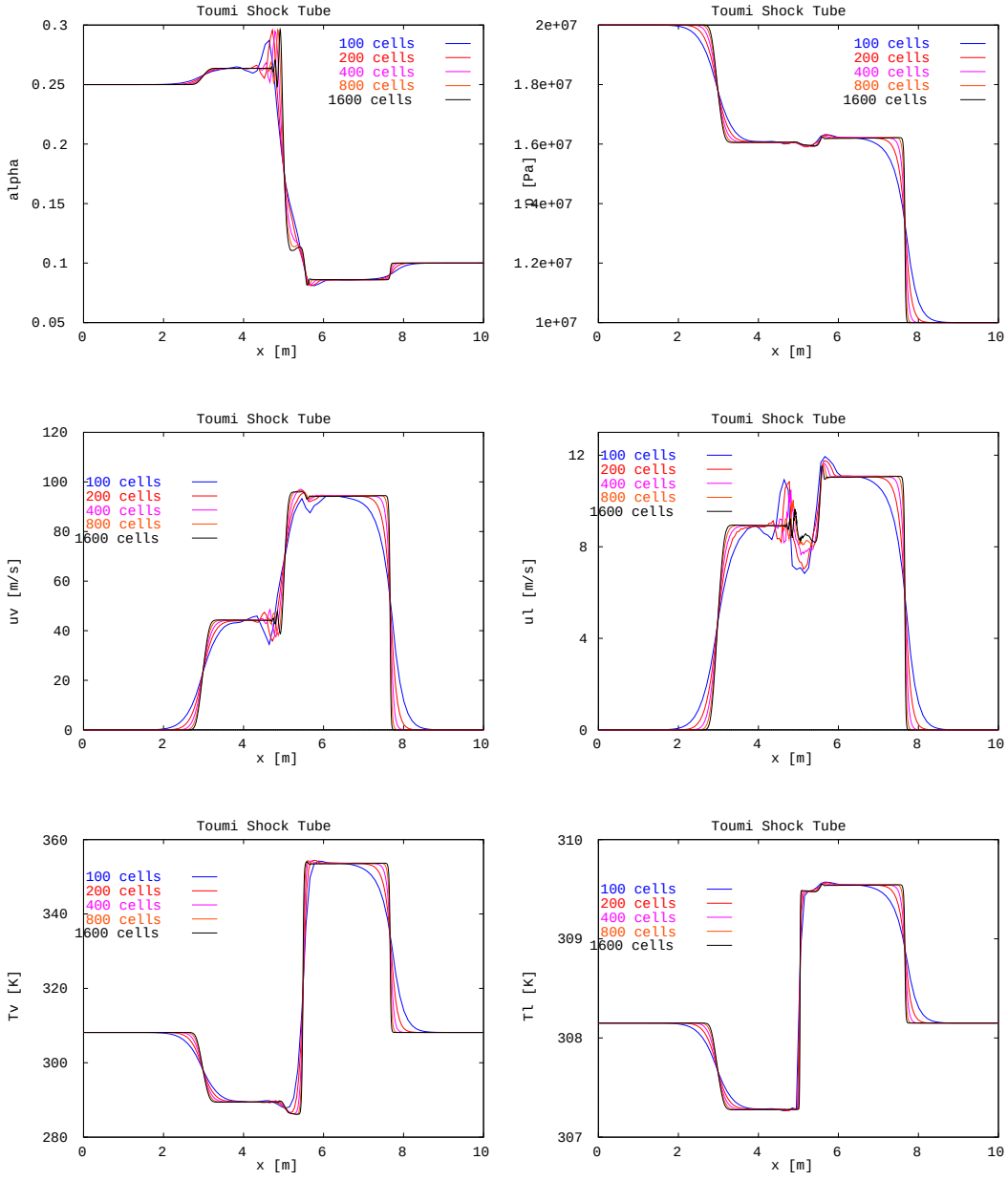

FIGURE 5.36. Toumi's shock tube, 2^{nd} order AUSMDV: Grid convergence study with the AUSMDV scheme, $\sigma = 2.0$. From top to bottom, left to right, void fraction, pressure, gas velocity, liquid velocity, gas temperature, liquid temperature.

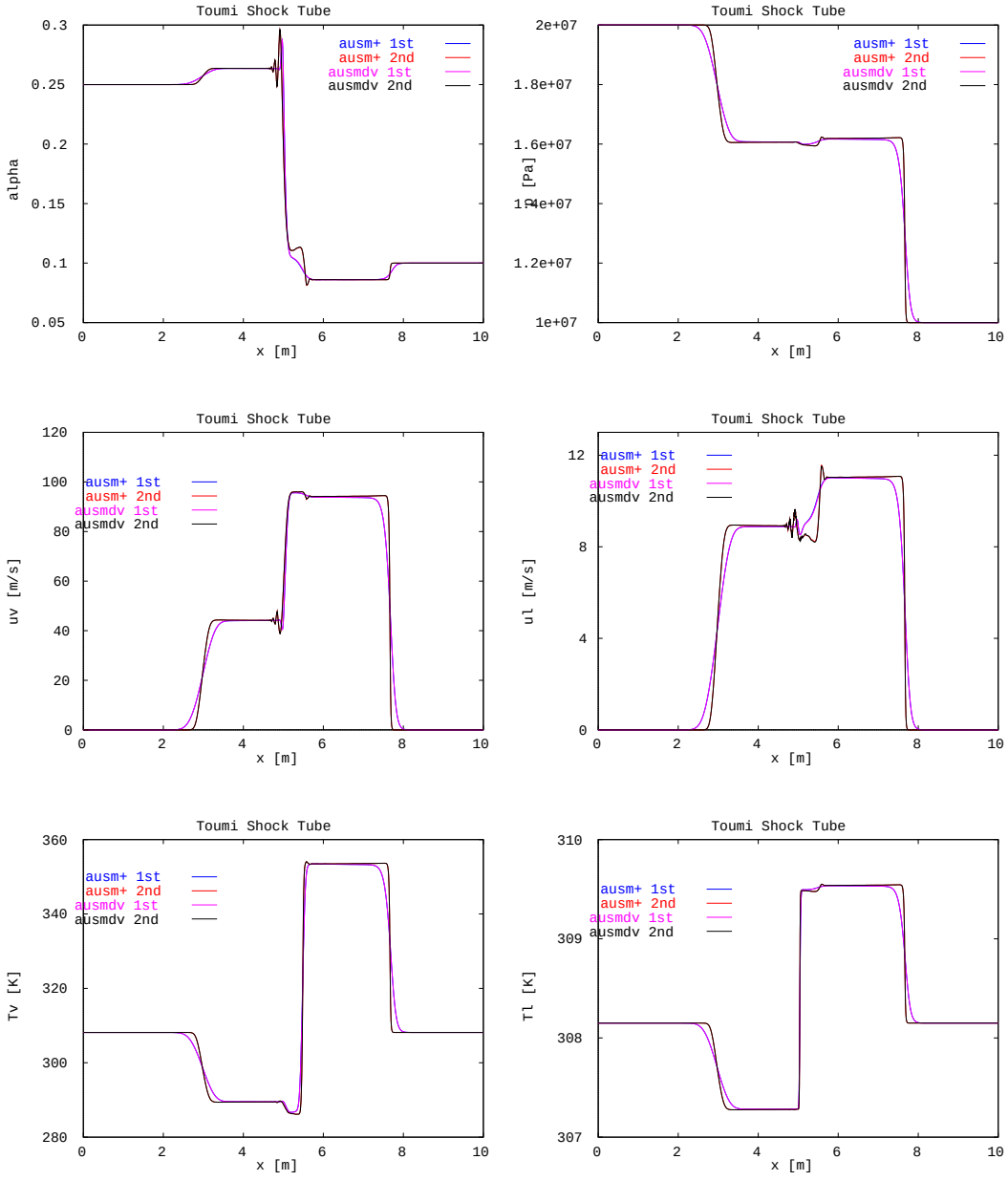

FIGURE 5.37. Toumi's shock tube, Comparison among different AUSM schemes: first order AUSM+, second order AUSM+, first order AUSMDV and second order AUSMDV., $\sigma = 2.0$. From top to bottom, left to right, void fraction, pressure, gas velocity, liquid velocity, gas temperature, liquid temperature.

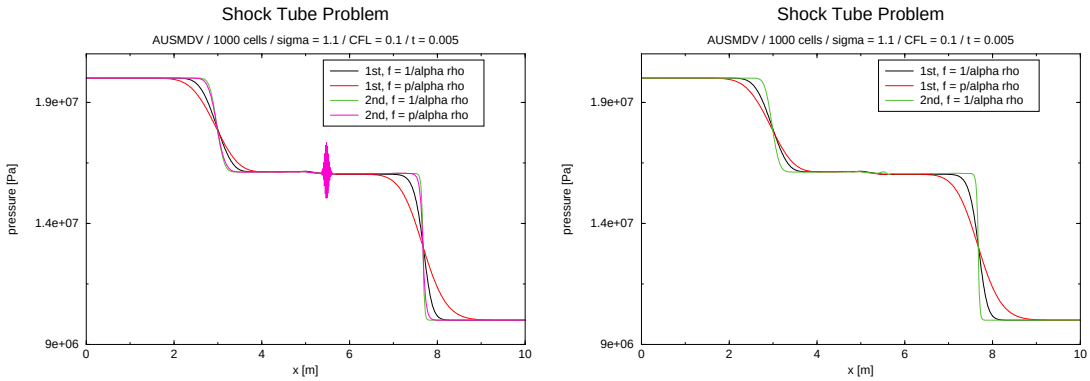

FIGURE 5.38. Results obtanied using different definitions of variable f in the shock tube test

In the extension of the AUSMDV scheme it has been necessary to redefine a variable call f

$$f = \frac{p}{\rho}.$$

It has been adapted to two phase flow by mean of two approaches, these are

$$f_k = \frac{p}{\alpha_k \rho_k} \qquad \text{or} \qquad f_k = \frac{1}{\alpha_k \rho_k},$$

the behaviour of the scheme has been checked when we choose one or another alternative, they provide somewhat different results (figure 5.38).

5.6.5.3. Phase Separation Test (Sedimentation Problem)

We have obtained the following profiles for void fraction (figure 5.39), pressure (figure 5.40), vapour and liquid velocities (figures 5.41 and 5.42). They have been obtained with CFL = 0.1, 50 cells and $\sigma = 1.1$ (no difference has been detected by using $\sigma = 0$).

sum

As commented at low Mach numbers we need of preconditioning, in such a way and following a particularization of the expressions in [**49**] to two phase flow we will consider a correction in the pressure term of the algorithm, $p_{\frac{1}{2}}$. So that we include a pressure diffusion term that couple the pressure and velocity fields at low Match number. At higher speeds the effects of the pressure-diffusion contribution will be reduced (AUSMDV) or eliminated (AUSM+).

In the limit of an incompressible flow, $\rho \approx$ constant, $a^2 >> \left|\overrightarrow{V}\right|^2$, the pressure diffusion contribution to the mass flux for both schemes can be approximated as

$$\dot{m} \approx C_{\frac{1}{2}} \frac{\rho_{\frac{1}{2}} a_{\frac{1}{2}}^2}{p_{\frac{1}{2}}} \frac{\sqrt{u_{\frac{1}{2}}^2 + 4V_*^2}}{V_*^2} (p_i - p_{i+1})$$

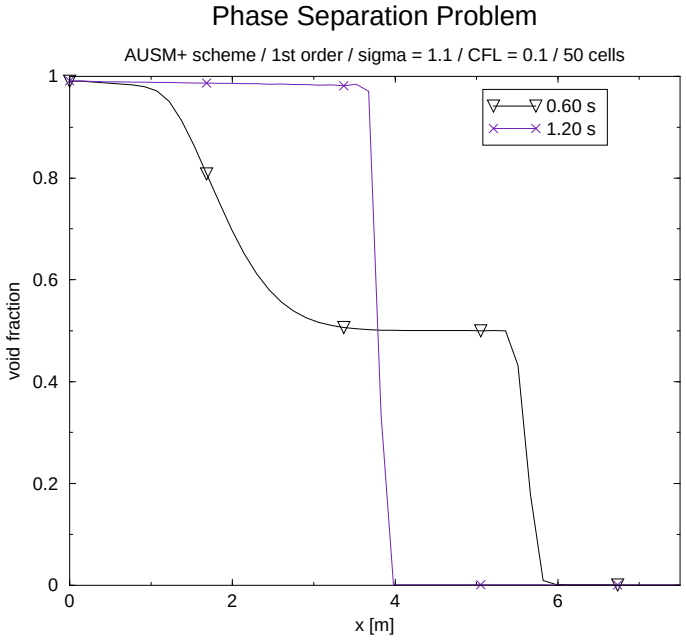

FIGURE 5.39. Void fraction

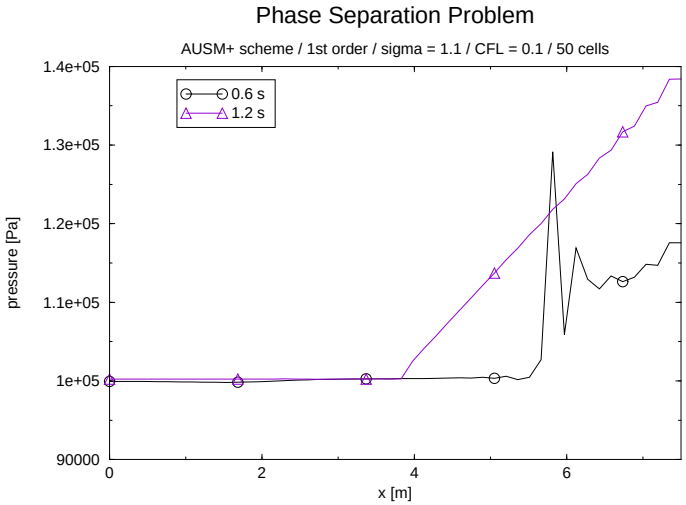

FIGURE 5.40. Pressure

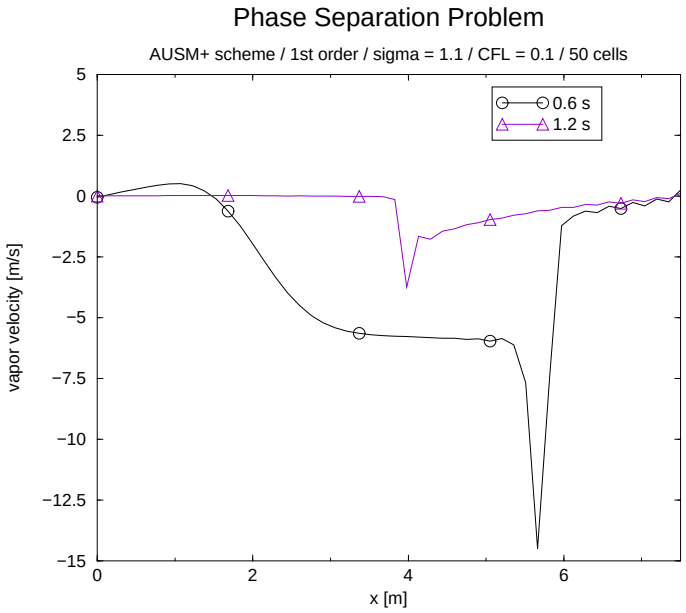

FIGURE 5.41. Vapour velocity

as it is recommended we have considered $C_{\frac{1}{2}} \approx 1$, $\frac{\rho_{\frac{1}{2}} a^2_{\frac{1}{2}}}{p_{\frac{1}{2}}}$ near one for gases but it may be larger than unity in liquid state, in our one dimension case $u^2_{\frac{1}{2}} = V^2_*$, so we have

$$\dot{m} \simeq \frac{\rho_{\frac{1}{2}} a^2_{\frac{1}{2}}}{p_{\frac{1}{2}} u_{\frac{1}{2}}} \sqrt{5}(p_i - p_{i+1})$$

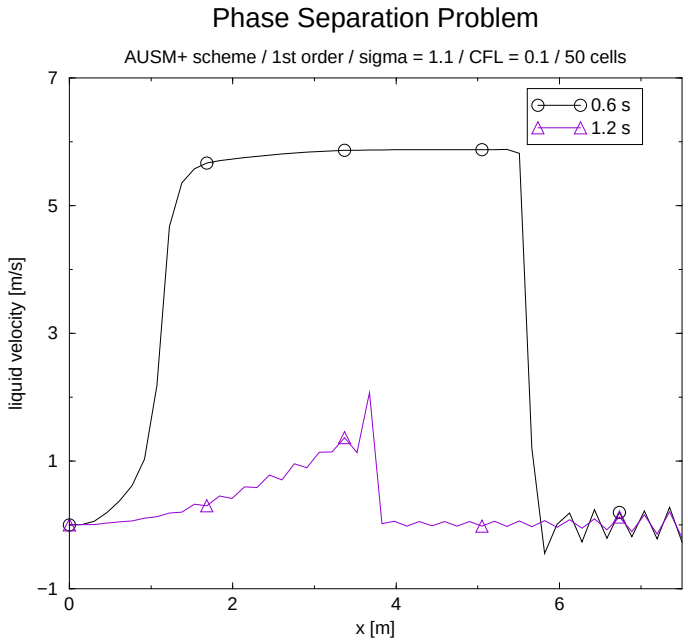

FIGURE 5.42. Liquid velocity

Another interesting aspect is what happens when we increase the number of mesh points, we have some improvements in the solution for void fraction although some oscillations appears for pressure. The computation time also increases too much. (Very high for a 500 cells mesh).

We have obtained the following figure 5.43 that plots the void fraction sequence until steady state is reached, compared with Städtke´ s results our figure does not provide symmetric curves, but we do not know the exact condition he uses for his test, similarity exists with the results shown by Coquel et al. in [**13**],

In addition it has been checked that AUSMDV is not able to solve the problem of contact discontinuities, unlike the previous tests where it was able to characterize shocks waves. In figure 5.44 we can see how AUSMDV behaves for the phase separation problem, it is also remarkable that the variables f must be redefined

$$f_k = \frac{p}{\rho_k}$$

because of the problem that implies having α or $1-\alpha$, in their denominators. Besides, we note that the code cannot reach more that 1.2 second of computing time.

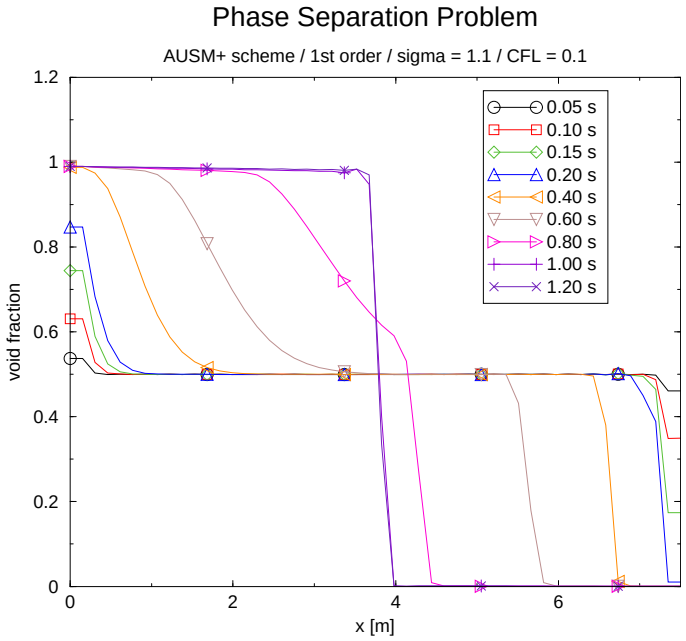

FIGURE 5.43. Void fraction sequence for the phase separation problem

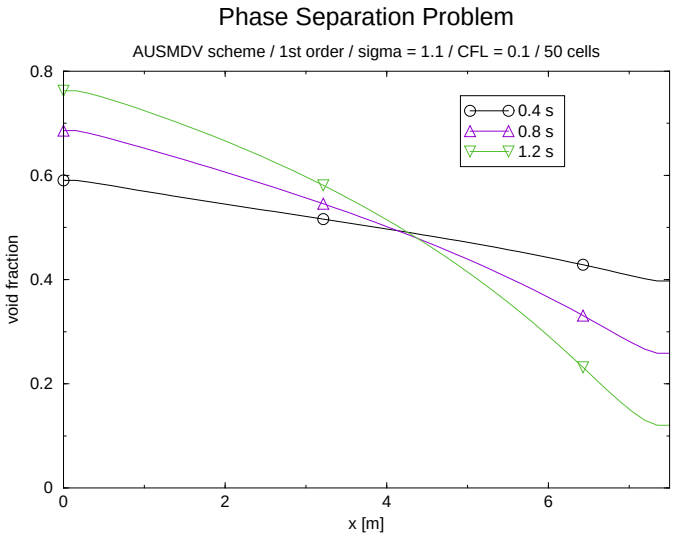

FIGURE 5.44. Void fraction profile for the phase separation test using AUSMDV

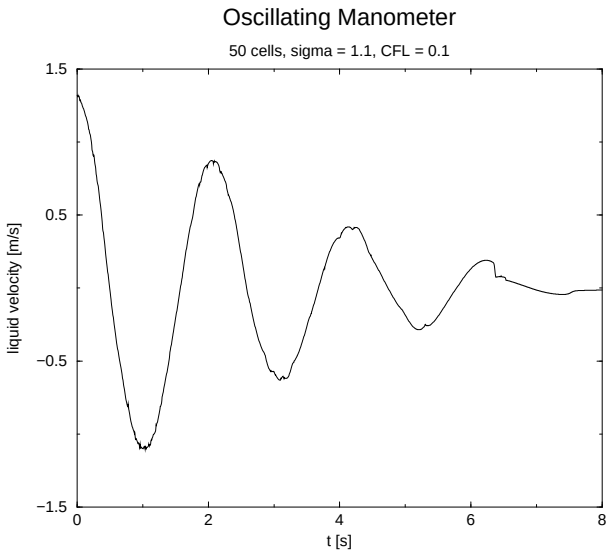

FIGURE 5.45. Velocity of liquid phase for a 50 cells mesh

5.6.5.4. Oscillation Manometer

The results obtained for the oscillating manometer are included in figures 5.45, 5.46 and 5.47. We can observed how the numerical method introduced too much numerical diffusion, this is the reason of this muffled behaviour of the fluid. In the ideal case, when no friction is considered, the fluid is always in motion. A poor resolution for the pressure is obtained and very bad results are obtained when the number of cells increases. We show in figure 5.48 the poor results the scheme has yielded for a 100 cells mesh.

Similar results for this benchmark can be found in some works such as those by Städtke et al. in [**64**], Petelin and Tiselj in [**54**], both analyse the problem with RELAP, and present the muffling due to friction, we are not considering this phenomenon, therefore the effect is due to numerical dissipation introduced by the scheme as has been commented. hacer algún tipo de comentario a lo de Pailler et al. in [**51**]

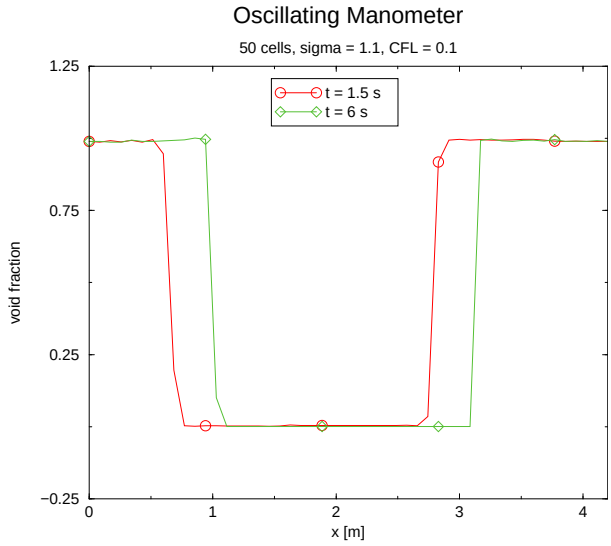

FIGURE 5.46. Void fraction of the oscillating manometer, 50 cells mesh

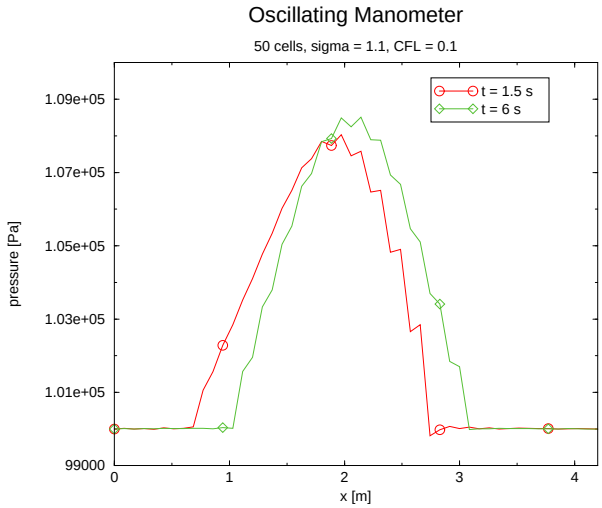

FIGURE 5.47. Pressure distribution of the oscillating manometer, 50 cells mesh

5.7. Conclusions and Future Research

This thesis has been centred in the development of conservative schemes for the solution of the system of equations of 1D unsteady two phase flow. Most of the existing

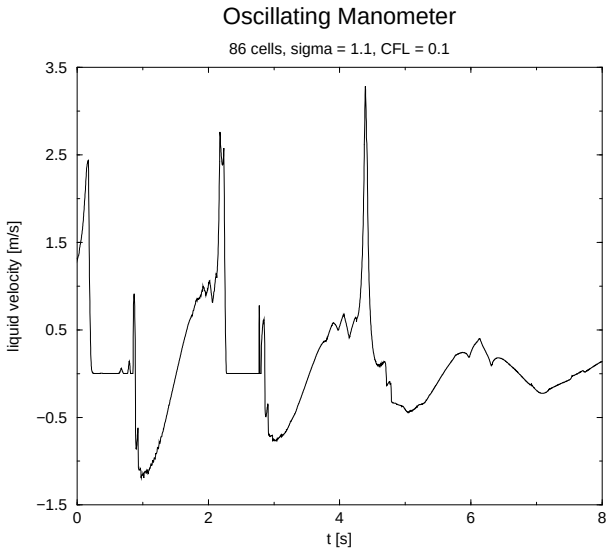

FIGURE 5.48. Velocity of the liquid phase for a 86 cells mesh

methods are based on the utilization of non conservative schemes that follow the non conservative nature of the conservation equations of this sort of problems. This non conservative character is caused by the coupling between the equations of the liquid and the vapour, as they share the conduct cross section and the pressure. So far, researchers have been working on improving the conservative character of the system, we shall highlight the contributions of Toumi, Stadtke, Ghidaglia, Tiselj among others.

The main conclusions derived from this thesis are summarized in the following. Firstly we have to stand out that we have not been able to develope a scheme that allows a good solution for all the tests analyzed. However, we will say in our favour that the number of tests cover a very wide variety of flux situations which are perhaps too different.

The main problems have been found in the oscillating manometer test and in the sedimentation test. This seems to indicate that these family of schemes do not allow to deal with phase discontinuities in a suitable manner, in the sense of $\alpha = 0$, $\alpha = 1$ or $u_r = 0$. With the exception of these tests, the TVD and AUSM families of schemes extended to two phase flow, provide good solutions and have demonstrated to be sufficiently efficient in the solutions of the other tests.

In general, we can state that the AUSM schemes are the most efficient as they have provided very good results and with reasonable computational time. Their easy adaption to the problems allows to model different fluid models compressible/incompressible

without too many changes. It offers good perspectives in its extension to two and three dimensions. Its main drawback has been the solution of problems with low Mach number, in which the use of a simple preconditioning of the schemes has been necessary. This has made the solution of the sedimentation and the manometer benchmarks possible.

The second order version of the AUSM schemes has contributed with high accuracy to the solutions of the water faucet problem and the shock tube test. It does not introduce any improvement in the case of the sedimentation and the manometer tests.

The extension of the AUSMDV scheme to two phase flow has been very simple as well, it has yielded a high characterization of discontinuities in the problems with shock waves.

These hybrid schemes have also demonstrated to be very fast techniques, as it does not make the calculation of the eigenstructure of the system. The results in the oscillating manometer test have shown a high numerical diffusion. It would be necessary to look for a solution of this problem and to check whether it appears in problems in which more calculation time is required.

A big effort has been done in the development of TVD schemes for the solution of one dimensional two phase flow. The main problems found have derived from the discretization of the spatial derivatives of the void fraction. We have demonstrated in the case of the water faucet test that an upwind discretization leads to better results than a centred one.

The difficulty of the diagonalization of the jacobian matrix has been avoided by means of the sign of the matrix algorithm described in appendix A. It has behaved much more efficiently from the point of view of the calulation time. The adaption of the TVD, following the philosophy of [**24**], has not permited to solve these problems. During the analysis of this bad behaviour we arrived at the conclusion that the strong coupling between vapour and liquid was the main cause of the problems found. This led us to the development of a scheme of the same characteristics but applied to the vapour and liquid equations in a decoupled way and neglecting the spatial variation of pressure in the liquid equation when we solve the Riemann problem at the intercell. The resulting scheme has proved to produce good results in some cases better that the AUSM. However we have not been able to obtain good results for the sedimentation and manometer tests. These good results recommend exploring the possibilities and capabilities of the scheme. Anyway, it still consumes many computational time with respect to the AUSM.

In the case of the TVD schemes the second order extension has not introduced apparent improvements.

We have also studied the adaption of classic schemes such as the Lax and Wendroff scheme. They have shown very sharp oscillations which have spoiled the solution in most of the cases. It has been necessary to use very low CFL numbers.

It is worthwhile to stand out that we have presented in this work explicit expressions for the calculation of the eigenstructure of the jacobian matrices corresponding to the homogeneous and separated models. We have tackled the preliminary studies for the analysis of processes with change of phase through the study of homogeneous two phase flow. With the results obtained we have adapted a TVD scheme, providing good results although the scheme have been ineffective from the computational point of view. In the case of the boiling tube test, the heat transfer process has a characteristic time several orders of magnitude bigger than the gas dynamic time. This has made the explicit scheme completely inefficient.

With regard to future developments we consider the following research lines of primary importance:

- After the very good results demonstrated by the AUSM schemes, its extension to two and three dimensions appears to be the next step to follow.
- The possibility of decoupling the liquid and vapour equations neglecting the pressure variations in the liquid equation should be fully investigated.
- The application of the scheme studied to problems with change of phase will be another continuation line. The water hammer test and other depressurization tests raise as first possible benchmarks to study this phenomena.

Appendix A

Some Useful Tools

A.1. On the Sign of a Matrix

In some occasions, when computing the numerical flux in a numerical method, it is necessary to evaluate what has been called *the sign of a matrix*. Such a matrix used to be the jacobian matrix or any other matrix depending on the scheme we consider.

Let us consider a general matrix A, we define the sign of A as

$$\mathrm{sgn}(A) = P \begin{pmatrix} sgn(\lambda_1) & & 0 \\ & \ddots & \\ 0 & & sgn(\lambda_6) \end{pmatrix} P^{-1}$$

where P and P^{-1} are the matrices of right and left eigenvectors, λ_i the eigenvalues and $\mathrm{sgn}(\lambda_i)$ is defined as

$$\mathrm{sgn}(\lambda_i) = \begin{cases} 1 & \text{if } \lambda_i > 0 \\ -1 & \text{if } \lambda_i < 0 \\ 0 & \text{if } \lambda_i = 0 \end{cases} .$$

In order to determine the sign of the matrix we can use different methods with more or less difficulty. In two phase flow, problems can be found with hyperbolicity when our matrices yield complex eigenvalues, this problem can be solved by considering the real part of those complex eigenvalues and the complex matrix of eigenvectors as suggested in [**80**]. Despite we have solved this problem it used to be necessary to determine the eigenstructure of the system which increases enormously the computing time and the complexity of our calculations. This can be avoided by using the methods of determining the sign of the matrix, they arebriefly summarized in this section.

The simplest method to determine the sign is the Newton-Schultz algorithm:

$$\begin{aligned} A_0 &= A \\ A_{n+1} &= \frac{3A_n - A_n^3}{2}, \end{aligned}$$

In [**28**] is presented an alternative method which improve convergence. The method assumes that the eigenvalues of A are clustered in $[L_0, -1] \cup \{0\} \cup [1, L_0]$, and if

$$\begin{aligned} a_0 &= \frac{1}{L_0(L_0+1)} \\ A_0 &= A \end{aligned}$$

then

$$\begin{aligned} A_{n+1} &= P_{a_n}(a_{n+1}), \\ L_{n+1} &= \frac{2(a_n+1)}{3}\sqrt{\frac{a_n+1}{3a_n}}, \\ a_{n+1} &= \frac{1}{L_{n+1}(1+L_{n+1})} \end{aligned}$$

where the polynomial function P_a is defined by

$$P_a(X) = -aX^3 + (a+1)X,$$

we referred to [**2**] for more details.

The parameter L_0 has been chosen considering that the bigger eigenvalue is always lower than this

$$L_0 = \frac{(u_v + a_v)(u_l + a_l)}{(1-\alpha)(u_v + a_v) + \alpha(u_l + a_l)}$$

Another option to determine the sign of the matrix was introduced and successfully applied by Viozat in [**83**], despite the complication that obtaining the eigenvalues implies in the six equation model, it is important to note the possibilities this method introduces. The sign of the matrix is given by

$$\operatorname{sgn}(A) = \sum_{i=0}^{n} \alpha_i A^i,$$

where

$$A^i = \begin{cases} I(\text{Identity}) & \text{if } i = 0 \\ AA^{i-1} & \text{if } i \in N^+ \end{cases}$$

and the coefficients α_i are obtained using

$$\begin{bmatrix} \alpha_1 \\ \vdots \\ \alpha_6 \end{bmatrix} = (C^{-1})^t \begin{bmatrix} \operatorname{sgn}(\lambda_1) \\ \vdots \\ \operatorname{sgn}(\lambda_6) \end{bmatrix}$$

and

$$C = \begin{bmatrix} 1 & \cdots & 1 \\ \lambda_1 & \cdots & \lambda_6 \\ \vdots & & \vdots \\ \lambda_1^5 & \cdots & \lambda_6^5 \end{bmatrix}.$$

This development is based on the work by Dutoya in [**21**].

A.2. From Conserved Variables to Primitive Variables

Every time step conserved variables are calculated, but we need to know the primitive ones as well. In order to do this we will consider the vectors of conserved and primitive variables:

$$w = \begin{bmatrix} \alpha\rho_g \\ (1-\alpha)\rho_f \\ \alpha\rho_g u_g \\ (1-\alpha)\rho_f u_f \\ \alpha\rho_g E_g \\ (1-\alpha)\rho_f E_f \end{bmatrix} \qquad v = \phi(w) = \begin{bmatrix} \alpha \\ u_v \\ u_l \\ p \\ T_v \\ T_l \end{bmatrix} = \begin{bmatrix} v_1 \\ v_2 \\ v_3 \\ v_4 \\ v_5 \\ v_6 \end{bmatrix}$$

Once we know w, we can calculate directly the velocities of each phase as

$$\begin{aligned} v_2 &= u_v = \frac{w_3}{w_1} \\ v_3 &= u_l = \frac{w_4}{w_2}, \end{aligned}$$

and the internal energies since

$$e_v = E_v - \frac{u_v^2}{2} = \frac{w_5}{w_1} - \frac{1}{2}\left(\frac{w_3}{w_1}\right)^2, \qquad e_l = E_l - \frac{u_l^2}{2} = \frac{w_6}{w_2} - \frac{1}{2}\left(\frac{w_4}{w_2}\right)^2,$$

so the temperature of vapour, using its quations of state, is

$$v_5 = T_v = \frac{\gamma_v e_v}{c_{pv}}.$$

If we call

$$\begin{aligned} A &= (\gamma_v - 1)e_v w_1 \\ B &= (\gamma_l - 1)e_l w_2 \\ \Delta &= (-A - B + \gamma_l p_\infty)^2 + 4\gamma_l p_\infty A \end{aligned}$$

we have

$$v_4 = p = \frac{A + B - \gamma_l p_\infty + \sqrt{\Delta}}{2}.$$

Using that $w_1 = \alpha\rho_v$

$$v_1 = \alpha = \frac{A}{p}.$$

Finally the liquid temperature can be obtained

$$v_6 = T_l = \frac{\gamma_l e_l}{c_{pl}\left(1 + \frac{p_\infty(\gamma_l - 1)}{p + p_\infty}\right)}.$$

Appendix B

Numerical Benchmarks

B.1. Introduction

In this appendix we describe the numerical benchmarks we have used to analyse the behaviour of the proposed schemes. We can be find in the literature much more tests besides those we have considered here, among them we stand out some classical tests that can be found in [**34**]. In a first step we have used for the study of separated two phase flow four of the most representative tests involving mixtures of air and water and a test with boiling water for the study of the homogeneous two phase flow. They are very common and frequently utilized in other recent works which will allow us to compare our results with the results of other researchers. These tests are:

- Water faucet.
- Shock tube.
- Phase separation.
- Oscillating manometer.
- Boiling tube.

B.2. Water Faucet Test

This test was proposed by Ramson (Numerical Bench. Test 2.1) in [**34**], it is summarized in the following sections, figure B.2 illustrates the initial and the steady state of this benchmark.

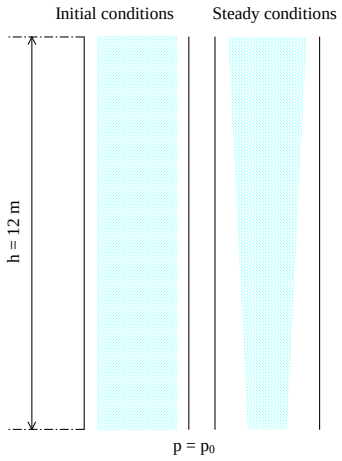

FIGURE B.1. Scheme of the water faucet test.

B.2.1. Initial Conditions

The initial conditions of the faucet test are summarized in the following table

Initial Conditions	
vertical tube	
length (m)	12
diameter (m)	1
T (^{o}C)	50
p (Pa)	10^5
u_v (m/s)	0
u_l (m/s)	10
α_l	0.8

B.2.2. Boundary Conditions

Boundary conditions are summarized in the following table

Boundary Conditions	
inlet	
T (n^{o}C)	50
u_v(m/s)	0
u_l (m/s)	10
α_l	0.8
outlet	
p (Pa)	10^5

B.2.3. Analytical Solution

Let us consider the equations of conservation of mass and momentum of the liquid phase

$$\frac{\partial(1-\alpha)\rho_l}{\partial t} + \frac{\partial(1-\alpha)\rho_l u_l}{\partial x} = 0, \tag{B.2.1}$$

$$\frac{\partial(1-\alpha)\rho_l u_l}{\partial t} + \frac{\partial(1-\alpha)\rho_l u_l^2}{\partial x} + (1-\alpha)\frac{\partial p}{\partial x} = (1-\alpha)\rho g. \tag{B.2.2}$$

Let us assume that the liquid is incompressible and the variation of pressure in the liquid phase is neglected, then we can transform B.2.1 and B.2.2 into

$$\frac{\partial \alpha}{\partial t} + \alpha\frac{\partial u_l}{\partial x} + u_l\frac{\partial \alpha}{\partial x} = 0, \tag{B.2.3}$$

$$\frac{\partial u_l}{\partial t} + u_l\frac{\partial u_l}{\partial x} = g, \tag{B.2.4}$$

thereby if we take into account that

$$dx = u_l dt \tag{B.2.5}$$

we can arrive at the following expressions for the liquid velocity

$$u_l(t,x) = u_0 + g(t-t_0), \tag{B.2.6}$$

$$u_l(t,x) = \sqrt{g(x-x_0)+u_0^2}, \tag{B.2.7}$$

and if we substitute B.2.6 in B.2.5 we have

$$x = x_0 - u_0(t-t_0) + \frac{1}{2}g(t-t_0)^2 \tag{B.2.8}$$

and finally if we substitute the expression of u_l (eq. B.2.7) in B.2.3 then

$$(1-\alpha) = \frac{(1-\alpha_0)u_0}{u_0 + g(t-t_0)}.$$

The analytical solution is obtained by using eq. B.2.8

$$\alpha = 1 - \frac{(1-\alpha_0)u_0}{\sqrt{u_0^2 + 2g(x-x_0)}}$$

for $x < \frac{g}{2}t^2 + u_0 t$.

In figure B.2 we show the exact solution at time $t = 0.5$ s which we will use to compare with the results yielded by our developments. On the left side of this figure steady state has been represented as well.

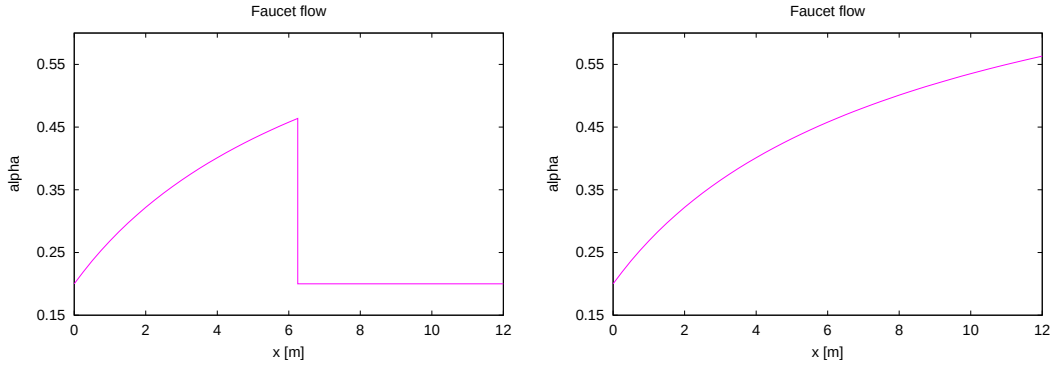

FIGURE B.2. Faucet test: Exact solution at $t = 0.5$ s (left) and at steady state (right).

B.3. Toumi's Shock Tube

This test was proposed by Toumi in [**78**] and it is summarized in the following sections.

B.3.1. Initial Conditions

The initial conditions are in the following table, they are a modified version respect to the original ones, both velocities have been put to zero.

Initial Conditions			
horizontal tube			
left side		rigth side	
length (m)			10
$T^L_{v,l}$ (^{o}C)	35	$T^R_{v,l}$ (^{o}C)	35
p^L (MPa)	20	p^R (MPa)	10
u^L_v (m/s)	0	u^R_v (m/s)	0
u^L_l (m/s)	0	u^R_l (m/s)	0
α^L	0.25	α^R	0.1

B.3.2. Boundary Conditions

The boundary conditions are summarized in the following table

Boundary Conditions	
left end	rigth end
$\alpha_{l1} = \alpha_{l2}$	$\alpha_{ln} = \alpha_{ln-1}$
$u_{v1} = -u_{v2}$	$u_{vn} = -u_{vn-1}$
$u_{l1} = -u_{l2}$	$u_{ln} = -u_{ln-1}$
$p_1 = p_2$	$p_n = p_{n-1}$
$T_{v1} = T_{v2}$	$T_{vn} = T_{vn-1}$
$T_{l1} = T_{l2}$	$T_{ln} = T_{ln-1}$

There is no exact solution of this problem. In order to analyse our results, we can compare with the results provided by other researchers, among them we have the results by Toumi in [**80**] or by Tiselj in [**72**] for example.

B.4. Phase Separation Test (Sedimentation Problem)

This test consist of a tube filled up with a two phase mixture of water and air and with a void fraction of $\alpha = 0.5$, this is a variation of the one described by Young (Numerical Benchmark Test 2.4) in [**34**] or by Städke in [**64**], in the next section we will

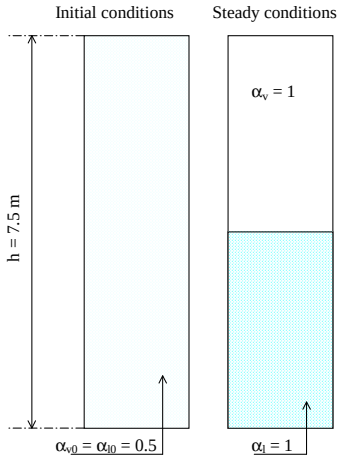

FIGURE B.3. Scheme of the phase separation test.

give some details about its implementation in the next sections. We have represented in figure B.4 the initial and steady conditions.

B.4.1. Initial Conditions

In this case we have the following initial conditions

Initial Conditions
vertical tube
length 7.5 m
$\alpha = 0.5$
$u_v = u_l \ = 0$ m/s
$p = 0.1$ MPa
$T_v = T_l = 50\ ^o$C

B.4.2. Boundary Conditions

The boundary conditions are the same that in shock tube problem.

Boundary Conditions	
bottom	top
$\alpha_{l1} = \alpha_{l2}$	$\alpha_{ln} = \alpha_{ln-1}$
$u_{v1} = -u_{v2}$	$u_{vn} = -u_{vn-1}$
$u_{l1} = -u_{l2}$	$u_{ln-1} = -u_{ln-1}$
$p_1 = p_2$	$p_n = p_{n-1}$
$T_{v1} = T_{v2}$	$T_{vn} = T_{vn-1}$
$T_{l1} = T_{l2}$	$T_{ln} = T_{ln-1}$

In this test, the steady state solution is characterized by constant void fraction at each part of the tube, $\alpha = 0$ in the liquid side and $\alpha = 1$ in the vapour side. With respect to the pressure we will have constant pressure in the vapour side and a hydrostatical distribution of this variable in the liquid side, this has been depicted in figure B.4.

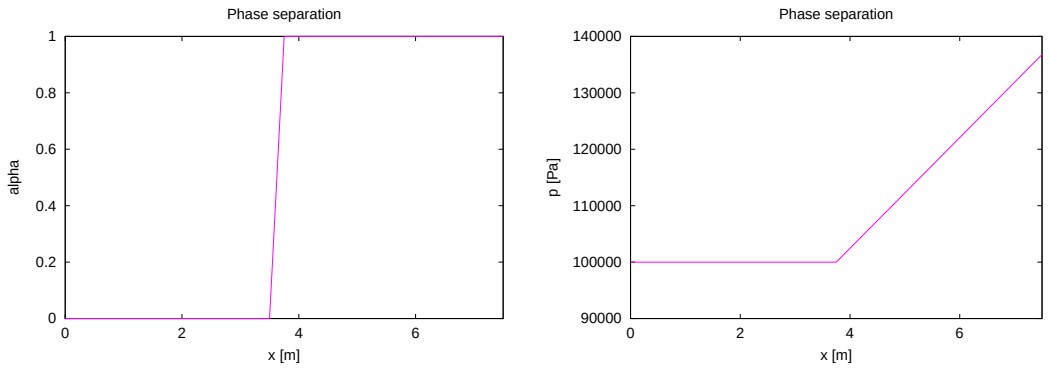

FIGURE B.4. Phase separation test: Steady state solution for void fraction (left) and pressure (right).

B.5. Oscillating Manometer

This test consist of a U tube, partially filled up with water, which after taking it out of equilibrium, water oscillates (A schematic figure of the experiment is shown in figure B.5). We have again water and air with void fractions of $\alpha = 0$ and 1, although

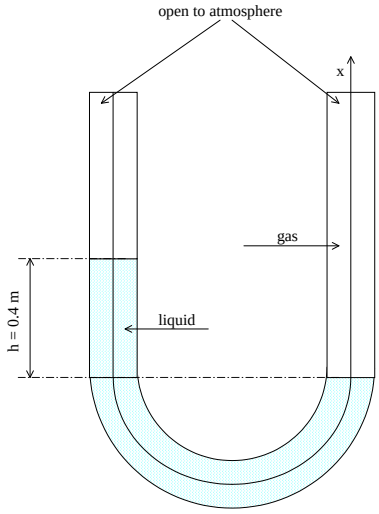

FIGURE B.5. Scheme of the oscillating water column in a U-tube manometer.

we actually have not a two phase mixture we will be able to predict its behaviour. This test was described by Ransom (Numerical Bench. Test 2.2) in [**34**], we give some details about its implementation, we note that it differs a bit from the original one.

B.5.1. Initial Conditions

In this case we have the following initial conditions

Initial Conditions
U tube
length 4.2 m, see geometry in figure
$\alpha = 0$ if gas $\alpha = 1$ if liquid
$u_v = u_l = 1.32$ m/s
$p = 10^5$ Pa (gas side)
$p = 10^5 + \rho_l g h$ Pa (liquid side)
$T_v = T_l = 27\ ^o$C

The pressure of the liquid phase is the hydrostatical pressure, we could calculate it by considering a constant density of the liquid (1000 kg/m^3) or by including its dependence respect to pressure, as expected the results obtained are very similar.

In order to model the problem efficiently, we have chosen the initial velocity of the column equal to 1.32 m/s avoiding some computational problems related to the start stage of the program.

B.5.2. Boundary Conditions

In this case boundary conditions have been chosen in this way

Boundary Conditions	
bottom	top
$\alpha_{l1} = \alpha_{l2}$	$\alpha_{ln} = \alpha_{ln-1}$
$u_{v1} = u_{v2}$	$u_{vn} = u_{vn-1}$
$u_{l1} = u_{l2}$	$u_{ln-1} = u_{ln-1}$
$p_1 = 10^5$ (Pa)	$p_n = 10^5$ (Pa)
$T_{v1} = T_{v2}$	$T_{vn} = T_{vn-1}$
$T_{l1} = T_{l2}$	$T_{ln} = T_{ln-1}$

The velocity of the liquid particles will be equal to

$$u_l = 1.32 \sin\left(\sqrt{\frac{2g}{L}}\right)$$

with

$g = 9.81$ m/s^2.

$L = 1.8$ m, that is the lineal length of the liquid column.

Such results correspond to the case in which no friction is considered. The velocity of the liquid as a function of time has been represented in figure B.6.

B.6. Boiling Tube Test

This test was introduced in [**69**] and the experiment consists of a horizontal heat pipe in which water flows with constant mass flow rate.

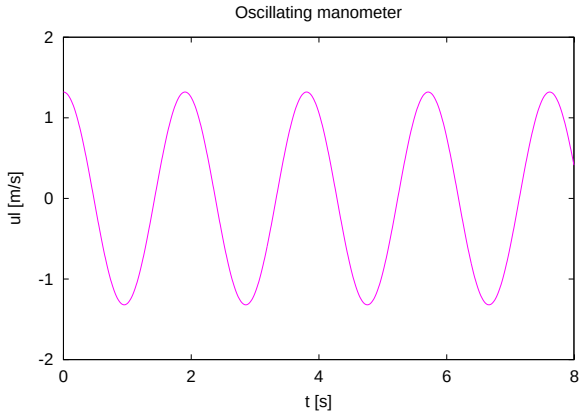

FIGURE B.6. Oscillating manometer: Evolution of the liquid velocity when friction is not considered.

B.6.1. Initial Conditions

The initial conditions differs a bit from the original as

$$\begin{aligned} \rho u &= 1 \\ p &= 10^5 \text{Pa} \\ h &= h(p = 10^5 \text{Pa}, x = 0.001). \end{aligned}$$

A constant heat source of $\phi = 450.000$ W/m has been considered in the tests.

B.6.2. Boundary Conditions

The boundary conditions used in this test are the following:

Boundary Conditions	
inlet	outlet
$\rho u = 1$	$s_n = s_{n-1}$
$u_1 = u_2$	$u_n = u_n - 1$
$h_1 = h(p = 10^5 \text{Pa}, x = 0.001)$	$p_n = 10^5$ Pa

Bibliography

[1] L.J. Agee, S. Banerjee, R.B. Duffey, and E.D. Hughes. Some aspects of two-fluid models for two-phase flow and their numerical solution. In *2nd OECD/NEA Specialists Meeting on Transient Two-Phase Flow*, Paris, June 1978.

[2] F. Alouges. Matrice signe et systemes hyperboliques, in aspects theoriques et pratiques de la simulation numerique de quelques problemes physiques. Memorie d'habilitation, Universite Paris-Sud., 1999.

[3] S. Banerjee and A.M.C. Chan. Separated models i, analysis of the averaged and local instantaneous formulations. *Int. J. Multiphase Flow*, 6:1–24, 1980.

[4] S. Banerjee, R.L. Ferch, W.G. Mathers, and B.H. Mc Donald. The dynamics of two phase flow in a duct. *Heat Transfer*, 1:345–350, 1978.

[5] S. Banerjee and W.T. Hancox. Transient thermohydraulics analysis for nuclear reactors. *Heat Transfer*, 6:311–337, 1978.

[6] F. Barre and M. Bernard. The cathare code strategy and assessment. *Nuclear Engineering and Design*, 124:257–284, 1990.

[7] F. Berger and J.F. Colombeau. Numerical solution of one-pressure models in multifluid flows. *SIAM J., Numer. Anal.*, 32(4):1139–1154, 1995.

[8] J.A. Borkowski and N.L. Wade. *TRAC-BF1/MOD1 Models and Correlations*. NUREG/CR-1391, 1992.

[9] M. Boucker. *Modelisation Numerique Multidimensionnelle d'Ecoulements Diphasiques Liquide-gas en Regimenes Transitoire et Permanent: Methodes et Applications*. PhD thesis, Ecole Normale Superieure de Cachan, 1998.

[10] J.A. Boure. On the form of the pressure terms in the momentum and energy equations of two phase flow models. *Int. J. of Multiphase Flow*, 5:159–164, 1979.

[11] J.G. Collier and J.R. Thome. *Convective Boiling and Condensation*. Oxford University Press, 3rd edition, 1996.

[12] C. Comino, M. De Salve, and P. Gregorio. Depressurization transient simulation by flux vector splitting method. In *ICONE5:* 5^{th} *International Conference on Nuclear Engineering*, May 1997.

[13] F. Coquel, K. El Amine, E. Godlewski, B. Perthame, and P. Raselet. A numerical method using upwind schemes for the resolution of two phase flows. *Journal of Computational Physics*, 136:272–288, 1997.

[14] F. Coquel and M.S. Liou. Field by field hybrid upwind splitting methods. In 11_{th} *AIAA CFD Conference*, 1993. AIAA Paper 93-3302-CP.

[15] J.M. Corberan and Ll. Gascón. Alternative treatment of strong source terms in non linear hyperbolic conservation laws.application to unsteady 1-d compressible flow in pipes with variable

cross section. *Eurotherm Seminar: Advanced Concepts and Techniques in Thermal Modelling*, 53, 1998.

[16] J. Cortes. *Etude des Régimes Transitoires d'Écoulements Diphasiques à Faible Rapport de Densité*. PhD thesis, Universite de Paris XI, Centre d'Orsay, 1999.

[17] Bestion D. The physical closure laws in the cathare code. *Nuclear Engineering and Design*, 124:229–245, 1990.

[18] V. De Henau and G.D. Raithby. A transient two fluid model for the simulation of slug flow in pipelines i, theory. *Int. J. Multiphase Flow*, 21:335–349, 1995.

[19] F. De Vuyst, J.M. Ghidaglia, and G. Le Coq. A numerical simulation of flows with changes of state and strong gradients using the hem. *AMIF-ESF Workshop*, 12-14 January 2000.

[20] J.M. Delhaye and J.L. Achard. On the averaging operators introduced in two phase flow modeling. In *Transient Two Phase Flow, Proceeding of the CSNI Specitalists Meeting*, pages 5–84. Atomic Energy of Canada Ltd., August 3-4 1976.

[21] D. Dutoya and P. Errera. Une décomposition formelle du jacobien des Équations d'euler. application a des schéma numériques decentrés. *La Recherche Aérospatiale*, 1:25–35, 1992.

[22] J.R. Edwards. A low-diffursion flux splitting scheme for navier-stokes calculations. *Computer and Fluids*, 26(6):635–659, 1997.

[23] J.R. Edwards and M.L. Liou. Low diffusion flux-splitting methods for flows at all speeds. *AIAA Journal*, 36(9):1610–1617, 1998.

[24] Ll. Gascón Martínez. *Estudio de Esquemas en Diferencias Finitas para el Cálculo del Flujo Compresible, Unidimensional, no Estacionario y no Isentrópico*. PhD thesis, Universidad Politécnica de Valencia, Spain, 1995.

[25] Ll. Gascón Martínez and J.M. Corberán Salvador. Construction of second-order tvd schemes for nonhomogeneous hyperbolic conservation laws. *Journal of Computational Physics*, 171:1–37, 2001.

[26] J.M. Ghidaglia, A. Kumbaro, and Le Coq G. On the numerical solution to two fluid models via cell centered finite volume methods. preprint version, 2000.

[27] J.M. Ghidaglia, A. Kumbaro, and G. Le Coq. Une méthode volumenes finis a flux caractéristiques pour la résolution numérique des systemes hyperboliques de lois de consevation. *JC. R, Acad Sc. Paris*, 322(I):981–988, 1996.

[28] J.M. et al. Ghidaglia. An overview of the vffc methods and tools for the simulation of two phase flows. Technical report, Universidad de Cachan, 1999. Report Note HT-33/99/005/A.

[29] D. Gidaspow. Raund table discussions, modelling two phase flow. In *Proceedings of the Fifth International Heat Transfer Conference*, Tokyo, Sept 7 1974.

[30] A. Harten. High resolution schemes for hyperbolic conservation laws. *Journal of Computational Physics*, 49:357–393, 1983.

[31] A.H. Harvey, A.P. Peskin, and S.A. Klein. *NIST/ASME Steam Properties, Version 2.1, Users' Guide*, 1997.

[32] G. Hestroni, editor. *Handbook of Multiphase Systems*. Hemisphere Publishing Corporation, 1982.

[33] G. Hestroni and G. et al. Yadigaroglu. Introduction, definitions and conservation equations, 1999. in Short Course:Modelling and Computation of Multiphase Flows, Zurich, Switzerland, March 8-12.

[34] G.F. Hewitt, J.M. Delhaye, and N. Zuber, editors. *Numerical Benchmark Test*, volume 2 of *Multiphase Science and Technology*. John Wiley & Sons Ltd., 1987.

[35] C. Hirsch, editor. *Numerical Computation of Internal and External Flows*, volume 2. John Wiley & Sons Ltd., 1990.

[36] D.D. Holm and B.A. Kuperschimidt. A multipressure regularization for multiphase flow. *Int. J. Multiphase Flow*, 47:681–69, 1986.

[37] YH. Hwang and NM. Chung. Analysis of the two-fluid model equations for the computation of two-phase flow. preprint version, May 2000.
[38] M. Ishii. Thermo-fluid dynamic theory of two phase flow. Eyrolles, Paris, 1975.
[39] R.T. Lahey. The prediction of the phase distribution and separation phenomena using two-fluid models. *Boiling Heat Transfer*, pages 85–121, 1992.
[40] S.J Lee. *A Hyperbolic Solution for Two Phase Flow Using Surface Tension Effects*. PhD thesis, Korea Advanced Institute of Science and Technology, 1997.
[41] S.J. Lee, K.S. Chang, and K. Kim. Pressure wave speeds from characteristics of two fluids, two phase hyperbolic equation system. *Int. J. Multiphase Flow*, 24:855–866, 1998.
[42] R.J. Leveque, editor. *Numerical Methods for Conservation Laws*. Lectures in Mathematics. Birkhäuser Verlag, ETH Zürich, 1992.
[43] M.S. Liou. A sequel to ausm: Ausm+. *Journal of Computational Physics*, 129:364–382, 1996.
[44] M.S. Liou. Mass flux schemes and connection to shock instability. *Journal of Computational Physics*, 160:623–648, 2000.
[45] M.S. Liou and C.J. Steffen. A new flux splitting scheme. *Journal of Computational Physics*, 107:23–29, 1993.
[46] R.W. Lyczkowski, D. Guidaspow, C.W. Solbrig, and E.D. Hughes. Characteristics and stability analyses of transient one dimensional two phase flow equations and their finite difference approximations. *Nuclear Science and Engineering*, 66:378–396, 1978.
[47] J.M. Masella. *Quelques Méthodes Numeriques pour les Ecoulements Diphasiques Bi-Fluide en Conduites Petrolières*. PhD thesis, Université Paris 6, 1997.
[48] J.M. Masella, Q.H. Tran, D. Ferre, and C. Pauchon. Transient simulation of two phase flow in pipes. *Int. J. Multiphase Flow*, 24:739–755, 1998.
[49] Liou M.S. and Edwards J.R. Ausm schemes and extensions for low mach and multiphase flows. VKI Lecture Series 1999-03, von Karmann Institute for Fluids Dynamics, 1999.
[50] K.L. Nguyen. One dimensional models for transient two phase separated flow. In *Transient Two Phase Flow, Proceeding of the 3rd CSNI Specialist Meeting*, pages 389–402, 1981.
[51] H. Paillere, C. Corre, and J.R. García Cascales. On the extension of the ausm+ scheme to compressible two-fluid models. *accepted in Computer and Fluid*, submitted in Dec 2000.
[52] H. Paillere, A. Kumbaro, C. Viozat, S. Clerc, A. Broquet, and C. Corre. A comparison of roe, vffc and ausm+ schemes for two phase water/steam flows. *Godunov Methods: Theory and Applications, Edited Review*, 2000.
[53] Whalley P.B. *Two Phase Flow and Heat Transfer*. Oxford University Press, 1996.
[54] S. Petelin, B. Mavko, and I. Tiselj. Two fluid model verification with utube liquid oscillation. *ZAMM, Z angew Math. Mech*, 75:359–360, 1995.
[55] V.H. Ramshaw and J.A. Trapp. Charecteristics, stability, and short wavelength phenomena in two phase flow equation systems. *Nuclear Science and Engineering*, 66:93–102, 1978.
[56] V.H. Ransom and D.L. Hicks. Hyperbolic two pressure models for two phase flow. *Journal of Computational Physics*, 53:124–151, 1984.
[57] L. Sainsaulieu. Contribution à la modelisation mathematique et numerique des Écoulaments diphasiques constitués d'un nuage de particules dans un ecoulaments de gas, 199? Demande D'Habilitation a Diriger Des Recherches.
[58] R. Saurel and R. Abgrall. A multiphase godunov method for compressible multifluid and mltiphase flows. *Journal of Computational Physics*, 150:425–467, 1999.
[59] W.T. Sha and S.L. Soo. On the effect of p term in the multiphase mechanics. *Int. J. Multiphase Flow*, 5:153–158, 1979.
[60] A.S. Shieh, Ransom V.H., and Krishnamurthy R. *Validation of Numerical Techniques in RELAP5/MOD3, RELAP5/MOD3 Code Manual, NUREG/CR-5535*, 1994.

[61] K.M. Shyue. An efficient shock -capturing algorithm for compressible multicomponent problems. *Journal of Computational Physics*, 142:208, 1998.

[62] H. Städtke, G. Franchello, and B. Worth. Numerical simulation of multi-dimensional two-phase flow based on flux vector splitting. *Nuclear Engineering and Design*, 177:199–213, 1997.

[63] H. Städtke, G. Franchello, and B. Worth. Characteristic-based upwind methods for two-phase flow - present status and future perspective. In *Proceeding of the* 4^{th} *International Conference on Multiphase Flow*, New Orleans, USA, May 27 - June 1 2001.

[64] H. Städtke and R. Holtbecker. Hyperbolic model for inhomogeneous two phase flow. In *International Conference on Multiphase Flows*, University of Tsukuba, Japan, Sept. 24-27 1991.

[65] H. Städtke and R. Holtbecker. Numerical simulation of two phase flow based on hyperbolic flow equations. In *Sixth International Topical Meeting on Nuclear Reactor ThermalHydraulics, NURETH-6*, Granoble, France, Octuber 5-8 1993.

[66] H.B Stewart. Stability of two phase flow calculation using two fluid models. *Journal of Computational Physics*, 33:259–270, 1979.

[67] H.B Stewart and B. Wendroff. Two phase flow: Models and methods. *Journal of Computational Physics*, 6:363–409, 1984.

[68] Y. Taitel and A.E. Dukler. A model for predicting flow regime transitions in horizontal and near horizontal gas liquid flow. *AIChE Journal*, 22:47–55, 1976.

[69] M. Tajchman and Freydier P. Schéma vffc: application à l'étude d'un cas test d'ebullition en tuyau droit représentant le fonctionnement en bouillotte d'un coeur. Technical report, EDF, 1998. REP. Note EDF HT 33/98/033/A.

[70] I. Tiselj and S. Petelin. Eigenvalues and eigenvectors of two fluid models of two-phase flow. In *Proceeding of the First International Symposium on Finite Volumes for Complex Applications*, pages 225–232, 1996.

[71] I. Tiselj and S. Petelin. High resolution shock capturing schemes for two-phase flow. In *Proceedings of the ASME FED Summer Meeting*, pages 251–256, 1996.

[72] I. Tiselj and S. Petelin. Modelling of two-phase flow with second order accurate scheme. *Journal of Computational Physics*, pages 503–521, 1997.

[73] I. Tiselj and S. Petelin. First and second order accurate schemes for two-fluid models. *ASME Journal of Fluids Engineering*, 20:363–368, 1998.

[74] I. Tiselj and S. Petelin. How to get second-order accurate solutions from the first-order accurate relap5 code. In *Proceedings of the ASME Nuclear Engineering Division*, 1998.

[75] E.F. Toro. Riemann-problem-based techniques for computing reactive two-phase flows. *Numerical Combustion, Lectures Notes in Physics*, page 351, 1989.

[76] E.F. Toro. *Riemann Solvers and Numerical Methods for Fluid Dynamics, A Practical Introduction*. Springer Verlag, 1997.

[77] I. Toumi. A weak formulation of roe's approximate riemann solver. *Journal of Computational Physics*, 102:360–373, 1992.

[78] I. Toumi. An upwind numerical method for two fluid two phase flow models. *Nuclear Science and Engineering*, 123:147–168, 1996.

[79] I. Toumi and A. Kumbaro. An approximate linearized riemann solver for a two fluid model. *Journal of Computational Physics*, 124:286–300, 1996.

[80] I. Toumi, A. Kumbaro, and H. Paillere. Approximate riemann solvers and flux vector splitting schemes for two phase flow. VKI Lecture Series 1999-03, von Karmann Institute for Fluids Dynamics, 1999.

[81] I. Toumi and P. Raymond. Upwind numerical scheme for two-fluid two-phase model. In *Proceeding of the 14th International Conference on Numerical Methods in Fluid Dynamics*, number 453 in Lecture Notes in Physics, pages 299–306. Springer-Verlag, Jul 11-15 1995.

[82] B. Van Leer. Flux-vector splitting for the euler equations. In *Proceeding of the 8^{th} International Conference on Numerical Methods in Fluid Dynamics*, pages 507–512. Springer-Verlag, 1982.

[83] C. Viozat. Calcul d'ecoulements diphasiques dans une tuyere: Influence de la renormalisation du schema de flux. Technical report, CEA, 2000. Raport DMT/SYSCO/LGLS/RT/00-014.

[84] G. Yaridaroglu and Jr.T. Lahey. On the various forms of the conservation equations in two phase flow. *Int. J. Multiphase Flow*, 2:477–494, 1976.

[85] N. Zuber and J.A. Findlay. Average volumetric concentration in two phase flow systems. *Journal of Heat Transfer*, 87:453, 1965.